Spring 2018 – Systems Biology of Reproduction
Discussion Outline – Ovary Systems Biology
Michael K. Skinner – Biol 475/575
CUE 418, 10:35-11:50 am, Tuesday & Thursday
March 1, 2018
Week 8

Ovary Systems Biology

Primary Papers:

1. Wigglesworth, et al. (2015) Biology of Reproduction 92(1):23, 1-4
2. Grøndahl, et al. (2013) Mol Human Reprod 19:600-617
3. Nilsson, et al. (2010) PLoS ONE 7:e11637

Discussion

Student 23: Reference 1 above

- What cumulus and mural granulosa cells?
- What gene categories and networks were identified?
- What oocyte paracrine interactions were identified?

Student 24: Reference 2 above

- What are the technology used and objectives?
- What did the expression patterns show about oocytes?
- What insights are provided about the extreme oocyte states during folliculogenesis?

Student 25: Reference 3 above

- What is the experimental and systems approach?
- What new insights provided on primordial follicle development?
- What gene signaling networks were identified for primordial follicle development?

BIOLOGY OF REPRODUCTION (2015) **92**(1):23, 1–14
Published online before print 5 November 2014.
DOI 10.1095/biolreprod.114.121756

Transcriptomic Diversification of Developing Cumulus and Mural Granulosa Cells in Mouse Ovarian Follicles[1]

Karen Wigglesworth,[3] Kyung-Bon Lee,[4] Chihiro Emori,[5] Koji Sugiura,[5] and John J. Eppig[2,3]

[3]*The Jackson Laboratory, Bar Harbor, Maine*
[4]*Department of Biology Education, College of Education, Chonnam National University, Buk-gu, Gwangju, Korea*
[5]*Laboratory of Applied Genetics, Graduate School of Agriculture and Life Sciences, The University of Tokyo, Tokyo, Japan*

ABSTRACT

Cumulus cells and mural granulosa cells (MGCs) have functionally distinct roles in antral follicles, and comparison of their transcriptomes at a global and systems level can propel future studies on mechanisms underlying their functional diversity. These cells were isolated from small and large antral follicles before and after stimulation of immature mice with gonadotropins, respectively. Both cell types underwent dramatic transcriptomic changes, and differences between them increased with follicular growth. Although cumulus cells of both stages of follicular development are competent to undergo expansion in vitro, they were otherwise remarkably dissimilar with transcriptomic changes quantitatively equivalent to those of MGCs. Gene ontology analysis revealed that cumulus cells of small follicles were enriched in transcripts generally associated with catalytic components of metabolic processes, while those from large follicles were involved in regulation of metabolism, cell differentiation, and adhesion. Contrast of cumulus cells versus MGCs revealed that cumulus cells were enriched in transcripts associated with metabolism and cell proliferation while MGCs were enriched for transcripts involved in cell signaling and differentiation. In vitro and in vivo models were used to test the hypothesis that higher levels of transcripts in cumulus cells versus MGCs is the result of stimulation by oocyte-derived paracrine factors (ODPFs). Surprisingly ~48% of transcripts higher in cumulus cells than MGCs were not stimulated by ODPFs. Those stimulated by ODPFs were mainly associated with cell division, mRNA processing, or the catalytic pathways of metabolism, while those not stimulated by ODPFs were associated with regulatory processes such as signaling, transcription, phosphorylation, or the regulation of metabolism.

cumulus cells, mouse, mural granulosa cells, oocyte, oocyte-derived paracrine factors, ovarian follicle, transcriptome

INTRODUCTION

The cellular architecture of the ovarian follicle of most mammalian species becomes clearly diversified at the preantral to antral follicle transition. The granulosa cells of preantral follicles sort into two more differentiated populations at the time of follicular antrum formation: mural granulosa cells (MGCs), which line the follicular wall, and cumulus granulosa cells, which are associated with the oocyte. Generally, cumulus cells are thought to support oocyte development, while MGCs carry out endocrine function(s) indicative of functional as well as cellular architectural diversity. However, these are not strict divisions of labor because interactions between MGCs and cumulus cells can play crucial roles in oocyte maturation and ovulation [1–3]. The two populations have very different fates after the preovulatory surge of luteinizing hormone (LH). The MGCs remain within the ovary and participate in the formation of the corpus luteum. In contrast, the cumulus cells undergo a dramatic morphological change, producing and becoming embedded in a mucinous matrix in a process often referred to as cumulus expansion; they accompany the metaphase II oocyte to the oviduct during ovulation [4–6]. Before the LH surge, the cumulus cells communicate with the oocyte via gap junctions, which allow the exchange of low molecular weight molecules and facilitate both metabolic cooperation between cumulus cells and oocytes and regulation of meiosis [7–11]. The cumulus cells in the first layer around the oocyte are referred to as the corona radiata; and both the corona cells and the cumulus cells in outer ranks communicate with the oocyte via membrane extensions that reach around the corona cells to contact the oocyte, thus forming a pseudostratified communicating epithelium [12]. Oocyte-derived paracrine factors (ODPFs), sometimes in cooperation with other ligands, play crucial roles in the development and function of the cumulus cells [13, 14]. Oocytes are required for the formation of cumulus cells during the preantral to antral follicle transition [15]. This transition is generally correlated with the acquisition of oocyte competence to resume the first meiotic division [16]. These early cumulus cells are competent to undergo expansion in vitro [17] in a manner that appears similar to that of cumulus cells within large Graafian follicles in situ. These specific roles reveal considerable cellular and developmental complexity, but, in fact, very little is known about the global nature of the transcriptomes that support this cellular and functional diversification, which is the goal of this study.

The levels of some transcripts that are different in the cumulus cell and MGC populations in large Graafian follicles even before the LH surge and the induction of cumulus expansion, provide information on how the transcriptome reflects architectural diversity. For example, transcripts encoding enzymes participating in glycolysis and cholesterol production are expressed more highly by cumulus cells than by MGCs. Other transcripts enriched in cumulus cells versus MGCs of Graafian follicles include those encoding an amino acid transporter SLC38A3, the androgen receptor AR, the

[1]Supported by grants from the Eunice Kennedy Shriver National Institute of Child Health and Human Development HD23839, HD 21970 (K.W., K-B.L., K.S., and J.J.E.) and a Grant-in-Aid for Scientific Research from the Ministry of Education, Culture, Sports, Science and Technology of Japan (C.E. and K.S.).
[2]Correspondence: John J. Eppig, The Jackson Laboratory, 600 Main Street, Bar Harbor, ME 04609. E-mail: john.eppig@jax.org

Received: 22 May 2014.
First decision: 29 June 2014.
Accepted: 3 November 2014.

eISSN: 1529-7268 http://www.biolreprod.org
ISSN: 0006-3363

ligand AMH, and the natriuretic receptor 2 (NPR2) [3, 13, 18]. Expression of these transcripts is seen by in situ hybridization as a gradient with highest expression by cells closest to the oocyte and decreasing with increased distance outward from the oocyte [3, 13, 19]. Some periantral granulosa cells express these transcripts at levels higher than those seen in mural cells closer to the basal lamina. This suggests that periantral MGCs receive ODPF signals at levels sufficient to affect gene expression but that these levels are rapidly diluted with increasing distance from the oocyte. Microsurgical removal of oocytes (oocytectomy, OOX) from isolated cumulus-oocyte complexes (COCs) results in reduced expression of these transcripts, but these levels are maintained by ODPFs, particularly BMP15, GDF9, FGF8, or combinations of these [13, 19, 20]. This demonstrates that ODPFs promote the expression of genes characteristic of the cumulus cell phenotype. On the other hand, follicle-stimulating hormone (FSH) occurs in a diffusion gradient in the follicle opposite to that of ODPFs and promotes the expression of genes characteristic of the MGC phenotype, such as *Lhcgr* encoding the LH-receptor and *Cyp11a1* encoding the P450 cholesterol side chain cleavage enzyme [13, 21]. Actions of FSH are augmented when MGCs contact components of the follicular basal lamina [22, 23]. ODPFs often abrogate the action of FSH and promote the cumulus cell phenotype instead. For example, ODPFs suppress the expression of *Lhcgr* mRNA by granulosa cells despite stimulation with FSH and culture on basal lamina [24]. Cells in intermediate zones between the gradients of FSH and ODPFs exhibit intermediate phenotypes depending upon their relative proximity to either the basal lamina or the oocyte.

Cumulus expansion in vivo occurs just before ovulation when follicles are stimulated by LH and produce EGF-like growth factors (EGFLGFs), which are first generated by MGCs in response to LH, and then by the cumulus cells via autocrine reinforcement [1, 2]. Cumulus expansion in response to stimulation of the EGF receptor requires the presence of ODPFs [25]. Moreover, expansion requires the expression of at least four factors (HAS2, PTGS2, PTX3, and TNFAIP6) because loss of expression of the genes encoding any of these factors dramatically compromises expansion [5, 26–29]. In addition to these expansion-related factors, the levels of many transcripts in cumulus cells change as a consequence of triggering cumulus expansion by gonadotropins in vivo [30–33]. However, the transcriptomes of cumulus cells and MGCs during the transition of small to large antral follicles (hereafter, SAFs and LAFs, respectively), before the initiation of cumulus expansion and ovulation, have not been described.

Clearly, more global and systems views of the transcriptional complexity underlying the architectural diversification can provide rationale and impetus to future studies of follicular cellular and functional development before the LH surge. Thus, the first objective of this study was to obtain a more global perspective than provided by analyses of single transcripts or pathways by utilizing microarrays to characterize the transcriptomic diversity of cumulus cells and MGCs. Analyses of these data are made by performing pairwise transcriptomic comparisons, with each comparison enhancing our view of the transcriptome of specific cell states and types. The value of this relatively unbiased, but global approach to the transcriptome was demonstrated by a previous study that capitalized on microarray data to discover a key for maintaining oocyte meiotic arrest. From this microarray approach, we found that natriuretic peptide NPPC is a ligand produced by MGCs and this ligand binds to its cognate receptor, NPR2, which is most highly expressed by cumulus cells. NPR2 is a guanylyl cyclase whose product, cGMP, is then transferred from the cumulus cells to oocytes via gap junctions to maintain oocyte meiotic arrest [3, 11]. Now in the current study, we have compared the transcriptomes of cumulus and MGCs in both early antral follicles and in large follicles after eCG-stimulation of immature mice in vivo. Although the cumulus cells isolated from both stages of follicular development are competent to undergo expansion in vitro [17], and are morphologically indistinguishable, we found that cumulus cells undergo transcriptomic changes that are as dramatic as those occurring in MGCs during the SAF to LAF transition.

The second objective of this study was to test the hypothesis that ODPFs are responsible for the higher expression of transcripts in cumulus cells than MGCs. Two approaches were used to test this: 1) comparison of the transcripts expressed at higher levels in freshly isolated cumulus cells with those found previously to be stimulated in cumulus cells by ODPFs in vitro [34] and 2) comparison of the higher cumulus cell transcripts with those found previously to be lower in cumulus cells of mutants deficient in the ODPFs GDF9 and BMP15 versus wild-type (WT) cumulus cells in vivo [35].

MATERIALS AND METHODS

COCs were isolated from the SAFs and LAFs of 22-day-old B6SJLF1 mice that were raised in the research colonies of the authors at The Jackson Laboratory. The Administrative Panel on Laboratory Animal Care at The Jackson Laboratory approved animal protocols, and all the experiments were conducted in accordance with the National Institutes of Health Guide for the Care and Use of Laboratory Animals. In order to obtain sufficient and uniform populations of cumulus cells and MGCs for microarray analyses, development of SAFs to LAFs was stimulated by intraperitoneal injection of 5 international units eCG 44 h before obtaining the COCs. Thus, SAFs were from unstimulated ovaries of 22-day-old mice, while LAFs were from 22-day-old mice stimulated 44 h previously with eCG. It is uncertain whether the stimulation with exogenous hormones produces the same effects on granulosa cell transcriptomes as would occur with natural stimulation by endogenous hormones.

Only COCs completely enclosed by tightly packed cumulus oophorus were selected for analysis. Two hundred oocyte-cumulus cell complexes were collected using micropipets with the aid of a stereo microscope and washed free of all other cells by serial transfer through three dishes of culture medium. This removes all possibility of contamination by individual MGCs. The cumulus cells were then stripped from the oocytes by drawing them into a fine glass pipet with a diameter slightly smaller than the diameter of the oocytes, which were discarded, and the cumulus cells prepared for RNA extraction. Clumps of MGCs, which are easily distinguishable from oocyte-cumulus cell complexes using a stereo microscope, with a total mass approximately equal to that of the cumulus cells, were collected with micropipets, washed, and prepared for RNA extraction. Given this care, the separation of cell types was absolutely clean. As verification of this, no expression of *Lhcgr*, a marker of MGCs [13], was found in the cumulus cell preparations, and no expression of *Slc38a3*, a marker of cumulus cells from LAFs [13], was found in the MGC preparations as shown in Supplemental Figure S1 (all the supplemental data is available online at www.biolreprod.org). The cumulus cells and MGCs were collected from three groups of five pooled mice. Thus, there were three biological replicates of each sample. The samples were amplified and applied to Affymetrics 430V2 arrays by the Jackson Laboratory Gene Expression Service as described previously [19, 34].

Average signal intensities for each probeset within the arrays were calculated by the RMA function provided within the Affymetrix package for R using a custom (Ensembl Transcript) CDF file [36]. The RMA method incorporates convolution background correction, sketch-quantile normalization, and summarization based on a multiarray model fit robustly using the median polish algorithm. For this experiment, three pairwise comparisons were used to statistically resolve transcriptomic differences between treatment levels using the R/maanova analysis package [37, 38]: 1) cumulus cells of SAFs versus LAFs, 2) cumulus cells versus MGCs of SAFs, and 3) cumulus cells versus MGCs of LAFs. Specifically, differentially expressed transcripts were detected using F, a modified F-statistic incorporating shrinkage estimate of variance components from within the R/maanova package [37, 38]. Statistical significance levels of the pairwise comparisons were calculated by permutation analysis (1000 permutations) and adjusted for multiple testing using the false discovery rate (FDR), Q-value, method [39]. Differentially expressed genes are declared at an FDR Q-value threshold of 0.05. Therefore, the FDR was limited by this selection alone to 5%. Furthermore, an additional stringency was

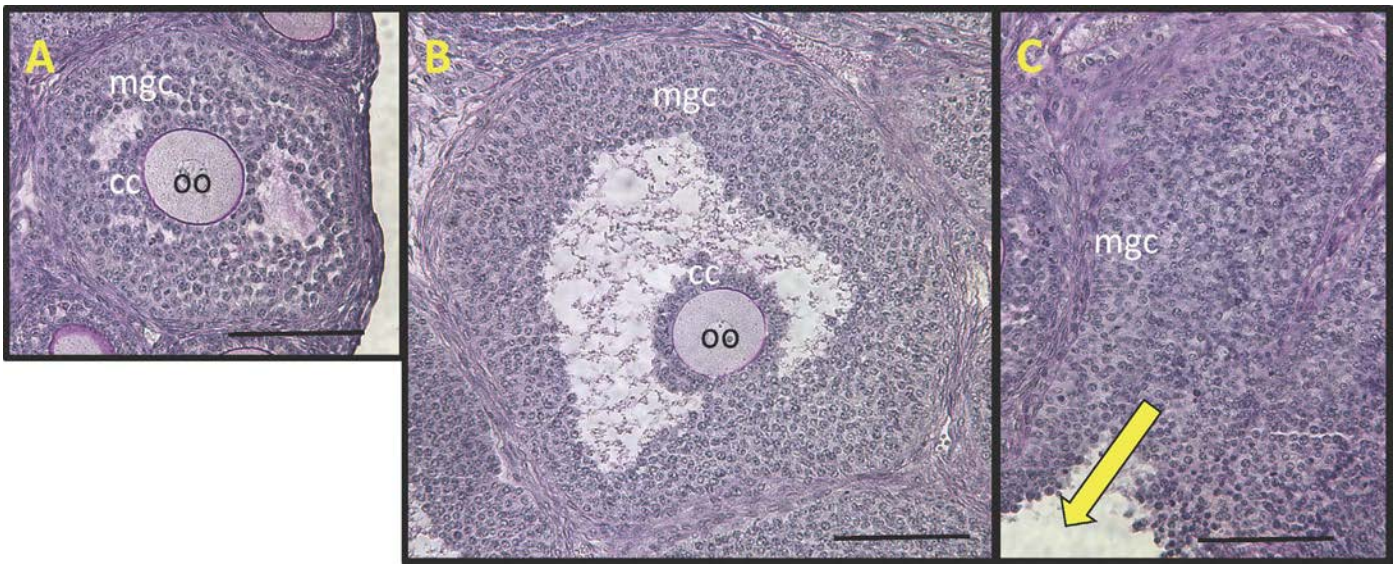

FIG. 1. Photomicrographs of histological sections of (**A**) a small antral follicle (SAF) typical of those in the ovaries of 22-day-old B6SJLF1 mice not stimulated with eCG and (**B**) a large antral follicle (LAF) typical of those in the ovaries 44 h postinjection with 5 international units eCG showing mural granulosa cells (MGC), cumulus cells (CC), and oocyte (oo). **C**) The follicular remnants after puncturing an LAF with a needle to express (yellow arrow) MGC and the oocyte cumulus cell complex. Note that many MGCs most immediately adjacent to the follicular basal lamina remain unexpressed and therefore not included in the microarray analyses. Bar = 100 μm.

imposed by requiring a 1.25-fold difference between contrasted groups for inclusion of transcripts in the cohort considered to be significantly enriched. The effective FDR was, therefore, less than 5%. Moreover, only those transcripts encoded by genes annotated in Mouse Genome Database (MGD) as having known biological functions (http://www.informatics.jax.org/function.shtml) are presented. Transcripts levels whose FDR *Q*-value was >0.05 and fold difference was <1.25 were considered to be not different. VLAD, a VisuaL Annotation Display tool (v. 1.5.1) (http://proto.informatics.jax.org/prototypes/vlad/) was used to identify biological function gene ontology (GO) terms defined by sets of enriched transcripts. GO terms, established by the GO Consortium (http://www.geneontology.org/), provide a standardized way to group genes or proteins according to their biological or molecular functions. Transcripts allocated to a specific GO term by electronic annotation alone were excluded. Therefore, assignment of a transcript to a GO term was based on curation of experimental data. Supplemental Figure S2 provides an illustration to aid in interpreting VLAD graphics.

For practical reasons, presentation of transcripts in contrasted groups was focused in two ways. First, only the transcripts associated with GO terms and annotated with known biological or molecular functions are presented; the entire lists of transcripts have been deposited in the Gene Expression Omnibus (http://www.ncbi.nlm.nih.gov/geo, dataset GSE55845). Additional transcriptomic analyses showing the effects of ODPFs on cumulus cell transcripts and on the effect of *Gdf9*$^{+/-}$ *Bmp15*$^{-/-}$ double mutation were deposited previously (GSE47967) [34] and (GSE7225) [19], respectively. Second, the top 50 transcripts exhibiting the greatest fold differences within the contrast are presented. Also for practical reasons, many references to general biological/molecular functions of the numerous specific gene products referred to here are not cited but can be found by searching the Mouse Genome Informatics database (http://www.informatics.jax.org/) or other resources.

To assess the ability of cumulus cells to elevate expression of cumulus expansion related transcripts *Has2, Ptx3, Ptgs2,* and *Tnfaip6*, in response to EGF, COCs were isolated from small and large follicles of ovaries of 22-day-old mice and cultured for 6 h with or without 10 ng/ml EGF. Transcript levels were assessed by quantitative RT-PCR (qRT-PCR). All procedures and reagents were exactly as described previously [15].

RESULTS

General Considerations of the Samples and Analyses of the Microarray Data

Cumulus and MGCs were obtained from either SAFs (200–350 μm diameter) of unstimulated ovaries or from LAFs (450–550 μm diameter) of eCG-stimulated ovaries (Fig. 1). The cumulus and MGCs of both groups appear morphologically indistinguishable by histological examination (Fig. 1, A and B). In addition to morphological resemblance, the COCs isolated from both groups were competent to undergo expansion in vitro ([17] and results presented here). During the collection process, rupturing follicles with needles expels COCs and clumps of MGCs. Examination of ovarian remnants after puncture of follicles showed that some MGCs were not extruded upon puncture, particularly those most closely associated with the basal lamina (Fig. 1C), suggesting that the MGCs used for analyses are probably a population biased toward the periantral MGCs.

Our previous studies [17] showed that COCs from SAFs underwent expansion in vitro, and, moreover, these experiments were conducted using FSH to stimulate expansion, that is, prior to demonstration of the prominent role of EGFLGFs in promoting cumulus expansion. Therefore, to provide more information on competence of the cumulus cells used for the transcriptomic studies described here, we tested the ability of these COCs to undergo expansion in response to EGF stimulation in vitro. As shown in Supplemental Figure S3, EGF dramatically stimulated the expression of the expansion-related transcripts *Has2, Ptx3, Ptgs2,* and *Tnfaip6* in COCs from both the SAFs from unstimulated ovaries and the LAFs from eCG-stimulated follicles. Nevertheless, in spite of the fact that COCs from both groups appeared maximally expanded (not shown), levels of these transcripts in the cumulus cells of SAFs were 50%–75% of those from LAFs.

In our previous studies, we reported differences in transcript levels between cumulus cells and MGCs using in situ hybridization and/or qRT-PCR or RNase protection assays [3, 13, 19, 20, 40–42]. It was shown that the following transcripts are expressed more highly in cumulus cells than in MGCs: *Slc38a3, Npr2, Mvk, Fdps, Pfkp, Ldha, Nog, Smad7, Tpi1,* and *Eno1*. In contrast, the following transcripts are expressed more highly in MGCs than in cumulus cells: *Grem1, Twsg1, Tob1, Nrip1, Cyp19a1, Cyp11a1, Lhcgr, Star,* and *Nppc*. All of these transcripts fell within the cutoffs defining the groups that were higher in cumulus or MGCs in the

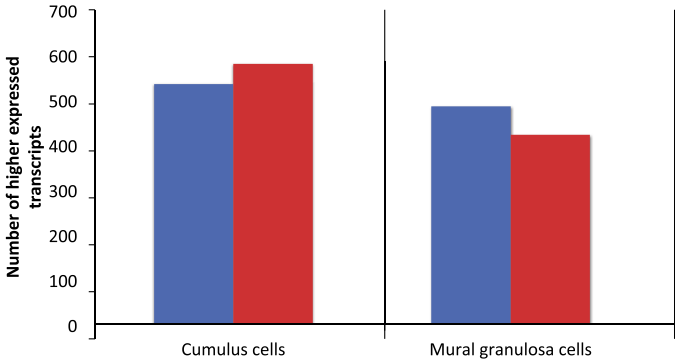

FIG. 2. Number of transcripts expressed at higher levels in SAFs of unstimulated ovaries (blue bars) versus those of LAFs 44 h post-eCG-stimulation (red bars) in cumulus cells or MGCs. Only transcripts that encode proteins with annotated biological functions are included.

microarray analyses presented here. As indicated in *Materials and Methods,* the cutoff to discriminate between higher or not higher in cumulus cells or MGCs in this study was set at fold difference > 1.25 and $Q < 0.05$. Thus, although arbitrary, the set discriminators for being different or not different produced outcomes that were highly correlated with results produced by the various other quantitative approaches. However, *Amh, Ar, Sqle,* and *Cyp51* were excluded from the higher in cumulus cells versus MGCs group despite evidence using alternative, and probably more reliable, methods showing that they are expressed at higher levels in cumulus cells than MGCs. The microarray-based fold increase and Q values for *Amh* were 1.25-fold and $Q = 0.09$, for *Ar* they were 1.12-fold and $Q = 0.08$, and for *Cyp51* they were 1.26-fold and $Q = 0.1$. Thus, these transcripts fell just outside the boundary that would have included them in the higher in cumulus cell cohort. The microarray data were validated for seven additional transcripts by qRT-PCR (Supplemental Fig. S1). Several issues could account for blurring of the boundary that would put transcripts inside or outside the inclusion groups. These include microarray probe factors, statistical confounding, biological factors (such as bias in the MGC populations that were analyzed toward the periantral MGCs, which express some transcripts typical of cumulus cells at higher levels than the MGCs located nearer to the basal lamina), or other artifacts that could be created by sample collection. Nevertheless, the results here, considered in their global perspective, are probably conservative, although any future studies based on the data presented here should include experimental verification of expression profiles for transcripts of interest.

Contrast: Cumulus Cells Isolated from SAFs Versus Cumulus Cells Isolated from LAFs

In the contrast between cumulus cells from SAFs versus LAFs, 535 transcripts were expressed at higher levels in cumulus cells from SAFs while 580 were expressed more highly in cumulus cells from LAFs (Fig. 2). Transcripts enriched in the cumulus cells from SAFs encode proteins that participate in metabolic processes, including those with catalytic activities (e.g., GO:0044281, small molecule metabolic process), such as those having transferase (GO:001670) or oxidoreductase activities (GO:0016491). In contrast, those enriched in cumulus cells from LAFs encode proteins involved with the regulation of metabolic and developmental processes, including those with protein-binding functions, such as those having protein- or small molecule-binding activities (e.g., GO:0048522, positive regulation of cellular processes). The relative enrichment of transcripts in the top GO terms are shown in Figure 3 and/or Supplemental Table S1, which presents the complete list of transcripts expressed differently in SAFs and LAFs for each GO term.

Transcripts with greatest fold differences. A list of the 50 top transcripts expressed more highly in cumulus cells from SAFs versus LAFs is shown on Table 1 and Supplemental Table S2. *Serpinf1,* encoding an antiangiogenic factor, heads

TABLE 1. Top 50 fold difference in cumulus cells of SAFs versus LAFs; gene names are presented in Supplemental Table S2.

Higher in SAF versus LAF cumulus cells				Higher in LAF versus SAF cumulus cells			
Fold difference	Gene symbol	Fold difference	Gene symbol	Fold difference	Gene symbol	Fold difference	Gene symbol
9.51	*Serpinf1*	2.71	*Mybpc3*	7.78	*Grem1*	3.26	*Scd1*
7.29	*Wt1*	2.71	*Mgp*	7.53	*Cbfa2t3*	3.03	*Aire*
7.00	*Nrip2*	2.70	*Gulo*	7.40	*Mrap*	3.02	*Fabp3*
5.19	*Lmo7*	2.69	*Cxcr7*	6.02	*Tubb2b*	3.01	*Vegfa*
5.13	*Ccbe1*	2.66	*Derl3*	5.86	*Cacna1a*	3.00	*Aicda*
4.88	*Gatm*	2.66	*Cspg4*	5.57	*Afap1l2*	2.98	*Mia1*
4.45	*Dsg2*	2.66	*Arnt2*	4.97	*Masp1*	2.95	*Dab1*
4.42	*Pik3ip1*	2.65	*Ror1*	4.43	*Vim*	2.94	*Hmgn3*
4.06	*Tdrd5*	2.63	*Perp*	4.31	*Plxnb1*	2.91	*Sdpr*
3.92	*Krt20*	2.62	*Cpeb2*	4.02	*Cml3*	2.91	*Lrp8*
3.79	*Plxna2*	2.58	*Tns3*	4.01	*Rbfox3*	2.91	*Adamts5*
3.78	*Slc18a2*	2.58	*Agtr2*	3.99	*Ppp1r3g*	2.91	*Rian*
3.66	*Maob*	2.55	*Sgms1*	3.95	*Cyp19a1*	2.88	*Gsta4*
3.43	*Calb1*	2.54	*Vnn1*	3.89	*Inhba*	2.85	*Fzd2*
3.34	*St3gal6*	2.54	*Plagl1*	3.82	*Cebpd*	2.82	*Cdkn1a*
3.29	*Itga6*	2.54	*Hnmt*	3.56	*Slit3*	2.82	*Gadd45g*
3.20	*Slc40a1*	2.51	*Sepp1*	3.51	*Timp2*	2.81	*Nmb*
3.19	*Kazald1*	2.47	*Hipk3*	3.39	*Meg3*	2.79	*Ralb*
3.19	*Mgst2*	2.47	*Abca1*	3.38	*Samd4*	2.76	*Fbxl15*
3.11	*Plin2*	2.47	*Slc38a3*	3.36	*Inhbb*	2.74	*Drd4*
3.07	*Runx1*	2.45	*Ntn4*	3.31	*Id2*	2.70	*Tmsb4x*
2.98	*Igfbp4*	2.42	*Irf6*	3.31	*P4ha2*	2.69	*Slc2a1*
2.95	*Eftud1*	2.41	*Cntn4*	3.30	*Gch1*	2.65	*Pfkp*
2.91	*Cd83*	2.41	*Hmga2*	3.27	*Ppfia3*	2.65	*Serpina5*
2.76	*Gadd45a*	2.39	*Sik1*	3.26	*Id1*	2.65	*Gsg1l*

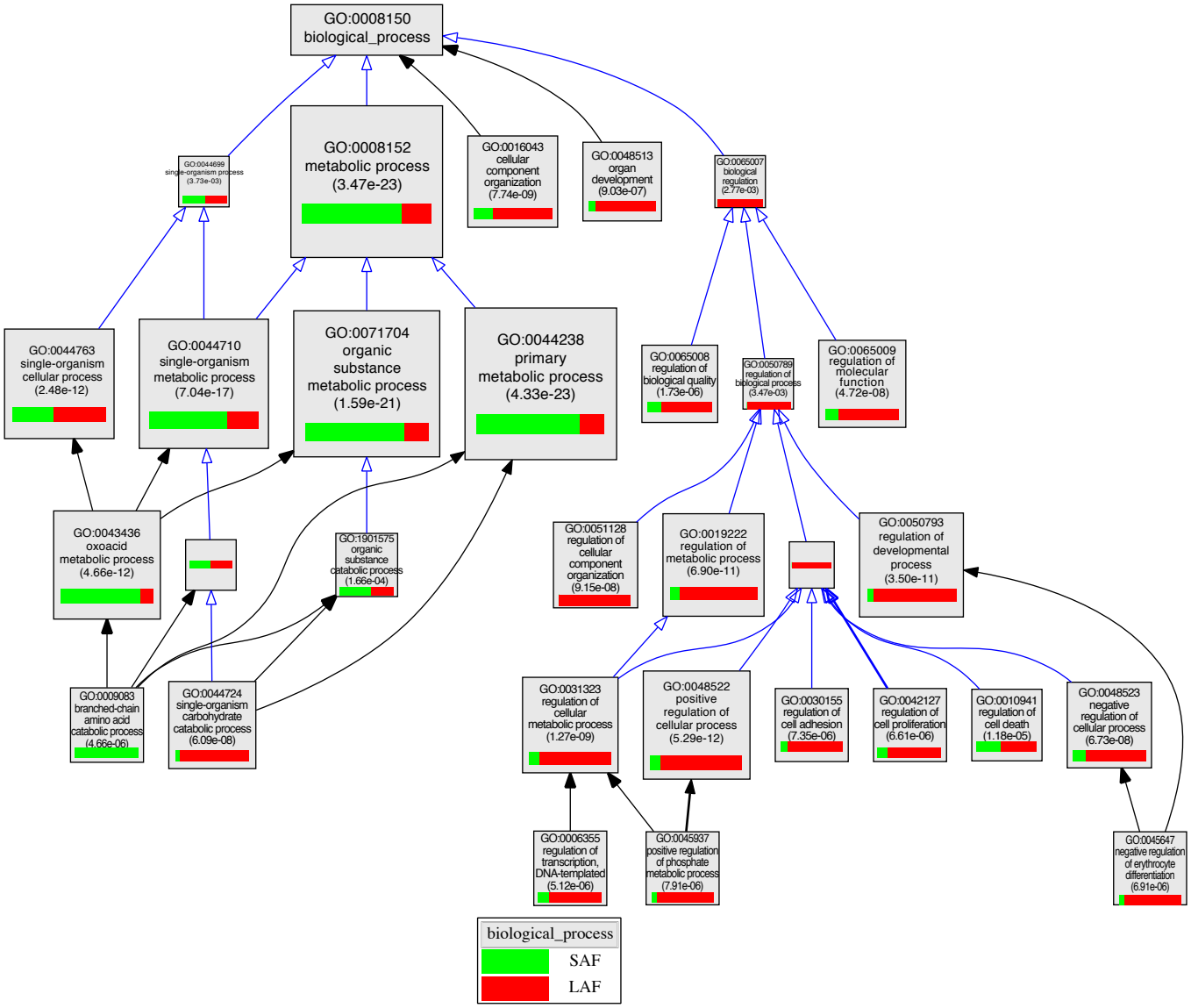

FIG. 3. VLAD depiction of GO terms in the contrast of cumulus cells from SAFs versus LAFs. The top 25 GO terms, selected by VLAD on the basis of local maximum *P* value, are shown. A local maximum term is one whose significance (−log [p]) is greater than its immediate neighbors (children or parents). The size of the rectangle is proportional to the *P* value; the larger the rectangle the lower, and more significant, is the *P* value. The green portion of the rectangle shows the relative contribution of cumulus cell transcripts from SAFs to that GO term while the red portion shows the relative contribution of transcripts from LAFs. Supplemental Table S1 presents a complete list of transcripts expressed differently in SAFs and LAFs for each GO term.

the list followed by the *Wt1* transcription factor and *Nrip2*, which encodes a nuclear corepressor of hormone action. The transcription factor *Runx1*, encoding a transcription factor, and *Agtr2*, encoding an angiotensin receptor, are also much more highly expressed by cumulus cells of SAFs.

Grem1, *Inhba*, and *Inhbb*, encoding ligands in the TGFβ superfamily, were among the transcripts included on the list of the top 50 transcripts most highly expressed in cumulus cells of LAFs compared to SAFs (Table 1 and Supplemental Table S2). Included on this list are *Id1* and *Id2*, which encode DNA-binding inhibitors involved in developmental processes promoted by various bone morphogenetic proteins (BMPs), *Vegfa*, *Fzd2*, and *Cdkn1a* (also known as *p21*), which encodes a cell cycle-related protein associated with cell differentiation. Oocytes probably regulate the expression of *Id1* and *Id2* in cumulus cells ([43, 44] and results presented here).

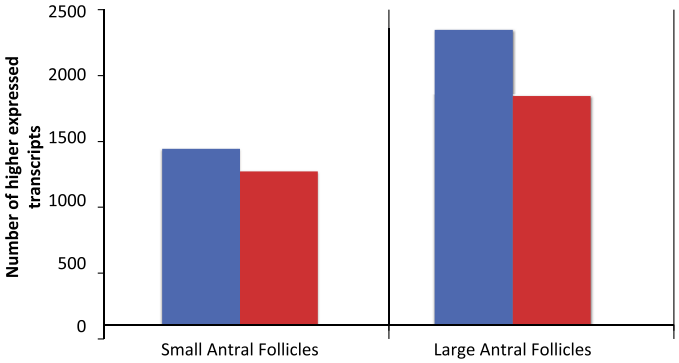

FIG. 4. Number of transcripts expressed at levels higher in cumulus cells versus MGCs (blue bars) or higher in MGCs versus cumulus cells (red bars). Samples were taken from the SAFs of 22-day-old mice or the LAFs of 22-day-old mice 44 h poststimulation with eCG. Only transcripts that encode proteins with annotated biological functions are included.

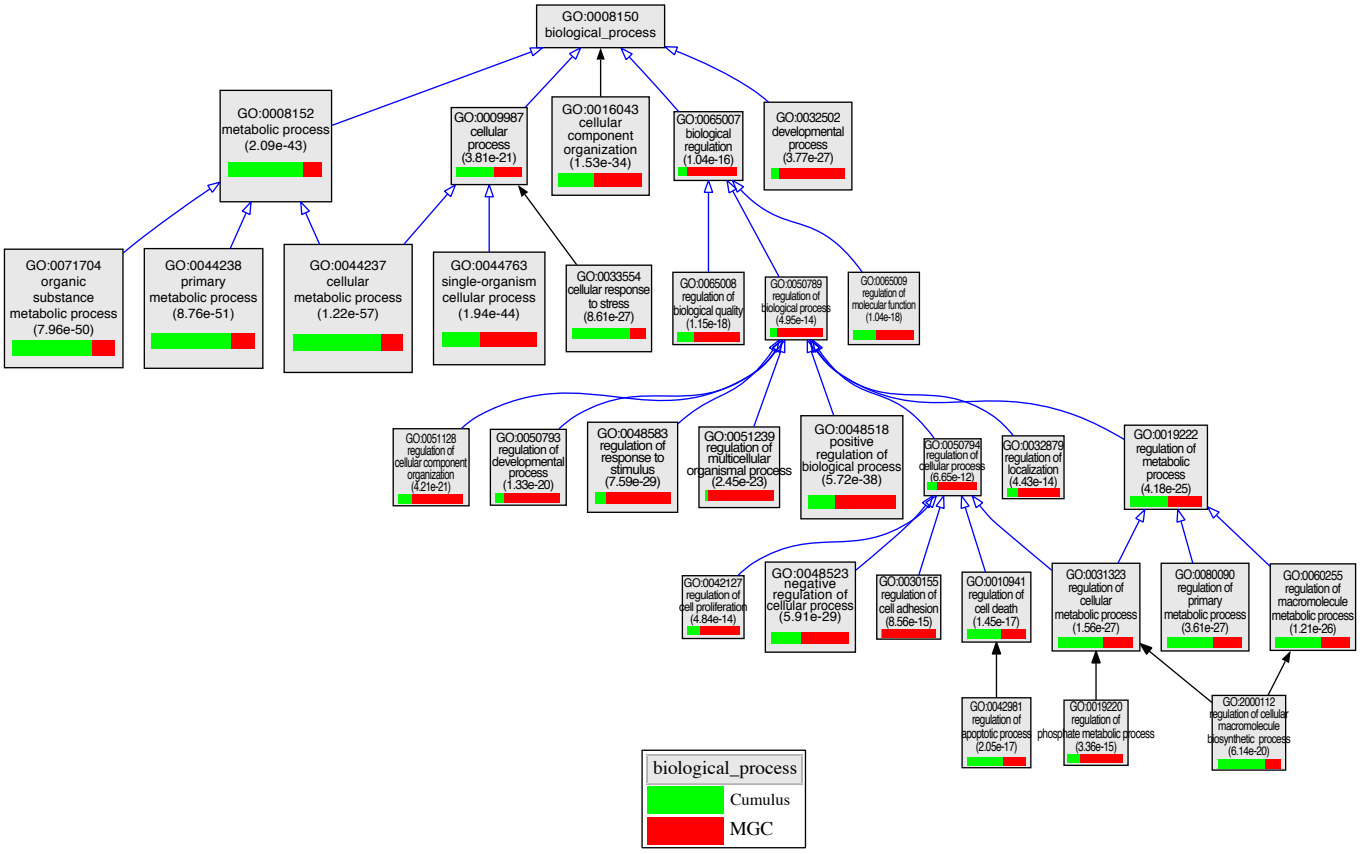

FIG. 5. VLAD depiction of GO terms in the contrast of cumulus cells versus MGCs from SAFs. The top 25 GO terms, selected by VLAD on the basis of local maximum *P* value, are shown. The size of the rectangle is proportional to the *P* value; the larger the rectangle the lower, and more significant, is the *P* value. The green portion of the rectangle shows the relative contribution of cumulus cell transcripts from SAFs to that GO term while the red portion shows the relative contribution of MGC transcripts from SAFs. Supplemental Table S3 presents a complete list of transcripts expressed differently in SAFs and LAFs for each GO term.

As shown in Figure 3 and/or Supplemental Table S1, transcripts in cumulus cells of SAFs relative to LAFs are enriched in transcripts generally associated with small molecule metabolic pathways (GO:0044281, GO:0019752, GO:0009083). In contrast, cumulus cells of LAFs are enriched in transcripts associated with enzymatic pathways involved in monosaccharide catabolic processes (GO:0046365), including glycolysis (GO:0006096), and cholesterol biosynthetic processes (GO:0006695) in accordance with our previous results [19, 20, 40]. Moreover, the cumulus cells of LAFs were enriched in transcripts associated with developmental processes (GO:0032502), regulation of molecular function (GO:0065009), positive and negative regulation of cellular processes (GO:0048522 and 0048523), and positive regulation of transcription (GO:0045893). Cumulus cells, therefore, become enriched in transcripts encoding components of metabolic pathways important for supporting cellular developmental processes and oocyte metabolism during the SAF to LAF transition.

Contrast: Cumulus Cells Versus MGCs

Cumulus cells expressed 1385 transcripts at levels higher than in MGCs of SAFs, and 2318 were higher in cumulus cells of LAFs (Fig. 4); 944 were commonly higher in cumulus cells versus mural cells in both SAFs and LAFs. Therefore, in SAFs and LAFs together, 2759 different transcripts were expressed at higher levels in cumulus cells than MGCs. MGCs expressed 1217 transcripts at levels higher than in cumulus cells of SAFs and 1814 transcripts were higher in MGCs of LAFs (Fig. 4); 878 transcripts were commonly higher in MGCs in both SAFs and LAFs.

In SAFs, transcripts encoding proteins involved in cell proliferation (e.g., GO:0022402; cell cycle process), cellular response to stress (GO:0033554), and ribosome biogenesis (GO:0042254) were enriched in cumulus cells relative to MGCs. In contrast, transcripts encoding proteins participating in the regulation of cell communication (GO:0010646), regulation of signal transduction (GO:0009966), cell morphogenesis (GO:0000902), regulation of cell adhesion (GO:0030155), the regulation of cellular component movement (GO:0051270), and the negative regulation of cell proliferation (GO:0008285) were enriched in MGCs relative to the cumulus cells in SAFs (Fig. 5 and Supplemental Table S3).

As shown in Figure 6 and/or Supplemental Table S4, cumulus cells of LAFs were enriched, relative to MGCs, in transcripts associated with cell cycle process (GO0022402), noncoding RNA processing (GO:0034470), primary metabolic processes (GO:0044238), which includes cholesterol biosynthetic process (GO:0006695), glycolysis (GO:0006096), and cellular response to stress (GO:0033554). In contrast, MGCs were enriched, relative to cumulus cells, in transcripts encoding proteins involved in the regulation of signaling (GO:0023051), phosphorylation (GO:0016310), protein catabolism (GO:0006511 and GO:0016567), steroid biosynthetic process (GO:0006694), and the regulation of cell communication (GO:0010646).

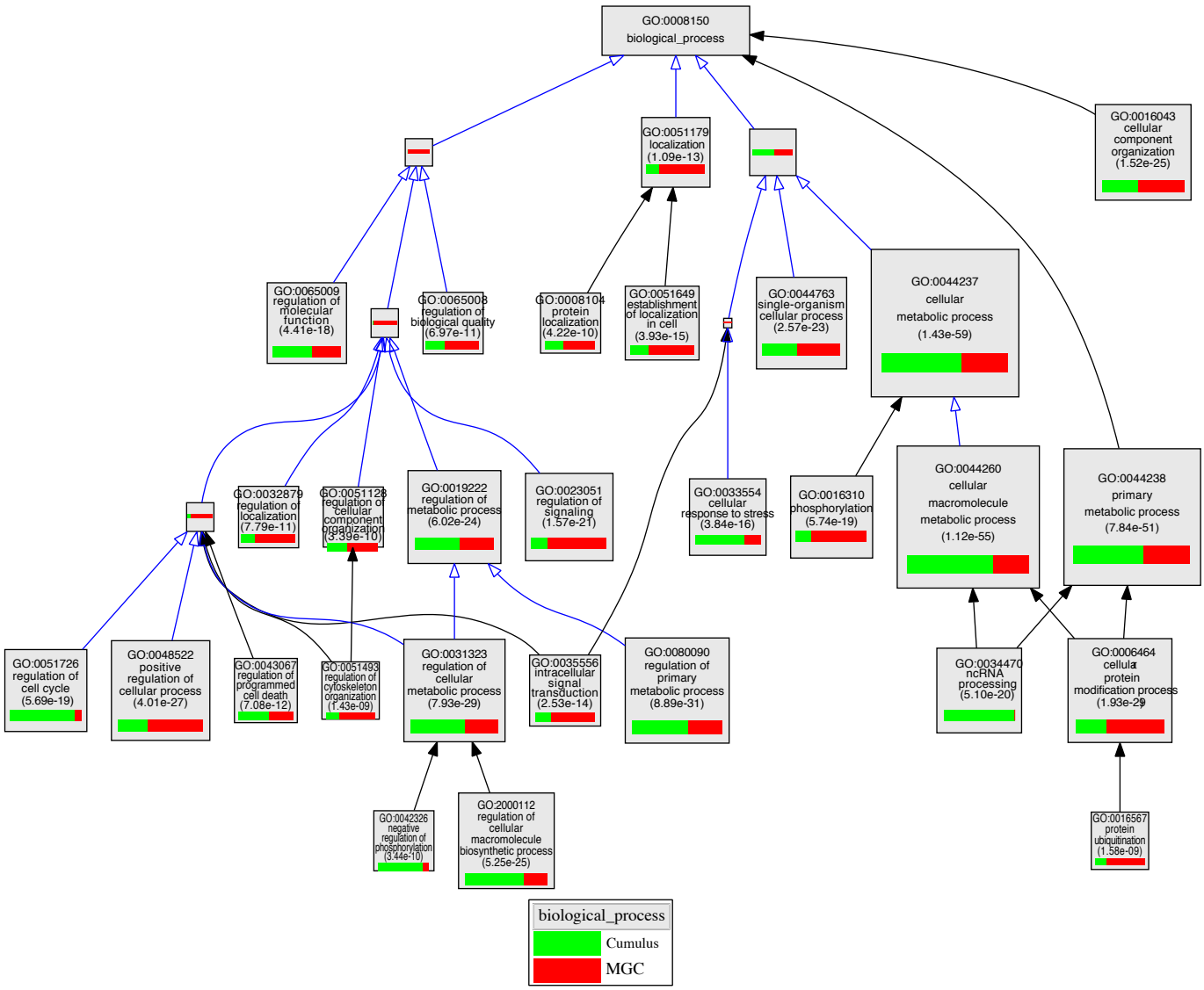

FIG. 6. VLAD depiction of GO terms in the contrast of cumulus cells versus MGCs from LAFs. The top 25 GO terms, selected by VLAD on the basis of local maximum *P* value, are shown. The size of the rectangle is proportional to the *P* value; the larger the rectangle the lower, and more significant, is the *P* value. The green portion of the rectangle shows the relative contribution of cumulus cell transcripts from LAFs to that GO term while the red portion shows the relative contribution of transcripts from LAFs. Supplemental Table S4 presents a complete list of transcripts expressed differently in SAFs and LAFs for each GO term.

Transcripts Expressed at Higher Levels in Cumulus Cells Versus MGCs

Transcripts with greatest fold differences. Table 2 and Supplemental Table S5 show the top 50 lists of transcripts expressed at higher levels in cumulus cells versus MGCs. Among the top 50 transcripts more highly expressed in cumulus cells versus MGCs, 23 are in common in SAF and LAF contrasts; those in the top 10 are particularly notable. They include two members of the FOS proto-oncogene family, *Fos* and *Fosb,* and two members of the JUN proto-oncogene family *Jun* and *Junb*. Members of these two families form heterodimers to produce the AP1 transcription factor complex, which has been associated with granulosa cell differentiation [45]. Also in these top 10 groups are *Klf4*, which has been implicated in stem cell-like capacity [46], and *Cyr61*, which encodes a protein that binds to various integrin receptors and to heparan sulfate proteoglycans involved in cell adhesion and signaling processes. Transcripts commonly expressed in the top 50 also include *Rhob*, a member of the Rho GTP-binding family, and *Arhgdig*, which affects the functioning of RHOB and, potentially, amplifies the actions of small G protein-signaling pathways. Also included in this group are *Shb*, which encodes an adapter protein that interacts with FGFR1 and is important for oocyte and follicular development [47]; *Smad7,* which encodes a member of TGFβ family and antagonizes the actions of the TGFβ type 1 receptor; *Dusp1,* which encodes a phosphatase that interacts with MAPK14, MAPK1, and MAPK8 (also known as p38, ERK2, and JNK1, respectively) that are well established to participate in a wide variety of signaling pathways in granulosa cells [48–56]; *Ank1,* which encodes a protein integral to the plasma membrane involved cell motility and the maintenance of specialized membrane domains; *Ednrb,* which encodes a G protein-coupled receptor of endothelin that is thought to have important roles in follicular development [57], including the induction of oocyte

TABLE 2. Top 50 fold difference higher in cumulus cells versus MGCs; gene names are presented in Supplemental Table S5.

Higher in SAF cumulus cells versus MGCs				Higher in LAF cumulus cells versus MGCs			
Fold difference	Gene symbol	Fold difference	Gene symbol	Fold difference	Gene symbol	Fold difference	Gene symbol
33.05	*Fosb**	2.85	*Dusp9**	28.25	*Fosb**	4.27	*Tex14*
14.32	*Jun**	2.84	*Arhgdig**	22.94	*Cyr61**	4.15	*Bmp6*
11.99	*Klf4**	2.83	*Nfkbiz*	14.79	*Aqp8**	4.12	*Zfp36**
9.71	*Ier2*	2.78	*Slc26a3**	14.39	*Egr1*	4.08	*Pfkp**
8.34	*Junb**	2.76	*Dntt*	11.42	*Junb**	4.07	*Mgp*
7.93	*Dusp1**	2.75	*Cnga1**	11.18	*Egr2**	4.06	*Rph3al*
7.62	*Cyr61**	2.75	*Calb1*	9.15	*Fos**	4.02	*Hps1*
6.05	*Fos**	2.75	*Loxl2*	7.59	*Arhgdig**	4.01	*Pdgfrb*
5.02	*Zfp36**	2.75	*Stat3*	6.96	*Jun**	4.00	*Dusp9**
4.63	*Btg2*	2.74	*Eftud1*	6.53	*Klf4**	3.99	*Slit3*
4.61	*Egr2**	2.74	*Plp1*	6.48	*Fbp1*	3.98	*Slc26a3**
4.06	*Rhob**	2.71	*Klf1**	5.87	*Klf1**	3.89	*Maff*
3.89	*Mt1*	2.68	*Aqp8**	5.75	*Dusp1**	3.88	*Cxcl1*
3.66	*Dnajb1*	2.68	*Id1*	5.63	*Smad7**	3.79	*Ablim1*
3.53	*Sik1*	2.67	*Smad7**	5.40	*Otof**	3.76	*Irx3*
3.36	*Ednrb**	2.63	*Pfkp**	5.22	*Shb**	3.74	*Slc38a3*
3.35	*Lnx1*	2.60	*Shb**	5.11	*Afap1l2*	3.71	*Abcc3*
3.15	*Runx1*	2.56	*Socs3*	4.92	*Gadd45b*	3.69	*Pdia2*
3.14	*Ucp2*	2.54	*Fgfbp3*	4.90	*Ank1**	3.68	*Cnga1**
3.05	*Btg1*	2.54	*Gadd45g*	4.49	*Rhob**	3.67	*Alpk3*
3.04	*Ank1**	2.53	*Chn2*	4.47	*Slc18a2*	3.64	*Apoa1*
3.02	*Malat1*	2.50	*Gatm*	4.46	*Nr4a1*	3.58	*Heyl**
3.00	*Klf2*	2.49	*Igfbp1*	4.34	*Angpt4*	3.56	*Rgcc*
2.92	*Otof**	2.49	*Cd83*	4.34	*Ednrb**	3.54	*Aicda*
2.90	*Elf3*	2.43	*Heyl**	4.27	*Vegfa*	3.54	*Trp53*

* Transcripts common to both SAFa and LAFs (N = 23).

maturation [58]; *Pfkp,* whose levels are known to be regulated by ODPFs and encodes an enzyme important for providing products of glycolysis to oocytes [20, 40]; *Slc26a3,* which encodes a member of the sulfate anion transporter family and mediates chloride and bicarbonate ion exchange, and *Cnga1,* which encodes a cyclic nucleotide gated ion channel; and *Heyl,* which encodes a transcription factor that mediates the action of NOTCH family receptors [59] involved in cell fate decisions and thought to participate in the regulation of granulosa cell proliferation [60, 61].

Vegfa is among the top 50 transcripts uniquely expressed more highly in cumulus cells versus MGCs of LAFs (Table 2 and Supplemental Table S5). This transcript encodes a member of the platelet-derived growth factor family of ligands thought to play a role in folliculogenesis [62, 63]. Suggestively, *Pdgfrb* is also included in the top 50 transcripts in this contrast, although no direct association of VEGFA and PDGFRB has yet been demonstrated. *Bmp6* transcripts are also higher in cumulus cells versus MGCs of LAFs as are *Trp53* transcripts encoding the tumor suppressor TRP53 (also known as p53).

Transcripts Expressed at Higher Levels in MGCs Versus Cumulus Cells

Transcripts with greatest fold differences. Some transcripts were expressed at higher levels in MGCs than in cumulus cells in both SAFs and LAFs. Among these on the top 50 lists, 11 were common to both size follicles (Table 3 and Supplemental Table S6) and encode steroidogenic hormone enzymes CYP11A1 (also known as P450 side chain cleavage enzyme) and CYP19A1 (also known as aromatase); the ligand CTGF; transcription factors and coregulators CITED2, NRIP1, and PBX1; apoptosis regulators GSN, STRADB, and TIA1; cell adhesion PCDH8; and receptor/ion channel GABRB2. NRIP1, also known as RIP140, is a nuclear receptor cofactor expressed by MGCs that regulates expression of amphiregulin and is necessary for normal cumulus expansion and ovulation [64]; its expression by cumulus cells is suppressed by oocytes [65].

Transcripts on the top 50 list of transcripts that are uniquely expressed higher in MGCs versus cumulus cells in SAFs (Table 3 and Supplemental Table S6) included those encoding receptors GHR and PLXNB1; ligands BMP2, INHBA, and NTN4; and cytoskeletal- and extracellular-related components ACTA2, COL3A1, FBN2, KRT20, MTAP2, SPNB2, and VIM.

The top 50 list of transcripts uniquely expressed higher in MGCs than cumulus cells in LAFs (Table 3 and Supplemental Table S6) include those encoding receptors LHCGR, PRLR, PTGFR, AHR, and EPHA5; ligands KITL and NPPC; cell adhesion/extracellular matrix-related molecules CD34, VCAM1, CCBE1, MATN2, LAMA4, and VCAN; and enzymes ADH1, CTSH, CYP17A1, ALDH1A1, and PRKAR2B. The ephrin receptor protein EPHA5 has been localized in MGCs by immunocytochemistry, regulated by FSH, and thought to participate in cell adhesion processes [66]. The transcript with the greatest differential between MGCs and cumulus cells in LAFs was *Comp*. It was previously suggested that *Comp* expression could be used as a marker of terminal follicular development because it was identified as the transcript most highly regulated by gonadotropin treatment in MGCs and during follicular development in vitro [67]. However, deletion of the *Comp* gene had no apparent effect on fertility, though quantitative data on fertility were not presented [68].

Role of ODPFs in the Differential Expression of Transcripts in Cumulus Cells and MGCs

These data reveal considerable differences in transcript levels in cumulus cells versus MGCs. Several factors could influence this differential expression: exposure to ODPFs, direct contact with oocytes and/or communication via gap

TABLE 3. Top 50 fold difference higher in MGCs versus cumulus cells; gene names are presented in Supplemental Table S6.

Higher in MGCs versus cumulus cells in SAFs				Higher in MGCs versus cumulus cells in LAFs			
Fold difference	Gene symbol	Fold difference	Gene symbol	Fold difference	Gene symbol	Fold difference	Gene symbol
7.23	*Vim*	3.70	*Gabrb2**	64.45	*Comp*	5.54	*Slc26a7*
7.21	*Plxnb1*	3.68	*Fabp3*	51.51	*Lhcgr*	5.43	*Ahr*
6.32	*Acta2*	3.68	*Krt20*	33.36	*Cyp11a1**	5.39	*Ccbe1*
6.25	*Gsn**	3.65	*Bmp2*	26.54	*Gabrb2**	5.22	*Fmnl2*
5.99	*Cald1*	3.65	*Ctgf**	19.74	*Cd34*	5.19	*Nrip1**
5.97	*Col11a1*	3.62	*Ctnna1*	16.45	*Cited2**	5.19	*Cyp19a1**
5.28	*Timp2*	3.61	*Gsta4*	15.14	*Gsn**	5.04	*Satb1*
4.90	*Tia1**	3.59	*Spnb2*	13.99	*Vcam1*	5.00	*Stradb**
4.89	*Tmsb4x*	3.56	*Etl4*	13.36	*Lrp11*	4.94	*Pappa*
4.76	*Col3a1*	3.54	*Rbm5*	13.06	*Prlr*	4.94	*Kcne2*
4.73	*Ntn4*	3.54	*Stk38*	10.06	*Adh1*	4.92	*Prkar2b*
4.73	*Nrip1**	3.47	*Cited2**	9.54	*Cyp17a1*	4.91	*Vcan*
4.71	*Stradb**	3.47	*Fbn2*	9.38	*Scara5*	4.86	*Nppc*
4.71	*Foxp1*	3.44	*F11r*	9.36	*Ctsh*	4.85	*Neb*
4.37	*Ghr*	3.44	*Mysm1*	9.34	*Ctgf**	4.82	*Hao2*
4.27	*Cyp11a1**	3.42	*Rgmb*	8.55	*Ptgfr*	4.80	*Matn2*
4.22	*Ctsf*	3.40	*Fbxl7*	7.75	*Olfm1*	4.68	*Epha5*
4.22	*Fhl1*	3.39	*Rala*	7.62	*Tnfsf11*	4.68	*Tia1**
3.99	*Cntf*	3.38	*Mtap2*	6.87	*Tulp2*	4.48	*Fosl2*
3.97	*Cyp19a1**	3.35	*Rab5b*	6.44	*Acsbg1*	4.36	*Pcdh8**
3.89	*Inhba*	3.35	*Pbx1**	6.36	*Kcnh2*	4.33	*Zeb2*
3.86	*Bcl9*	3.35	*Dzip1*	6.29	*Aldh1a1*	4.32	*Lama4*
3.85	*Col5a2*	3.34	*Itch*	6.11	*Socs2*	4.27	*Malat1*
3.80	*Hsd3b1*	3.32	*Fzd2*	5.79	*Kitl*	4.22	*Dpyd*
3.74	*Atxn10*	3.29	*Pcdh8**	5.64	*Pbx1**	4.21	*Hunk*

* Transcripts common to both SAFs and LAFs (N = 11).

junctions, interactions with basal lamina, different hormone or growth factor concentrations, or other factors influencing cellular microenvironments or physical conditions. Because of our prior findings on the importance of ODPFs, we used two approaches to test the role of ODPFs in promoting higher levels of transcripts in cumulus cells versus MGCs. The first experimental paradigm, an in vitro approach, compared the transcripts expressed at higher levels in cumulus cells freshly isolated from SAFs and LAFs with those elevated in cumulus cells by ODPFs in vitro as reported previously [34]. The second approach, an in vivo one, compared the higher cumulus cell transcripts with those expressed at lower levels in cumulus cells of *Gdf9*$^{+/-}$ *Bmp15*$^{-/-}$ double mutant (hereafter, DM) cumulus cells compared to WT cumulus cells in vivo as reported previously [19].

For the in vitro analysis of the role of ODPFs on differential transcript expression, oocytes were microsurgically removed from COCs isolated from eCG-stimulated ovaries and cultured for 20 h without or with coculture with two oocytes/μl of medium. After removal of the oocytes, the cumulus cells are referred to as OOX cumulus cells. We reported effects of ODPFs on the transcriptome of OOX cumulus cells previously [34], and the Jackson Laboratory Gene Expression Service carried out all the sample preparation and microarray protocols. The same boundaries for significance established for the present study, $Q < 0.05$ and fold change > 1.25, were applied to all data sets. Transcripts whose steady state levels were elevated by ODPFs in OOX cumulus cells were compared to the transcripts differentially expressed by freshly isolated cumulus cells and MGCs. Those transcripts expressed significantly more highly in freshly isolated cumulus cells versus MGCs and those whose expression was stimulated in OOX cumulus cells by oocytes in vitro are probably expressed at higher levels in cumulus cells because of exposure to ODPFs in situ.

All the transcripts with annotation of biological function expressed at higher levels in cumulus cells than MGCs, from both SAFs and LAFs, were compared with those increased by oocytes in OOX cumulus cells. In total, 1099 transcripts were higher in freshly isolated cumulus cells and were also stimulated by ODPFs in OOX-cumulus cells. Unexpectedly, 1660 transcripts that were higher in the freshly isolated cumulus cells compared with MGCs were not significantly stimulated by ODPFs in vitro.

To further test the surprising result that many cumulus transcripts expressed at higher levels than MGCs are not stimulated by ODPFs, we used an in vivo model. In a previous study [19], we assessed the transcriptomes of cumulus cells in *Gdf9*$^{+/-}$ *Bmp15*$^{-/-}$ DM ovaries, wherein the oocytes are deficient in the production of ODPFs GDF9 and BMP15 compared to WT cumulus cells. Cumulus expansion is defective in the COCs of these mutant mice, and the defective expansion was not remedied by coculture with WT oocytes, indicating that differentiation of the cumulus cells during follicular development requires these ODPFs [35]. Here we compared the transcripts with significantly lower expression by the DM cumulus cells versus WT cumulus cells with the cohort of transcripts found in the present study to be expressed at levels significantly higher in cumulus cells versus MGCs. Lower expression is the consequence of deficiencies in ODPFs GDF9 and BMP15 throughout follicular development. Thus, this experimental paradigm tests the effects of chronic ODPF deficiency on the cumulus cell transcriptome in vivo in contrast to the model testing the acute effects of ODPFs on normal OOX cumulus cells in vitro. As in the in vitro experiment, the cumulus cell transcripts expressed higher than in MGCs from both SAFs and LAFs were pooled for comparison to the transcripts reduced in the DM cumulus cells. A total of 843 transcripts expressed lower in DM cumulus cells were also expressed higher in normal cumulus cells versus MGCs. Moreover, 1916 were expressed at higher levels in the normal cumulus cells versus MGCs but were unchanged in the DM cumulus cells versus WT. Of the 843 transcripts that were lower in DM cumulus cells, 487 were the same as those

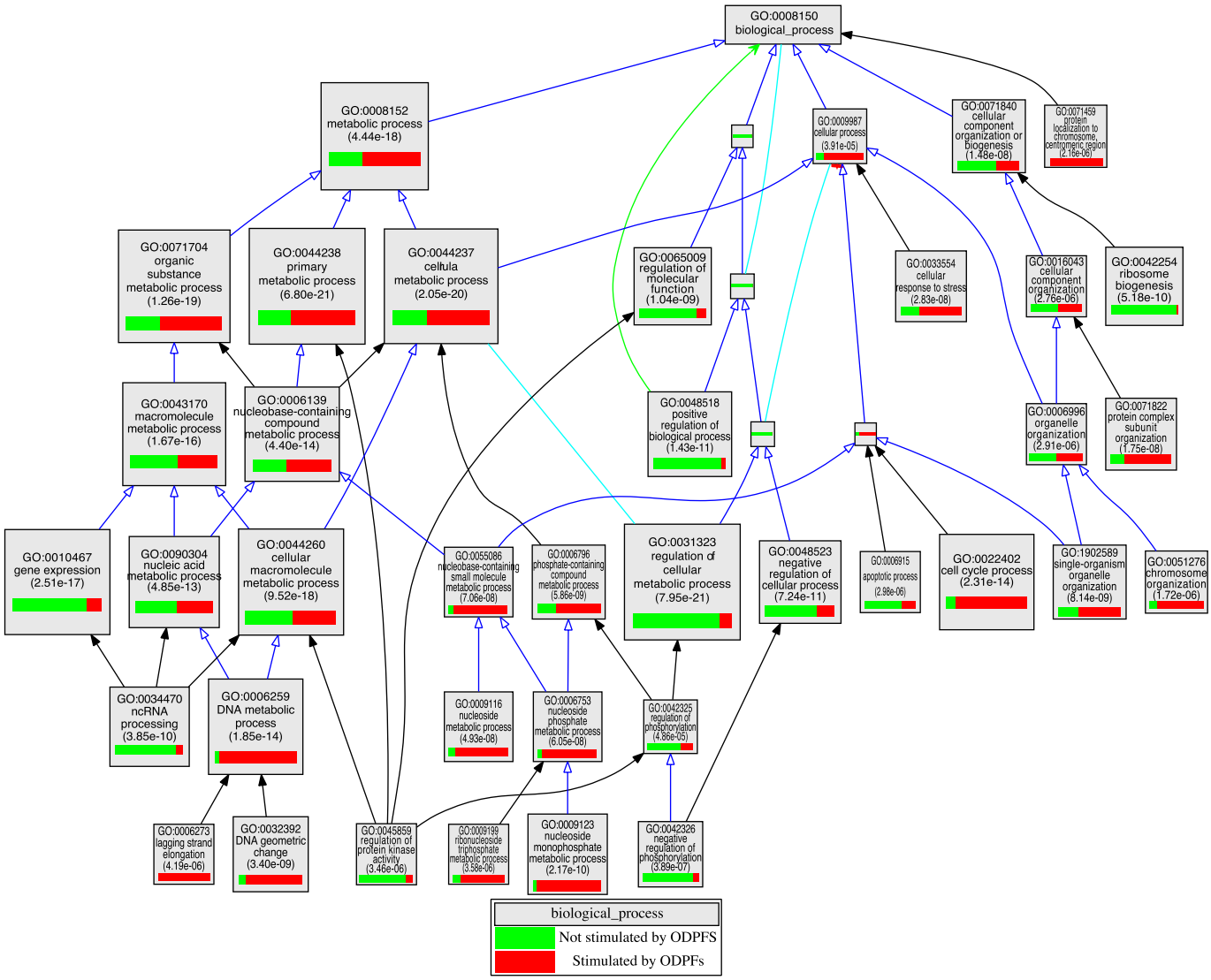

FIG. 7. VLAD depiction of GO terms in the contrast of consensus transcripts higher in cumulus cells than MGCs stimulated by ODPFs or not. The top 25 GO terms, selected by VLAD on the basis of local maximum *P* value, are shown. The size of the rectangle is proportional to the *P* value; the larger the rectangle the lower, and more significant, is the *P* value. The green portion of the rectangle shows the relative contribution of cumulus cell transcripts not stimulated by ODPFs to that GO term while the red portion shows the relative contribution of transcripts stimulated by ODPFs. Supplemental Table S8 presents complete list of transcripts expressed differently in SAFs and LAFs for each GO term.

stimulated by ODPFs in OOX cumulus cells in vitro. Thus, these 487 transcripts can be considered consensus transcripts whose expression in cumulus cells is stimulated by ODPFs (Supplemental Table S7). Importantly, of the 1916 transcripts that were lower in the DM relative to WT cumulus cells, 1301 were in common with the cohort of transcripts not stimulated by ODPFs in vitro (Supplemental Table S7). Thus, these can be considered consensus transcripts that are expressed more highly in normal cumulus cells, but the higher levels of expression is not due to stimulation by ODPFs.

The GO terms associated with consensus ODPF-stimulated versus not stimulated are compared in Figure 7 and Supplemental Table S8. By definition, these transcripts are all more highly expressed in fresh cumulus cells than in MGCs. Analysis of the GO terms associated with the consensus transcripts for ODPF-stimulated or ODPF not stimulated processes was similar to that found for transcripts defined by either the in vitro or in vivo protocols, which are not shown. Transcripts that were higher in freshly isolated cumulus cells and consensus ODPF-stimulated cumulus cells included those enriched in biological function GO terms associated with catalytic processes in small metabolic processes, including glycolysis (GO:0006096, e.g., *Pfkp*) and cholesterol biosynthesis (GO:0008208, e.g., *Mvk*) as described previously [19, 20, 40]. Transcripts encoding molecules involved in other metabolic pathways such as GO:0009123 (nucleoside monophosphate metabolic process) were also promoted by consensus ODFPs. Previous studies have demonstrated that oocytes promote the proliferation of granulosa cells [69–71]. Transcripts associated with cell proliferation GO terms such as GO:0022402 (cell cycle process) and GO:0006259 (DNA metabolic process) are therefore not surprisingly found in the consensus ODPF-regulated group. The transcripts encoding receptors EDNRA, EDNRB, EGFR, and ESR1 as well as ligands IGF1, VEGFA, and VEGFB are also among those that are more highly expressed by both cumulus cells in situ and stimulated by ODPFs in OOX cumulus cells.

Notable among the consensus transcripts expressed at levels higher in cumulus cells than MGCs but not promoted by ODPFs were the proto-oncogenes *Fosb, Jun,* and *Junb*. In addition to these components of the AP1 transcription complex, *Ap1b1* and *Ap1g1,* encoding AP1 complex adaptor proteins, are in the group of consensus transcripts expressed higher in cumulus cells than MGCs but not regulated by ODPFs. Transcripts also apparently not regulated by ODPFs were apoptosis-regulating factors *Bad*, the transcription factor involved in follicular development *Foxo3*, all of the early growth response genes (*Egr1/2/3*), the ligands *Efna1, Gh, Ghrl, Shh, Tgfa, Pdgfa,* and *Wnt4*, and transcripts encoding receptors *Acvr2b, Adra2c, Fgfr1, Igf1r, Ntrk3,* and *Pdgfra*. In general, GO terms enriched with transcripts not controlled by ODPFs include those that encode regulators of biological processes while those controlled by ODPFs encode proteins involved in cell division and catalytic metabolic pathways (Fig. 7 and Supplemental Table S8).

DISCUSSION

This study has delineated, at a global level, major transcriptomic dynamics that underlie the structural and functional architecture of the ovarian follicle. The analysis has revealed not only transcriptomic complexity, but also unanticipated regulatory differences that control cumulus cell diversification, development, and function. Scrutiny of gene lists and GO terms has revealed functions in cumulus cells and MGCs not previously fully appreciated. For example, although cumulus cells of both stages of follicular development are competent to undergo expansion in vitro, they were otherwise remarkably dissimilar with transcriptomic changes quantitatively equivalent to those of MGCs. GO analysis revealed that cumulus cells of small follicles were enriched in transcripts generally associated with catalytic components of metabolic processes, while those from large follicles were involved in regulation of metabolism, cell differentiation, and adhesion. Contrast of cumulus cells versus MGCs revealed that cumulus cells were enriched in transcripts associated with metabolism and cell proliferation while MGCs were enriched for transcripts involved in cell signaling and differentiation. Together, these findings validate that global systems approaches, such as that taken here, can provide a richness of information that complements other more focused (biased) approaches.

Oocytes are required for the progression of preantral (secondary) follicles to the early antral (tertiary) follicle stage [15]. This pivotal transition in folliculogenesis propels the structural and functional divergence of the cumulus cell and MGC lineages. Although it is well established that gonadotropins drive the development of SAFs to LAFs and promote the expression of genes key to steroidogenesis and the ability to respond to LH by MGCs, an analysis of the developmental changes in gene expression in the cumulus and MGC somatic compartments before the LH-surge (or hCG-treatment) has been lacking. Such information is essential to define the transcriptomic foundation of the cellular and functional architecture of the follicle and to determine how differential gene expression relates to the fates of both the somatic and oocyte compartments.

The cumulus cells of SAFs are competent to undergo expansion in vitro in a manner that appears similar to that of cumulus cells retrieved from LAFs isolated from follicles before the preovulatory LH surge ([17] and results presented here [Supplemental Fig. S3]). Despite this similarity, this study has shown that transcripts of cumulus cells from SAFs are actually quite different than those in cumulus cells from LAFs. In fact, the transcriptome changes in cumulus cells during the SAF to LAF development is qualitatively and quantitatively as significant as the transcriptomic transformation of the MGC population during the same follicular developmental span. Previous studies demonstrated that cumulus cells provide small nutritional and regulatory molecules to the oocyte via the gap junctions that couple the metabolism of these cells. In fact, oocytes, via ODPFs, promote pathways in cumulus cells, such as the glycolytic and cholesterol-generating pathways, in which the oocytes themselves are deficient [19, 40]. Moreover, previous studies have shown that ODPFs promote cumulus cell division [69–71]. A general emerging theme is that the cumulus cell transcriptome is enriched in the transcripts of workhorse molecules that drive both metabolism and cell division. As shown here, as the cumulus cells develop, they also become enriched in transcripts that regulate metabolic and developmental pathways. Curiously, however, most of the regulatory transcripts appear controlled by factors other than ODPFs, although the catalytic pathways themselves are often driven by ODPFs. Moreover, it is not yet clear how, or if, these transcriptomic changes in the cumulus cells relate to the qualitative changes in oocytes during the SAF to LAF developmental transition, when they increase their embryonic developmental competence [72].

Follicular microenvironments are influential in defining the functional diversity of the granulosa cell compartments. As shown both here and in other studies that focused on the expression patterns of individual transcripts or pathways [73], cumulus cells and MGCs differ in their patterns of gene expression and these patterns change during the SAF to LAF transition. What determines these lineage diversifications? ODPFs diffusing from the oocyte are a major influence in establishing the cumulus cell lineage [13]. It has been suggested that factors in apposition to the influence of ODPFs, such as FSH, diffuse from outside of the follicle to establish the reversed gradients in levels of several transcripts, for example, for *Lhcgr* versus *Pfkp*. *Lhcgr* is expressed at highest levels near the follicular-basal lamina [22, 74] while *Pfkp* is expressed at highest levels near the oocyte [20]. ODPFs suppressed expression of *Lhcgr* by granulosa cells that was stimulated by both FSH and contact with basal lamina [24], suggesting that ODPFs are the most influential factors in lineage determination. In fact, evidence suggests that ODPFs orchestrate the rate of follicular development [75], probably by promoting essential metabolic pathways and cell division.

We hypothesized that the higher levels of expression of most transcripts expressed higher in cumulus cells are promoted by ODPFs. There were 2759 total transcripts expressed more highly by cumulus cells than MGCs of SAFs and LAFs together. Using data from both the in vitro and in vivo models used to test this hypothesis, a total of 52% (1455) of the transcripts depend upon ODPFs; 39% (843) were acutely stimulated using the in vitro model. Thus, there is a remarkable reliance on ODPFs to promote in cumulus cells higher levels of transcripts that are involved in cell division or catalytic metabolic pathways. Nevertheless, 48% of the transcripts that were higher in cumulus cells were apparently not stimulated by ODPFs. This unanticipated result indicates that factors other than ODPFs are also major determinants of transcriptomic diversity of cumulus cells and MGCs.

Discovering the mechanisms for apparent ODPF-independent elevated expression of some transcripts in cumulus cells versus MGCs is a future challenge. It is possible that oocytes stimulate expression by the cumulus cells via mechanism requiring direct contact rather than ODPFs. However, no differences were detected in the transcriptomes of cumulus

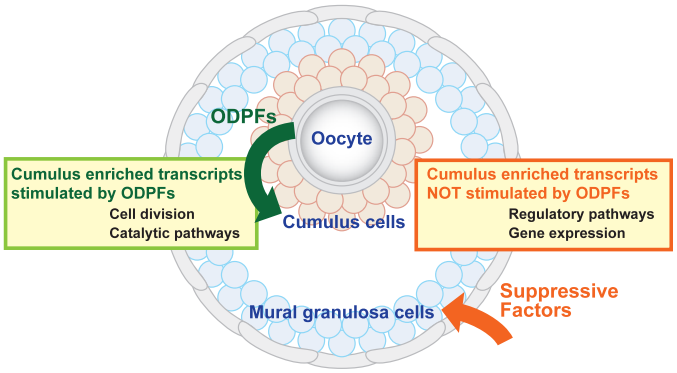

FIG. 8. Working model depicting possible mechanisms regulating the expression of two groups of transcripts enriched in cumulus cells relative to MGCs. These groups of transcripts affect the diversity in functions of these cell types. Both groups are expressed at higher levels in cumulus cells than in MGCs. One group of transcripts is elevated in cumulus by oocyte-derived paracrine factors (ODPFs) and the other is not. The group whose expression is stimulated by ODPFs includes, among others, transcripts enriched in the GO terms associated with cell division and catalytic enzymes of metabolic pathways. The transcripts not affected by ODPFs include, among others, transcripts enriched in the GO terms associated with the regulation of these pathways and various aspects of gene expression (see Fig. 7 and Supplemental Table S8). The transcripts unaffected by ODPFs may be expressed at higher levels in cumulus cells than MGCs because expression is suppressed in the MGCs.

cells cultured either as intact oocyte-cumulus cell complexes or OOX cumulus cells cocultured with denuded oocytes. This suggests that oocytes do not affect the cumulus cell transcriptome via juxtacrine or gap junction-mediated communication, at least under the culture conditions used in that study [34]. In the in vitro experimental approach, the action of ODPFs was determined by coculturing OOX cumulus cells with denuded fully grown oocytes. Thus, the ODPFs contained the natural cocktail of factors released by oocytes in vitro and not arbitrarily selected recombinant ODPFs used individually or in combination. This protocol has been used in several previous studies to demonstrate the ability of ODPFs to promote or suppress several transcripts in cumulus cells [13, 19, 24, 34]. It is possible that expression of some cumulus cell transcripts require that ODPFs act in concert with paracrine factors produced within the follicle or endocrine factors, such as FSH or estrogens.

What, if not ODPFs, results in the higher levels of these transcripts in cumulus cells? Clearly, this should be an objective of future studies, but our working hypothesis is presented in Figure 8. Although intrinsic developmental programs cannot be excluded, the relative level of transcript expression in cumulus cells versus MGCs is probably the net result of stimulation by ODPFs in cumulus cells, suppression in MGCs, or both. FSH suppresses levels of *Ar* and *Slc38a3* mRNAs in isolated COCs wherein ODPFs stimulated expression, thus imparting some MGCs-like phenotypic characteristics to cumulus cells [13]. Therefore, FSH could be a key factor in establishing or maintaining the diversity of granulosa cell lineages and is certainly needed, as well as ODPFs, for driving follicular development. Because FSH enters by diffusion from outside the follicle, and much of it is probably bound to FSH receptors abundant on MGCs [76], the concentration of FSH probably decreases with increasing depth into the follicle, minimizing the exposure of cumulus cells to FSH in vivo. Moreover, the follicular basal lamina, contacted by most MGCs [77], augments some actions of FSH [22, 24]. Thus, the combination of FSH and basal lamina could function to decrease the levels of expression of some transcripts in MGCs relative to cumulus cells, which would account for the transcriptomic diversity observed here. Other factors present in the granulosa cell microenvironments—estrogens and growth factors, for example—probably also participate in the architecture of transcriptomic diversity of cumulus cells and MGCs fundamental to cellular function and coordination during follicular development.

ACKNOWLEDGMENT

We are grateful to Tim Stearns of the Jackson Laboratory Computational Sciences Service for statistical analyses of microarray data and for spearheading the Gene Expression Omnibus submission of the data, to Chrystal Snow of The Jackson Laboratory Gene Expression Service for sample preparation and running the microarrays, and to Joel Richardson of the Mouse Genome Informatics Program for heroic assistance in the use of VLAD and for allowing us to have a small part in its evolution. We also thank Dr. Mary Ann Handel for her comments during the preparation of this manuscript

REFERENCES

1. Park JY, Su YQ, Ariga M, Law E, Jin SL, Conti M. EGF-like growth factors as mediators of LH action in the ovulatory follicle. Science 2004; 303:682–684.
2. Shimada M, Hernandez-Gonzalez I, Gonzalez-Robayna I, Richards JS. Paracrine and autocrine regulation of epidermal growth factor-like factors in cumulus oocyte complexes and granulosa cells: key roles for prostaglandin synthase 2 and progesterone receptor. Mol Endocrinol 2006; 20:1352–1365.
3. Zhang M, Su YQ, Sugiura K, Xia G, Eppig JJ. Granulosa cell ligand NPPC and its receptor NPR2 maintain meiotic arrest in mouse oocytes. Science 2010; 330:366–369.
4. Dekel N, Hillensjo T, Kraicer PF. Maturational effects of gonadotropins on the cumulus-oocyte complex of the rat. Biol Reprod 1979; 20:191–197.
5. Chen L, Russell PT, Larsen WJ. Functional significance of cumulus expansion in the mouse: roles for the preovulatory synthesis of hyaluronic acid within the cumulus mass. Mol Reprod Dev 1993; 34:87–93.
6. Salustri A, Yanagishita M, Hascall VC. Synthesis and accumulation of hyaluronic acid and proteoglycans in the mouse cumulus cell-oocyte complex during follicle-stimulating hormone-induced mucification. J Biol Chem 1989; 264:13840–13847.
7. Anderson E, Albertini DF. Gap junctions between the oocyte and companion follicle cells in the mammalian ovary. J Cell Biol 1976; 71: 680–686.
8. Gilula NB, Epstein ML, Beers WH. Cell-to-cell communication and ovulation. A study of the cumulus-oocyte complex. J Cell Biol 1978; 78: 58–75.
9. Schultz RM. Roles of cell-to-cell communication in development. Biol Reprod 1985; 32:27–42.
10. Albertini DF, Barrett SL. Oocyte-somatic cell communication. Reproduction 2002; 49–54.
11. Norris RP, Ratzan WJ, Freudzon M, Mehlmann LM, Krall J, Movsesian MA, Wang H, Ke H, Nikolaev VO, Jaffe LA. Cyclic GMP from the surrounding somatic cells regulates cyclic AMP and meiosis in the mouse oocyte. Development 2009; 136:1869–1878.
12. Anderson E, Wilkinson RF, Lee G, Meller S. A correlative microscopical analysis of differentiating ovarian follicles of mammals. J Morph 1978; 156:339–366.
13. Diaz FJ, Wigglesworth K, Eppig JJ. Oocytes determine cumulus cell lineage in mouse ovarian follicles. J Cell Sci 2007; 120:1330–1340.
14. Zhang M, Su YQ, Sugiura K, Wigglesworth K, Xia G, Eppig JJ. Estradiol promotes and maintains cumulus cell expression of natriuretic peptide receptor 2 (NPR2) and meiotic arrest in mouse oocytes in vitro. Endocrinology 2011; 152:4377–4385.
15. Diaz FJ, Wigglesworth K, Eppig JJ. Oocytes are required for the preantral granulosa cell to cumulus cell transition in mice. Dev Biol 2007; 305: 300–311.
16. Eppig JJ, Wigglesworth K, Chesnel F. Secretion of cumulus expansion enabling factor by mouse oocytes: relationship to oocyte growth and competence to resume meiosis. Dev Biol 1993; 158:400–409.
17. Vanderhyden BC, Caron PJ, Buccione R, Eppig JJ. Developmental pattern of the secretion of cumulus-expansion enabling factor by mouse oocytes

and the role of oocytes in promoting granulosa cell differentiation. Dev Biol 1990; 140:307–317.
18. Eppig JJ, Pendola FL, Wigglesworth K, Pendola JK. Mouse oocytes regulate metabolic cooperativity between granulosa cells and oocytes: amino acid transport. Biol Reprod 2005; 73:351–357.
19. Su YQ, Sugiura K, Wigglesworth K, O'Brien MJ, Affourtit JP, Pangas SA, Matzuk MM, Eppig JJ. Oocyte regulation of metabolic cooperativity between mouse cumulus cells and oocytes: BMP15 and GDF9 control cholesterol biosynthesis in cumulus cells. Development 2008; 135: 111–121.
20. Sugiura K, Pendola FL, Eppig JJ. Oocyte control of metabolic cooperativity between oocytes and companion granulosa cells: energy metabolism. Dev Biol 2005; 279:20–30.
21. Richards JS. Perspective: the ovarian follicle—a perspective in 2001. Endocrinology 2001; 142:2184–2193.
22. Furman A, Rotmensch S, Kohen F, Mashiach S, Amsterdam A. Regulation of rat granulosa cell differentiation by extracellular matrix produced by bovine corneal endothelial cells. Endocrinology 1986; 118: 1878–1885.
23. Huet C, Pisselet C, Mandon-Pepin B, Monget P, Monniaux D. Extracellular matrix regulates ovine granulosa cell survival, proliferation and steroidogenesis: relationships between cell shape and function. J Endocrinol 2001; 169:347–360.
24. Eppig JJ, Wigglesworth K, Pendola F, Hirao Y. Murine oocytes suppress expression of luteinizing hormone receptor messenger ribonucleic acid by granulosa cells. Biol Reprod 1997; 56:976–984.
25. Peng J, Li Q, Wigglesworth K, Rangarajan A, Kattamuri C, Peterson RT, Eppig JJ, Thompson TB, Matzuk MM. Growth differentiation factor 9: bone morphogenetic protein 15 heterodimers are potent regulators of ovarian functions. Proc Natl Acad Sci U S A 2013; 110:E776–E785.
26. Fulop C, Szanto S, Mukhopadhyay D, Bardos T, Kamath RV, Rugg MS, Day AJ, Salustri A, Hascall VC, Glant TT, Mikecz K. Impaired cumulus mucification and female sterility in tumor necrosis factor-induced protein-6 deficient mice. Development 2003; 130:2253–2261.
27. Ochsner SA, Day AJ, Rugg MS, Breyer RM, Gomer RH, Richards JS. Disrupted function of tumor necrosis factor-alpha-stimulated gene 6 blocks cumulus cell-oocyte complex expansion. Endocrinology 2003; 144: 4376–4384.
28. Ochsner SA, Russell DL, Day AJ, Breyer RM, Richards JS. Decreased expression of tumor necrosis factor-alpha-stimulated gene 6 in cumulus cells of the cyclooxygenase-2 and EP2 null mice. Endocrinology 2003; 144:1008–1019.
29. Varani S, Elvin JA, Yan C, DeMayo J, DeMayo FJ, Horton HF, Byrne MC, Matzuk MM. Knockout of pentraxin 3, a downstream target of growth differentiation factor-9, causes female subfertility. Mol Endocrinol 2002; 16:1154–1167.
30. Hernandez-Gonzalez I, Gonzalez-Robayna I, Shimada M, Wayne CM, Ochsner SA, White L, Richards JS. Gene expression profiles of cumulus cell oocyte complexes during ovulation reveal cumulus cells express neuronal and immune-related genes: does this expand their role in the ovulation process? Mol Endocrinol 2006; 20:1300–1321.
31. Shimada M, Hernandez-Gonzalez I, Gonzalez-Robanya I, Richards JS. Induced expression of pattern recognition receptors in cumulus oocyte complexes: novel evidence for innate immune-like functions during ovulation. Mol Endocrinol 2006; 20:3228–3239.
32. Xu F, Stouffer RL, Muller J, Hennebold JD, Wright JW, Bahar A, Leder G, Peters M, Thorne M, Sims M, Wintermantel T, Lindenthal B. Dynamics of the transcriptome in the primate ovulatory follicle. Mol Hum Reprod 2011; 17:152–165.
33. Ouandaogo ZG, Frydman N, Hesters L, Assou S, Haouzi D, Dechaud H, Frydman R, Hamamah S. Differences in transcriptomic profiles of human cumulus cells isolated from oocytes at GV, MI and MII stages after in vivo and in vitro oocyte maturation. Hum Reprod 2012; 27:2438–2447.
34. Emori C, Wigglesworth K, Fujii W, Naito K, Eppig JJ, Sugiura K. Cooperative effects of 17beta-estradiol and oocyte-derived paracrine factors on the transcriptome of mouse cumulus cells. Endocrinology 2013; 154:4859–4871.
35. Su YQ, Wu X, O'Brien MJ, Pendola FL, Denegre JN, Matzuk MM, Eppig JJ. Synergistic roles of BMP15 and GDF9 in the development and function of the oocyte-cumulus cell complex in mice: genetic evidence for an oocyte-granulosa cell regulatory loop. Dev Biol 2004; 276:64–73.
36. Dai M, Wang P, Boyd AD, Kostov G, Athey B, Jones EG, Bunney WE, Myers RM, Speed TP, Akil H, Watson SJ, Meng F. Evolving gene/transcript definitions significantly alter the interpretation of GeneChip data. Nucleic Acids Res 2005; 33:e175.
37. Wu H, Kerr MK, Cui XQ, Churchill GA. MAANOVA; A Software Package for the Analysis of Spotted cDNA Microarray Experiments in the Analysis of Gene Expression Data. An Overview of Methods and Software: Methods and Software. New York: Springer; 2003.
38. Cui X, Hwang JT, Qiu J, Blades NJ, Churchill GA. Improved statistical tests for differential gene expression by shrinking variance components estimates. Biostatistics 2005; 6:59–75.
39. Storey JD, Tibshirana R. Statistical significance for genomewide studies. Proc Natl Acad Sci USA 2003; 100:9440–9445.
40. Sugiura K, Su YQ, Diaz FJ, Pangas SA, Sharma S, Wigglesworth K, O'Brien MJ, Matzuk MM, Shimasaki S, Eppig JJ. Oocyte-derived BMP15 and FGFs cooperate to promote glycolysis in cumulus cells. Development 2007; 134:2593–2603.
41. Sugiura K, Su YQ, Li Q, Wigglesworth K, Matzuk MM, Eppig JJ. Fibroblast growth factors and epidermal growth factor cooperate with oocyte-derived members of the TGFbeta superfamily to regulate Spry2 mRNA levels in mouse cumulus cells. Biol Reprod 2009; 81:833–841.
42. Sugiura K, Su YQ, Eppig JJ. Does bone morphogenetic protein 6 (BMP6) affect female fertility in the mouse? Biol Reprod 2010; 83:997–1004.
43. Hogg K, Etherington SL, Young JM, McNeilly AS, Duncan WC. Inhibitor of differentiation (Id) genes are expressed in the steroidogenic cells of the ovine ovary and are differentially regulated by members of the transforming growth factor-beta family. Endocrinology 2010; 151: 1247–1256.
44. Verbraak EJ, van 't Veld EM, Groot Koerkamp M, Roelen BA, van Haeften T, Stoorvogel W, Zijlstra C. Identification of genes targeted by FSH and oocytes in porcine granulosa cells. Theriogenology 2011; 75: 362–376.
45. Sharma SC, Richards JS. Regulation of AP1 (Jun/Fos) factor expression and activation in ovarian granulosa cells. Relation of JunD and Fra2 to terminal differentiation. J Biol Chem 2000; 275:33718–33728.
46. Meissner A, Wernig M, Jaenisch R. Direct reprogramming of genetically unmodified fibroblasts into pluripotent stem cells. Nat Biotechnol 2007; 25:1177–1181.
47. Calounova G, Livera G, Zhang XQ, Liu K, Gosden RG, Welsh M. The Src homology 2 domain-containing adapter protein B (SHB) regulates mouse oocyte maturation. PLoS One 2010; 5:e11155.
48. Maizels ET, Cottom J, Jones JC, Hunzicker-Dunn M. Follicle stimulating hormone (FSH) activates the p38 mitogen-activated protein kinase pathway, inducing small heat shock protein phosphorylation and cell rounding in immature rat ovarian granulosa cells. Endocrinology 1998; 139:3353–3356.
49. Su YQ, Wigglesworth K, Pendola FL, O'Brien MJ, Eppig JJ. Mitogen-activated protein kinase activity in cumulus cells is essential for gonadotropin-induced oocyte meiotic resumption and cumulus expansion in the mouse. Endocrinology 2002; 143:2221–2232.
50. Su YQ, Denegre JM, Wigglesworth K, Pendola FL, O'Brien MJ, Eppig JJ. Oocyte-dependent activation of mitogen-activated protein kinase (ERK1/2) in cumulus cells is required for the maturation of the mouse oocyte-cumulus cell complex. Dev Biol 2003; 263:126–138.
51. Sela-Abramovich S, Chorev E, Galiani D, Dekel N. Mitogen-activated protein kinase mediates luteinizing hormone-induced breakdown of communication and oocyte maturation in rat ovarian follicles. Endocrinology 2005; 146:1236–1244.
52. Hunzicker-Dunn M, Maizels ET. FSH signaling pathways in immature granulosa cells that regulate target gene expression: branching out from protein kinase A. Cell Signal 2006; 18:1351–1359.
53. Diaz FJ, O'Brien MJ, Wigglesworth K, Eppig JJ. The preantral granulosa cell to cumulus cell transition in the mouse ovary: development of competence to undergo expansion. Dev Biol 2006; 299:91–104.
54. Miyoshi T, Otsuka F, Inagaki K, Otani H, Takeda M, Suzuki J, Goto J, Ogura T, Makino H. Differential regulation of steroidogenesis by bone morphogenetic proteins in granulosa cells: involvement of extracellularly regulated kinase signaling and oocyte actions in follicle-stimulating hormone-induced estrogen production. Endocrinology 2007; 148: 337–345.
55. Sriraman V, Modi SR, Bodenburg Y, Denner LA, Urban RJ. Identification of ERK and JNK as signaling mediators on protein kinase C activation in cultured granulosa cells. Mol Cell Endocrinol 2008; 294:52–60.
56. Liu Z, Fan HY, Wang Y, Richards JS. Targeted disruption of Mapk14 (p38MAPKalpha) in granulosa cells and cumulus cells causes cell-specific changes in gene expression profiles that rescue COC expansion and maintain fertility. Mol Endocrinol 2010; 24:1794–1804.
57. Cho J, Kim H, Kang DW, Yanagisawa M, Ko C. Endothelin B receptor is not required but necessary for finite regulation of ovulation. Life Sci 2012; 91:613–617.
58. Kawamura K, Ye Y, Liang CG, Kawamura N, Gelpke MS, Rauch R, Tanaka T, Hsueh AJ. Paracrine regulation of the resumption of oocyte meiosis by endothelin-1. Dev Biol 2009; 327:62–70.

59. Lavery DN, Villaronga MA, Walker MM, Patel A, Belandia B, Bevan CL. Repression of androgen receptor activity by HEYL, a third member of the Hairy/Enhancer-of-split-related family of Notch effectors. J Biol Chem 2011; 286:17796–17808.
60. Johnson J, Espinoza T, McGaughey RW, Rawls A, Wilson-Rawls J. Notch pathway genes are expressed in mammalian ovarian follicles. Mech Dev 2001; 109:355–361.
61. Zhang CP, Yang JL, Zhang J, Li L, Huang L, Ji SY, Hu ZY, Gao F, Liu YX. Notch signaling is involved in ovarian follicle development by regulating granulosa cell proliferation. Endocrinology 2011; 152: 2437–2447.
62. Artac RA, McFee RM, Smith RA, Baltes-Breitwisch MM, Clopton DT, Cupp AS. Neutralization of vascular endothelial growth factor antiangiogenic isoforms is more effective than treatment with proangiogenic isoforms in stimulating vascular development and follicle progression in the perinatal rat ovary. Biol Reprod 2009; 81:978–988.
63. Qiu Y, Seager M, Osman A, Castle-Miller J, Bevan H, Tortonese DJ, Murphy D, Harper SJ, Fraser HM, Donaldson LF, Bates DO. Ovarian VEGF(165)b expression regulates follicular development, corpus luteum function and fertility. Reproduction 2012; 143:501–511.
64. Nautiyal J, Steel JH, Rosell MM, Nikolopoulou E, Lee K, Demayo FJ, White R, Richards JS, Parker MG. The nuclear receptor cofactor receptor-interacting protein 140 is a positive regulator of amphiregulin expression and cumulus cell-oocyte complex expansion in the mouse ovary. Endocrinology 2010; 151:2923–2932.
65. Sugiura K, Su YQ, Li Q, Wigglesworth K, Matzuk MM, Eppig JJ. Estrogen promotes the development of mouse cumulus cells in coordination with oocyte-derived GDF9 and BMP15. Mol Endocrinol 2010; 24:2303–2314.
66. Buensuceso AV, Deroo BJ. The ephrin signaling pathway regulates morphology and adhesion of mouse granulosa cells in vitro. Biol Reprod 2013; 88:25.
67. Skory RM, Bernabe BP, Galdones E, Broadbelt LJ, Shea LD, Woodruff TK. Microarray analysis identifies COMP as the most differentially regulated transcript throughout in vitro follicle growth. Mol Reprod Dev 2013; 80:132–144.
68. Svensson L, Aszodi A, Heinegard D, Hunziker EB, Reinholt FP, Fassler R, Oldberg A. Cartilage oligomeric matrix protein-deficient mice have normal skeletal development. Mol Cell Biol 2002; 22:4366–4371.
69. Vanderhyden BC, Telfer EE, Eppig JJ. Mouse oocytes promote proliferation of granulosa cells from preantral and antral follicles in vitro. Biol Reprod 1992; 46:1196–1204.
70. Gilchrist RB, Ritter LJ, Armstrong DG. Mouse oocyte mitogenic activity is developmentally coordinated throughout folliculogenesis and meiotic maturation. Dev Biol 2001; 240:289–298.
71. Hickey TE, Marrocco DL, Amato F, Ritter LJ, Norman RJ, Gilchrist RB, Armstrong DT. Androgens augment the mitogenic effects of oocyte-secreted factors and growth differentiation factor 9 on porcine granulosa cells. Biol Reprod 2005; 73:825–832.
72. Pan H, O'Brien MJ, Wigglesworth K, Eppig JJ, Schultz RM. Transcript profiling during mouse oocyte development and the effect of gonadotropin priming and development in vitro. Dev Biol 2005; 286:493–506.
73. Su YQ, Sugiura K, Eppig JJ. Mouse oocyte control of granulosa cell development and function: paracrine regulation of cumulus cell metabolism. Semin Reprod Med 2009; 27:32–42.
74. Amsterdam A, Koch Y, Lieberman ME, Lindner HR. Distribution of binding sites for human chorionic gonadotropin in the preovulatory follicle of the rat. J Cell Biol 1975; 67:894–900.
75. Eppig JJ, Wigglesworth K, Pendola FL. The mammalian oocyte orchestrates the rate of ovarian follicular development. Proc Natl Acad Sci U S A 2002; 99:2890–2894.
76. Richards JS, Ireland JJ, Rao MC, Bernath GA, Midgley AR Jr, Reichert LE Jr. Ovarian follicular development in the rat: hormone receptor regulation by estradiol, follicle stimulating hormone and luteinizing hormone. Endocrinology 1976; 99:1562–1570.
77. Lipner H, Cross NL. Morphology of the membrana granulosa of the ovarian follicle. Endocrinology 1968; 82:638–641.

Molecular Human Reproduction, Vol.19, No.9 pp. 600–617, 2013
Advanced Access publication on April 18, 2013 doi:10.1093/molehr/gat027

MHR Basic science of reproductive medicine

ORIGINAL RESEARCH

The dormant and the fully competent oocyte: comparing the transcriptome of human oocytes from primordial follicles and in metaphase II

Marie Louise Grøndahl[1,2,*], Rehannah Borup[3], Jonas Vikesså[3], Erik Ernst[4], Claus Yding Andersen[1], and Karin Lykke-Hartmann[4]

[1]Laboratory of Reproductive Biology, University Hospital of Copenhagen, Rigshospitalet, Denmark [2]Fertility Clinic, University Hospital of Copenhagen, Herlev Hospital, Herlev, Denmark [3]Genomic Medicine, University Hospital of Copenhagen, Rigshospitalet, Denmark [4]Department of Biomedicine, Reproductive Laboratory, Aarhus University, Aarhus, Denmark

*Correspondence address. E-mail: marie.louise.groendahl@regionh.dk

Submitted on November 27, 2012; resubmitted on March 30, 2013; accepted on April 3, 2013

ABSTRACT: Oocytes become enclosed in primordial follicles during fetal life and remain dormant there until activation followed by growth and meiotic resumption. Current knowledge about the molecular pathways involved in oogenesis is incomplete. This study identifies the specific transcriptome of the human oocyte in the quiescent state and at the pinnacle of maturity at ovulation. *In silico* bioinformatic comparisons were made between the transcriptome of human oocytes from dormant primordial follicles and that of human metaphase II (MII) oocytes and granulosa cells and unique gene expression profiles were identified as well as functional and pathway enrichments associated with the oocytes from the two developmental hallmarks. A total of 729 genes were highly enriched in oocytes from primodial follicles and 1456 genes were highly enriched in MII oocytes (>10-fold, $P < 0.001$) representing functional categories such as cell cycle regulation, DNA protection and epigenetics, with representative genes validated by qPCR analysis. Dominating canonical pathways in the oocytes from primordial follicles were androgen, estrogen receptor, glucocorticoid receptor and PI3K/AKT signaling ($P < 0.001$). In the MII, mitotic roles of polo-like kinases, estrogen receptor, JAK/Stat signaling ($P < 0.001$) and the ERK/MAPK ($P < 0.01$) signaling were enriched. Some of the highly differentially expressed genes were completely new in human reproduction (*CDR1*, *TLC1A*, *UHRF2*) while other genes [*ABO*, *FOLR1* (folate receptor), *CHRNA3* (nicotine receptor)] may relate to clinical observations as diverse as premature ovarian failure, folic acid deficiency and smoking affecting female fertility. The *in silico* analysis identified novel reproduction-associated genes and highlighted molecular mechanisms and pathways associated with the unique functions of the human oocyte in its two extremes during folliculogenesis. The data provides a fundamental basis for future functional studies in regulation of human oogenesis.

Key words: folliculogenesis / transcriptome / oocytes from primordial follicles / metaphase II oocytes / microarray

Introduction

The human oocyte is a unique cell that differs from all other cells in the human body. First of all, it is the cell that possesses the capacity to form a new offspring and secure continuation of the gene pool and is of utmost importance from an evolutionary point of view. Further, the length of the oocyte cell cycle is extraordinarily long, potentially up to five decades under the condition that the oocyte becomes surrounded by somatic cells and forms the primordial follicle during fetal life. The follicle constitutes the functional unit of the ovaries and once primordial follicles becomes activated, the follicle will either develop to full maturity during approximately half a year containing a mature oocyte capable of sustaining fertilization and embryo development or undergo atresia at some point during growth and development.

The mechanisms that induce growth and maturation of the follicles are poorly understood, though it has been demonstrated that the oocyte itself plays a crucial role in the complex bidirectional interaction between the oocytes and granulosa cells (Eppig, 2001; Gilchrist *et al.*, 2008). During follicular development, the supporting granulosa cells proliferate and differentiate from ~30 pregranulosa cells (Westergaard *et al.*, 2007) to around 60 million mural granulosa cells in the human fully mature follicle (McNatty *et al.*, 1979) and support ovulation of an oocyte embedded in cumulus cells. In this process the oocyte grows in diameter from around 30 μm in the primordial follicle (Westergaard *et al.*, 2007) to 110 μm in the preovulatory follicle. The multiple processes that regulate folliculogenesis are very complex and far from being fully understood, especially in humans. One possible way of

further elucidating the processes involved in growth and development of human oocytes and the mechanisms that govern the cell cycle dormant stage to the development of metaphase II (MII) oocytes (the fully mature oocytes), is to compare the whole transcriptomes of oocytes from primordial follicles with those of MII oocytes and granulosa cells (Grondahl *et al.*, 2010; Markholt *et al.*, 2012). In addition, comparison between the transcriptomes of the two oocyte stages will provide data on the transcripts stockpiled in the MII oocyte during oogenesis. Thus, the aim of the present study was by *in silico* microarray analysis to describe the unique transcriptomes associated with the oocytes from two developmental hallmarks. We identified commonly expressed genes as well as genes specific to each stage and have for the first time described the unique biological network required during the two stages of oocyte maturation in human female reproduction.

Materials and Methods

Gene expression array data analysis

The microarray data used in this study is presented in the following papers: Primordial oocytes (Markholt *et al.*, 2012) MII oocytes (Grondahl *et al.*, 2010) and granulosa cell (Grondahl *et al.*, 2012; Table I). All studies were approved by the Danish Scientific Ethical Committee (Danish Scientific Ethical Committee Approval Number: KF 299017 and J/KF/01/170/99 and KF 299017, respectively). Participants provided their written consent to participate in this study. On behalf of the minors/child participants, written consents to participate in this study was obtained from parents. The ethics committees approved these consent procedures. The GeneChip Affymetrix HG_U133 2.0 probe array containing 54 675 probe sets (including affymetrix control probe sets $n = 62$) was used in the studies.

A total of 33 samples were analyzed. Three oocyte samples from primordial follicle [representing pools of laser capture microdissected 10 μm thick sections of (i) 620 oocytes from a 21-year-old woman, (ii) 332 oocytes and (iii) 330 oocytes from a 11-year-old girl donated in connection with a fertility preservation program]; 15 samples representing individual zona pellucida free MII oocytes and 15 samples representing mural granulosa cells from individual follicles donated from 15 women aged 27–39 years in connection with oocyte retrieval for IVF/ICSI treatment. The 33 Cel files from the microarray analysis were imported into the Partek Genomics Suite 6.5 software package and Robust Multichip Average (RMA) normalized using quantile normalization and 'Median Polish summarization' (Bolstad *et al.*, 2003). The modeled log-intensity of 54 675 probe sets was used for high-level analysis selecting differentially expressed genes.

All samples are MIAME compliant and are handled according to Standard Operating Procedures in the Microarray Center. The samples were submitted to ArrayExpress at 'European Molecular Biology Laboratory' using MIAMExpress. The experiment accession number for the oocytes of primordial follicles is E-MEXP-3454, E-MEXP-2347 for MII oocytes and E-MEXP-3641 for granulosa cells.

Table I Summary of data analysis.

	Oocytes from primordial follicles	MII oocytes	Granulosa cells
Patient	Fertility preservation program	IVF/ICSI treatment	IVF/ICSI treatment
Array data	DNA microarray on 3 pools of 620, 332 and 330 microdissected oocytes[a]	DNA microarray on 15 individual zona-free MII oocytes[b]	DNA microarray on 15 preovulatory follicles cells containing an MII oocyte[c]
Transcriptome comparison analysis	*In silico*: Normalization of the 3 + 15 + 15 raw expression files*		
RT–qPCR	Two independent pools of microdissected oocytes (10 nm thickness)*	Two individual zona-free MII oocytes*	

*Bioinformatic analysis and RT–qPCR described in materials and methods.
[a]Markholt *et al.* (2012); [b]Grondahl *et al.* (2010); [c]Grondahl *et al.* (2012).

Differentially expressed genes

To display overall differences in expression of the three cell types primordial oocyte ($n = 3$), MII oocyte ($n = 15$) and mural granulosa cells ($n = 15$), a multi-group comparison was performed using an *F*-test selecting the 2000 most significantly changed probe sets, corresponding to a *P*-value below 1.69E−13 (q<4.61E−12). The expression pattern of the 2000 probe sets was visualized by hierarchical clustering with average linkage of samples and genes as implemented in Qlucore Omics Explorer 2.2 software (www.glucore.com).

To identify transcripts regulated in oocytes from primordial follicle versus MII oocytes and granulosa cells, combined, and MII oocytes versus oocytes from primordial follicles, two-group comparisons were performed. Differentially expressed genes were defined as having more than 10-fold up- or down-regulation and show a significance level of $P < 10^{-4}$ (corresponding to a False Discovery Rate below 6.0 × 1E−4) in a Student's *t*-test. In order to address the differences in female age, between patients donating oocytes from primordial follicles (11–21 years) and MII oocytes (27–39 years), the intersection between MII gene expression influenced by women's age (Grondahl *et al.*, 2010) and the genes found to be highly enriched in MII in the present study were identified. The intersection was below 1.6% (data not shown).

Detection of expressed genes analysis

Probe sets were defined to be present if the average unlogged expression value exceeded an intensity of 100. Lists of expressed genes were generated by excluding redundant probe sets based on gene symbols. Intersections of the three gene lists were visualized in a Venn diagram and lists of selectively and overlapping transcripts were generated.

Gene function enrichment and biological networks

Biological networks of the differentially expressed genes were generated in Ingenuity pathway analysis tools from Ingenuity Systems Inc. (www.ingenuity.com). The list of differentially expressed genes was imported into Ingenuity and each gene identifier was overlaid onto a global molecular network developed from information contained in the Ingenuity Pathways Knowledge Base. Functions and networks of these genes were then generated based on their connectivity. A network score was calculated based on the hyper-geometric distribution and calculated with the right-tailed Fisher's exact test. The score is the negative log of this *P*-value. The score takes into account the number of network eligible molecules in the network and its size, as well as the total number of network eligible molecules analyzed and the total number of molecules in the knowledge base that could potentially be included in the network. The score represents the chance of getting a network containing at least the same number of network eligible

molecules by chance when randomly picking the number of genes that can be in networks from the knowledge base. The top molecular and cellular functions and networks are presented.

Validation of microarray results by quantitative RT–PCR

Validation of selected genes was performed by qPCR. Samples of independent pools of oocytes from primordial follicles and MII oocytes were collected from patients equivalent to those previously described (Grondahl *et al.*, 2010; Markholt *et al.*, 2012). Briefly, MII oocytes were donated by women (27–32 years) undergoing controlled ovarian stimulation followed by oocyte retrieval for ICSI with male indication. Primordial follicles were donated in connection with an ovarian cryo-preservation program (11 and 21 years). Total RNA was isolated from the microdissected oocytes from the primordial follicle on the Laser capture microdissection caps using a RNA extraction/isolation kit (KIT0310-NS Arcturus Paradise Plus qrt PCR kit, Molecular Devices, Sunnyvale, CA, USA), as described (Markholt *et al.*, 2012) and total RNA was extracted from MII oocytes using the PicoPure® RNA Isolation Kit (MDS, Inc., Ontario, Canada) as described (Grondahl *et al.*, 2010), according to the manufacture's recommendations. In this study, total RNA (25 ng) from primordial and MII oocytes, respectively, was used as input to an RNA amplification step using the WT-Ovation™ PicoSL WTA System A (cat 3312, NuGEN Technologies, Inc., CA, USA) including both oligo d(T) and random hexamers for cDNA amplifications, and 100 ng cDNA was used in each SYBR green (Applied Biosciences) qPCR reaction, as described (Markholt *et al.*, 2012). Primers were designed using an exon-spanning approach from Pearl Primer software (Marshall, 2004) and the NCBI Primer BLAST, and all primers were submitted to the primer BLAST search at NCBI to verify specificity; using Brilliant® SYBR Green Master Mix (Stratagene). PCR was run using 7500 Fast Real-Time PCR system (Applied Biosystems). The following program was used: 95°C for 10 min followed by 45 cycles of 30 s at 95°C, 1 min at 60°C and 1 min at 72°C. A dissociation curve verified individual PCR amplicons. A non-template control was included in each qRT–PCR run. PCR products were visualized on a 2% agarose gel containing EtBr for UV visualization (data not shown). Transcription levels of the genes were quantified using the relative quantification method based on comparative threshold cycle values (Ct). For selection of endogenous control genes, we used NormFinder (Andersen *et al.*, 2004) to define a stability value for 22 key reference genes based on the microarray data. The best of these candidates were furthermore tested by qRT–PCR to account for inherent differences between the two oocyte stages. There is no single gene that fulfills such criteria completely and we evaluated the results for recommended oocyte control genes (Mamo *et al.*, 2007; O'Connor *et al.*, 2012) before deciding which control gene was most suitable for normalization. The results of our control gene screening revealed the following (average Ct values for each triplicate measurements); GAPDH; Primordial oocyte; Ct 20.6413; MII oocyte; Ct 16.8896 (~4 point difference in Ct value), RPLN13A; Primordial oocyte; Ct 28.2355; MII oocyte; Ct 23.0020 (~5 point difference in Ct value), H2AFZ; Primordial oocyte; Ct 36.5701; MII oocyte; Ct 25.7762 (>10 point difference in Ct value), HPRT1; Primordial oocyte; Ct 25.8756; MII oocyte; Ct 23.0272 (~2 point difference in Ct value), PPIA; Primordial oocyte; Ct 32.8664; MII oocyte; Ct 30.4870 (~2 point difference in Ct value). Relative expression levels for each gene were calculated using the delta Ct method, where each gene was normalized to control genes using $2^{\Delta(Ct/Control(mean) - Ct/Gene(mean))}$, plotted with standard error bars ($2^{\Delta(Ct/Control(mean) - Ct/Gene(mean))} - 2^{\Delta((Ct/Control(value1)) - (Ct/Gene(value1)) - (Ct/Control(value2)) - (Ct/Gene(value2)) - (Ct/Control(value3) - Ct/Gene(value3))}$) using Microsoft Excel. For each comparison normalized to *HPRT1*, an unpaired *t*-test with Welch's correction was carried out (Prism6) for the qPCR data to evaluate the significant difference *P*-values.

Gene	Primers	Product size (nt)
hsZP3	F: 5′-ACGAGTGTGGCAACAGCA R: 5′-GGTCATGGAGCAGGAAGGT	68
hsOOEP	F: 5′-GCAGCTGCGTAGGTTACCA R: 5′-GGGTCTCTCAGTTCCTGCAC	80
hsDPPA3	F: 5′-CAATTTGAGGCTCTGTCATCAG R: 5′-ATCGGCGTCTTGACACAAC	77
hsFOLR1	F: 5′-GAGCAGAGCAGAAGCCTGA R: 5′-GGTGATCCTTTGGGTTCAGTT AACTGAACCC	69
hsBMP15	F: 5′-CCTAGAGAGAACCGCACCAT R: 5′-GAGGAAAGCCCAGGATCTGT	111
hsMOS	F: 5′-CACCAAGAACCGACTAGCATC R: 5′-GCAGCCTTGCTACGTTGAG	61
hsGAPDH	F: 5′-GTCTCCTCTGACTTCAACAG R: 5′-GTTGTCATACCAGGAAATGAGC	104
hsRPL13A	F: 5′-TGGCTAAACAGGTACTGCTGG R: 5′-CCGCTTTTTCTTGTCGTAGGG	282
hsH2AFZ	F: 5′-AGTGGGCCGTATTCATCGAC R: 5′-TGTGGAATGACACCACCACC	252
hsHPRT1	F: 5′-CCCTGGCGTCGTGATTAGTG R: 5′-CGAGCAAGACGTTCAGTCCT	138
hsPPIA	F: 5′-GTGGTATAAAAGGGGCGGGA R: 5′-TGAAGTCACCACCCTGACAC	281

Results

Novel gene expression profiling at the onset and end of folliculogenesis

Three pools of primordial oocytes (Markholt *et al.*, 2012), 15 MII oocytes (Grondahl *et al.*, 2010) and 15 pools of mural granulosa samples (Grondahl *et al.*, 2010) were expression profiled using the same Human Genome microarray platform. The three sample groups were compared by detect uniquely expressed genes and differences in expression level. The lists of genes expressed in oocytes from primordial follicles, MII oocytes and the mural granulosa cells, (Supplementary data, Table SI) show that a total of 2556 unique genes (3735 probe sets) were selectively present in the oocytes from primordial follicles and not expressed in the MII oocytes nor in the somatic cell compartment as presented by a Venn diagram (Fig. 1A). In the MII oocytes, 1387 genes were selectively expressed (1776 probe sets), whereas the granulosa cells selectively expressed 2234 genes (3049 probe sets; Fig. 1A). Interestingly, MII oocytes and the granulosa cells have a higher number of co-expressed genes (2585) when compared with (i) oocytes from primordial follicles and MII oocytes (1335) and (ii) oocytes from primordial follicles and granulosa cells (1191) (Fig. 1A; The gene lists representing each compartment of the Venn diagram are presented in Supplementary data, Table SII). Among genes expressed in the oocyte-specific overlap (1335) biological categories such as 'regulation of mitosis', 'chromosome condensation' and 'Meiosis I' were enriched ($P < 0.05$; Supplementary data, Table SIII).

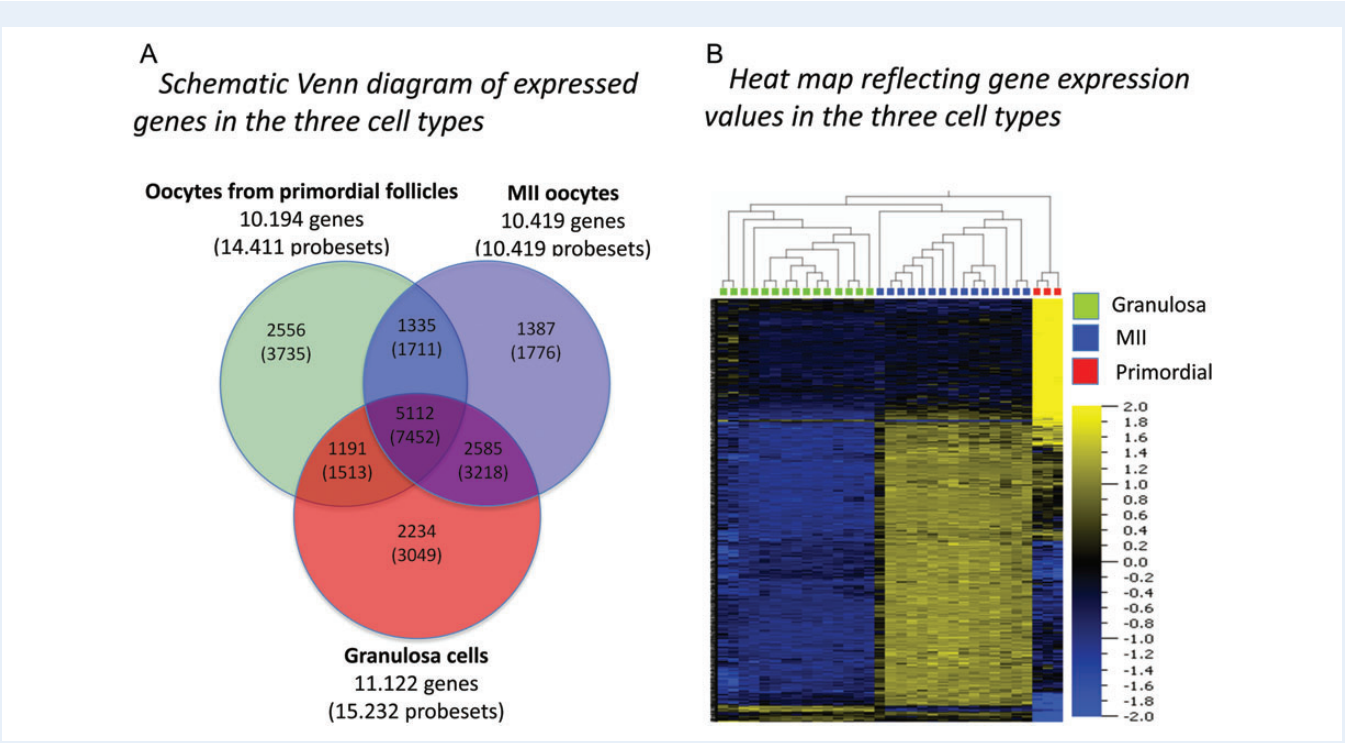

Figure 1 Comparisons between the transcriptomes of oocytes from primordial follicles, MII oocytes and somatic cells. (**A**) A Venn diagram of total expressed transcripts (red) and unique genes in human oocytes from the primordial follicle, MII oocytes and granulosa cells, respectively, divided to represent all possible relations of gene expression confined to either cell-specific or overlapping between two or three cell populations, as indicated by intersections (numbers are based on gene expressions with signal intensities above 100). (**B**) Hierarchical cluster of the 2000 transcripts with the most significant difference in expression level between human oocytes from the primordial follicle ($n = 3$) and MII oocytes ($n = 15$) and mural granulosa cells ($n = 15$). The expression level for each gene is standardized to have a mean value of 0 and standard deviation of 1. Black color represents the mean value, 0; yellow color represents a gene expression level above the mean; and blue color represents expression below the mean. The intensity of the pseudo color reflects the number of standard deviations from the mean as indicated by the color box.

None of the three lists of expressed genes represented the common leukocyte antigen CD45 (*PTPRC*, protein tyrosine phosphatase, receptor type, C), indicating no or negligible blood contamination to the samples.

Up-regulated genes in the primordial follicle

To identify transcripts that were enriched in oocytes from primordial follicles, a two-group comparison of oocytes from primordial follicles to MII oocytes and granulosa cells combined was performed. Differentially expressed genes were defined as having a 10-fold up- or down-regulation and exhibit a significance level in a Student's *t*-test of $P <$ 1E−10 (corresponding to a False Discovery Rate below 6.0 × 1E−4), resulting in 1333 unique genes (1846 probe sets) being differentially expressed. Of these, 729 unique genes (1107 probe sets) showed a higher expression in oocytes from primordial follicles (Supplementary data, Table SIVA). From this group, high expression levels were found for genes such as the transmembrane protein with EGF-like and two follistatin-like domains 2 (*TMEFF2*), the folate receptor 1 (*FOLR1*), the oligophrenin 1 (*OPHN1*) and the cerebellar degeneration-related protein 1 (*CDR1*) in oocytes from primordial follicles (Table II). Among the genes with high expression levels, several were found to be selectively expressed in oocytes from primordial follicles, i.e. *CDR1*, the glutamate-decarboxylase-like 1 (*GADL1*) and the Cyclin K (*CCNK*) and among genes with lower expression levels, genes as the meiosis-specific nuclear structure 1 (*MNS1*), the reelin (*RELN*) and the Heat shock transcription factor 3 (*HSF3*) were also selectively expressed in the oocyte in the (Table II).

Up-regulated genes in the MII oocyte

The comparison between MII oocyte and the oocytes from primordial follicle transcriptomes resulted in 2228 genes (3019 probe sets) meeting the criteria of being differentially expressed. Of these 1456 genes (1780 probe sets) were up-regulated in the MII oocytes (Supplementary data, Table SIVB). This showed that gene transcripts such as the zona pellucida glycoprotein 3 (*ZP3*), the developmental pluripotency associated 5 (*DPPA5*), the oocyte expressed protein homolog (*OOEP*) and other maternal-effect genes accumulate in human MII oocytes (Table III). In addition, the T-cell leukemia/lymphoma 1A (*TCL1A*) (T-cell leukemia/lymphoma 1A), the B-cell translocation gene 4 (*BTG4*), the ubiquitin-like with PHD and ring finger domains (*UHRF2*), the v-mos Moloney murine sarcoma viral oncogene homolog (*MOS*) and the spermatogenesis associated 2 (*SPATA2*) transcripts represent selectively expressed top (high expression level) genes in human MII oocytes. The bone morphogenetic protein 15 (*BMP15*) transcript was moderately and selectively expressed, while the epidermal growth factor (*EGF*), its receptor (*EGFR*), the spermatogenesis and oogenesis-specific basic helix-loop-helix 2 (*SOHLH2*), the FBJ murine osteosarcoma viral oncogene homolog (*FOS*), the relaxin 1 (*RLN1*) and the aurora kinase B (*AURKB*) represent selectively but lower expressed genes. Examples on

Table II Selectively and higher (>10-fold, $P < 0.001$) expressed genes in the human oocytes from primordial follicles relative to MII oocytes and somatic cells (granulosa cells).

Gene symbol	Gene title	Probe set ID	*P*-value#	Foldchange#	Primordial oocyte*	MII oocyte*	Granulosa cells*	Function
TMEFF2	Transmembrane protein with EGF-like and two follistatin-like domains 2	224321_at	4.02E−13	135	+++++	+	−	Tumor suppressor (Gery *et al.*, 2002)
FOLR1	Folate receptor 1 (adult)	211074_at	4.12E−13	55	+++++	+	+	Cell cycle regulation, adhesion, DNA methylation, DNA repair (Crott *et al.*, 2008)
MALAT1	Metastasis associated lung adenocarcinoma transcript 1 (non-protein coding)	231735_s_at	1.58E−05	30	+++++	+	++	Long non-coding mRNA, mediates gene activation programs (Yang *et al.*, 2011)
OPHN1	Oligophrenin 1	206323_x_at	1.16E−12	20	+++++	++	++	Intracellular signal transduction (Ramakers, 2002)
CDR1	Cerebellar degeneration-related protein 1, 34 kDa	207276_at	2.02E−36	1610	++++	−	−	Unknown
CCDC117	Coiled-coil domain containing 117	235330_at	1.00E−32	101	++++	+	+	Unknown
EPCAM	Epithelial cell adhesion molecule	201839_s_at	8.71E−25	32	++++	++	−	Marker for meiotic-competent germ cell-like cell (Chuang *et al.*, 2012)
CCNK	Cyclin K	219273_at	1.54E−25	116	+++	−	−	Genome maintenance (Yu and Cortez, 2011)
PNN	Pinin, desmosome-associated protein	1567213_at	2.67E−21	94	+++	−	−	RNA processing and transcriptional regulation (Bracken *et al.*, 2008)
GADL1	Glutamate-decarboxylase-like-1	1563533_at	2.18E−24	476	+++	−	−	Unknown
MND1	Meiotic nuclear divisions 1 homolog (S. cerevisiae)	223700_at	4.06E−20	38	+++	+	−	Meiotic recombination (Pezza *et al.*, 2010)
TP63	Tumor protein p63	211194_s_at	1.42E−20	67	+++	+	−	Survival of the oocyte pool (Levine *et al.*, 2011)
CHRNA3	Nicotine receptor cholinergic receptor, nicotinic, alpha 3	210221_at	1.17E−14	12	++	(+)	−	Generally unknown function in non-excitable cells
BUB1	Budding uninhibited by benzimidazoles 1 homolog	216275_at	3.71E−18	31	++	(+)	−	Cell cycle checkpoint; dysfunction linked to aneuploidy in female germ cells (Leland *et al.*, 2009)
ITGBL1	Integrin, beta-like 1 (with EGF-like repeat domains)	231993_at	1.58E−28	140	++	−	−	Unknown
CEP63	Centrosomal protein 63kDa	233650_at	2.95E−27	67	++	−	−	Spindle assembly, cell cycle regulation (Brown and Costanzo, 2009)
HSF2	Heat shock transcription factor 2	211220_s_at	2.91E−19	65	++	−	−	Stress response in oocyte and embryos (Le Masson and Christians, 2011)
MNS1	Meiosis-specific nuclear structural 1	219703_at	3.65E−18	51	++	−	−	Essential in spermiogenesis in mice (Zhou *et al.*, 2012)
RELN	Reelin	205923_at	3.50E−19	49	++	−	−	Extracellular glycoprotein. Tumor suppressor (Okamura *et al.*, 2011)
SKIL	SKI-like oncogene	206675_s_at	1.32E−22	38	++	−	−	Inhibition of TGFb signaling (Trombly *et al.*, 2009)
SMARCA2	SWI/SNF-related, matrix-associated, actin-dependent regulator of chromatin, subf	228926_s_at	1.15E−24	38	++	−	−	Chromatin remodeling (Ko *et al.*, 2008)

*Relative expression of max expression value: −: not expressed in appreciable levels (see definition in materials and methods); (+): low expression in some of the samples; +: 0.1–1%; ++: 1–10%, +++: 10–40%; ++++:40–70%; +++++: 70–100%. #: comparison between primordial oocytes and MII and granulosa cell.

Table III Selectively and higher (>10-fold, $P < 0.001$) expressed genes in the human MII oocytes relative to oocytes from primordial follices.

Gene symbol	Gene title	Probeset ID	*P*-Value#	Fold change#	Primordial oocyte*	MII Oocyte*	Granulosa cells*	Function
TCL1A	T-cell leukemia/lymphoma 1A	39318_at	1.52E−19	285	(+)	+++++	−	Inhibition of de novo DNA methylation (Palamarchuk *et al.*, 2012)
ZP3	Zona pellucida glycoprotein 3	204148_s_at	7.18E−10	12	++	+++++	+	Sperm receptor (Gupta *et al.*, 2009)
NLRP5/ MATER	NLR family, pyrin domain containing 5	1552405_at	−	−	++++	+++++	−	Maternal-effect gene. NLRP in reproduction. (Tian *et al.*, 2009)
DPPA3/ STELLA	Developmental pluripotency associated 3	231385_at	−	−	++++	+++++	−	Maternal-effect gene. Pluripotency. Chromatin condensation in oogenesis (Liu *et al.*, 2012)
BCAR4	Breast cancer anti-estrogen resistance 4	230854_at	1.69E−09	46	+	++++	−	Oncogene (Godinho *et al.*, 2011)
DNMT1	DNA (cytosine-5-)-methyltransferase 1	201697_s_at	8.36E−15	44	+	++++	+	Maintenance of DNA methylation in oocyte and zygote (Hirasawa *et al.*, 2008)
SOHLH2	Spermatogenesis and oogenesis-specific basic helix-loop-helix 2	220129_at	−	−	++++	++++	−	Transcription regulation during gametogenesis (Jagarlamudi and Rajkovic, 2012)
BTG4	B-cell translocation gene 4	220766_at	1.76E−17	1486	−	++++	−	Oocyte competence (Raty *et al.*, 2011)
DPPA5	Developmental pluripotency associated 5	241550_at	1.45E−17	35	++	++++	−	Control of cell pluripotency (Kim *et al.*, 2005)
PCNA	Proliferating cell nuclear antigen	201202_at	4.56E−14	19	+	++++	+	DNA replication and repair (Kirchmaier, 2011)
PTTG1	Pituitary tumor-transforming 1/Securin	203554_x_at	8.46E−11	33	+	++++	+	Sister chromatid segregation. Anaphase switch (Holt *et al.*, 2008)
OOEP	Oocyte-expressed protein homolog	238218_at	3.34E−09	60	+	++++	−	Maternal-effect gene (Tashiro *et al.*, 2010)
BOD1	Bi-orientation of chromosomes cell division	225030_at	4.45E−13	15	++	++++	+	Orientate chromsome (Compton, 2007)
CCNB1	Cyclin B1	228729_at	1.09E−12	24	++	+++	(+)	Part of the maturation-promoting factor (Kim *et al.*, 2011)
MELK	Maternal embryonic leucine zipper kinase	204825_at	8.84E−13	108	(+)	+++	(+)	Proliferation (Saito *et al.*, 2011)
NLRP11	NLR family, pyrin domain containing 11	1552531_a_a	5.21E−09	14	+	+++	−	Primate-specific, oocyte-specific NLRP. (Tian *et al.*, 2009)
NLRP13	NLR family, pyrin domain containing 13	1553525_at	7.67E−08	12	+	+++	−	Oocyte-specific NLRP (Tian *et al.*, 2009)
FIGLA	Folliculogenesis-specific basic helix-loop-helix	1570337_at	−	−	+++	+++	−	Maternal-effect gene (Zheng and Dean, 2007)
ZAR1	Zygote arrest 1	1555775_a_at	−	−	+++	+++	−	Maternal-effect gene (Zheng and Dean, 2007)
ZP2	Zona pellucida glycoprotein 2	207933_at	5.30E−09	19	+	+++	−	Sperm receptor (Gupta *et al.*, 2009)
GDF9	Growth differentiation factor 9	221314_at	1.24E−06	49	+	+++	−	Oocyte Growth and differentiation (Otsuka *et al.*, 2011)
UHRF2	Ubiquitin-like with PHD ring finger domains 2	225610_at	8.06E−20	449	−	+++	++	Maintenance of DNA methylation (Pichler *et al.*, 2011)
H1FOO	H1 histone family, member O, oocyte-specific	1553064_at	1.9E−11	35	+	+++	−	Coupled to initiation of oocyte growth (Tanaka *et al.*, 2005)
SOCS7	Suppressor of cytokine signaling 7	226572_at	1.38E−12	54	(+)	+++	+	DNA damage response (Kremer *et al.*, 2007)
CENPA	Centromere protein A	204962_s_at	2.45E−07	20	+	+++	−	Assembling and directing the organization of the kinetochore (Verdaasdonk and Bloom, 2011)
CHEK1	CHK1 checkpoint homolog	205394_at	1.27E−08	23	+	+++	−	Cell cycle arrest (G2) in response to DNA damage or unreplicated DNA (Flemr *et al.*, 2010)

Continued

TableIII *Continued*

Gene symbol	Gene title	Probeset ID	*P*-Value#	Fold change#	Primordial oocyte*	MII Oocyte*	Granulosa cells*	Function
ESPL1	Extra spindle pole bodies homolog 1/separase	38158_at	7.18E−12	85	(+)	+++	(+)	Stable cohesion between sister chromatids (Yanagida, 2009)
MOS	V-mos Moloney murine sarcoma	221367_at	9.45E−15	223	−	+++	−	Meiotic arrest upon fertilization (Dupre *et al.*, 2011)
SPATA2	Spermatogenesis associated 2	204434_at	2.61E−12	136	−	+++	(+)	Involved in more than spermatogenesis (Maran *et al.*, 2009)
ZP1	Zona pellucida glycoprotein 1	237335_at	9.89E−12	48	+	++	−	Sperm receptor (Gupta *et al.*, 2009)
AURKC	Aurora kinase C	211107_s_at	6.48E−07	17	+	++	(+)	Spindle organization in meiosis (Uzbekova *et al.*, 2008)
DCP1A	DCP1 decapping enzyme homolog A	225443_at	6.26E−11	35	(+)	++	+	Increase during meiosis and involved in activation of maternal mRNA storage (Flemr *et al.*, 2010)
CENPE	Centromere protein E, 312kDa	205046_at	2.07E−08	34	(+)	++	−	Assembling and directing the organization of the kinetochore. (Verdaasdonk and Bloom, 2011)
BMP15	Bone morphogenetic protein 15	221332_at	9.11E−07	77	−	++	−	Oocyte maturation, folliculogenesis (Gilchrist *et al.*, 2008)
ACVR1	Activin A receptor, type 1	203935_at	2.68E−08	33	−	++	+	Folliculogenesis (Kevenaar *et al.*, 2009)
FOS	FBJ murine osteosarcoma	209189_at	3.06E−10	38	−	++	++	cell proliferation, differentiation (Regassa *et al.*, 2011)
EGF	Epidermal growth factor	206254_at	1.36E−06	32	−	++	−	Growth, differentiation and proliferation (Hsieh *et al.*, 2009)
RLN1	Relaxin	211752_s_at	7.87E−10	30	−	+	+	Possible role of relaxin peptides in spermiogenesis (Edsgard *et al.*, 2011)
AURKB	Aurora kinase B	209464_at	4.85E−06	20	−	++	−	Spindle organization in meiosis and mitosis (Lampson and Kapoor, 2005)
EGFR	Epidermal growth factor receptor	1565483_at	5.10E−10	15	−	+	+	Growth, differentiation and proliferation (Hsieh *et al.*, 2009)

*Relative expression of max expression value: −: not expressed in appreciable levels (see definition in materials and methods); (+): very low expression in some of the samples; +: 0.1–1%; ++: 1–10%, +++: 10–40%; ++++:40–70%; +++++: 70–100%. #: Comparison between MII and primordial oocytes.

Bold genes are oocyte-specific genes/maternal-effect genes with moderate to high expression in both oocyte stages.

top genes meeting the criteria of being differentially expressed are the growth differentiation factor 9 (GDF9), the breast cancer anti-estrogen resistance 4 (*BCAR4*), the extra spindle pole bodies homolog 1/separase (*ESPL1*) and the proliferating cell nuclear antigen (*PCNA*) (Table III).

The overall difference in expression as detected by a multi-group comparison between the three cells types is visualized in the heat map, which show the 2000 genes that best separate the expression profiles of the three different cell types (Fig. 1B). The intense yellow cluster (top right) in the oocytes from primordial follicle samples represents a part of the genes that we found to be selectively or highly differentially expressed in the oocytes from primordial follicles.

Function enrichment analysis of differentially expressed genes

The two developmental stages of the human oocytes were illustrated by a gene set enrichment analysis using the IPA Ingenuity software (Ingenuity® Systems, www.ingenuity.com) of the 1107 probe sets enriched in the oocyte from the primordial follicle and of the 1780 probe sets enriched in the MII oocytes, respectively. The highly enriched ($P < 0.001$) bio-functions in the two stages of oocyte development clearly demonstrated several categories being present in both types of oocytes such as 'Cancer' and 'Genetic disorder', which were in the top of the *Disease and Disorder* category, as was 'Cell cycle' in the 'Molecular and Cellular Functions' category (Table IV).

Furthermore 'Transcription' and 'RNA post-transcriptional modification' were gene categories enriched in oocytes from primordial follicles (Table IV). The three top bio-functions represented genes such as the forkhead box N3 (*FOXN39*), the POU class 3 homeobox 2 (*POU3F2*) and the SRY (sex determining region Y)-box 5 (*SOX5*) in the 'Gene expression', whereas the UPF3 regulator of nonsense transcripts homolog B (*UPF3B*) was listed in the 'RNA Post-transcriptional Modification' group and genes such as *BRCA2*, the mouse double minute 2 (*MDM2*), the budding uninhibited by benzimidazoles 1 homolog (*BUB1*) and the tumor protein p63 (*TP63*) were filed in the 'cell cycle' (Supplementary data, Table SVA).

MII oocyte up-regulated genes represented bio-functions as 'Cell cycle', 'Cell death' and 'DNA replication, recombination and repair' and were represented by genes such as *AURKB*, the transforming growth factor, beta receptor III (*TGFBR3*) and *FOS*, respectively (Table IV). In the functional annotated term referred to as 'cell division process' listed in the 'cell cycle ' function, 139 genes were listed, and of those, 26 genes were categorized as 'decreases cell division process', while 27 genes listed as 'increases the cell division process' (Supplementary data, Table SVB).

Enriched networks and pathways

The functional analysis of the two gene sets (enriched in oocytes from primordial follicles and MII oocytes, respectively) listed 'cell cycle network' as particular enriched, which, interestingly, revealed very distinct networks (Fig. 2A and B, respectively). The oocytes from primordial follicles 'cell cycle network' category was highly represented by tumor suppressor genes, i.e. Familial Adenomatous Polyposis (*APC*), *BUB1* and catenin beta 1 (*CTNNB1*) (Fig. 2A), whereas MII oocyte 'cell cycle network' showed a high representation of genes involved in cell cycle progression, i.e. cyclin B1 (*CCNB1*), cyclin E1 (*CCNE1*) and separase (*ESPL1*) (Fig. 2B).

The top canonical pathways enriched in the unique transcriptome from oocytes from primordial follicles were 'androgen signaling' ($P < 0.0001$), 'actin cytoskeleton signaling' ($P < 0.001$), 'PI3K/AKT signaling' ($P < 0.001$; Fig. 3A), 'glucocorticoid receptor signaling' ($P < 0.001$) and 'estrogen receptor signaling' ($P < 0.001$). In the MII oocyte transcriptome, the enriched pathways consisted of 'mitotic roles of polo-like kinases' ($P < 0.001$; Fig. 3B), 'estrogen receptor signaling' ($P < 0.001$), 'JAK/Stat' ($P < 0.001$) and the 'ERK/MAPK' ($P < 0.01$) signaling.

Relative quantification of selected genes in oocytes from primordial follicles and MII oocytes

To verify the relative expression of genes represented in oocytes from primordial follicles and MII oocytes, genes were selected for qPCR

Table IV Top Bio-Functions in the genes highly up-regulated in oocyte in the primordial follicle and the MII oocyte, respectively.

Top bio-functions categories	Oocytes from primordial follicle	MII oocytes
Molecular and cellular functions	Gene expression (122), RNA post-transcriptional modification (29), Cell cycle (78), Protein metabolism (13), Cellular development (76), Cell morphology (35), Cellular assembly (56), Cellular organization and maintenance (29)	Cell cycle (141), Cell death (162), Carbohydrate metabolism (14), DNA replication recombination and repair (44), Nucleic acid metabolism (5), Small molecule biochemistry (23), Post-translational modification (102), Cellular growth and proliferation (62)
Disease and Disorders	Endocrine disorders (155), Gastrointestinal disorders (217), Genetic disorders (242), Metabolic disease (159), Immunological disease (79), Cancer (222), Infectious disease (69), Hematological disease (125)	Cancer (381), Reproductive system disease (189), Hematological disease (51), Organismal injury and abnormalities (16), Genetic disorders (679)
Physiological Systems Development and function	–	Tissue development (15)

The enriched bio-functions ($P < 0.001$) are generated in Ingenuity® from the gene lists representing genes highly (10-fold, $P < 0.001$) up-regulated in the two oocyte stages. The bio-functions are listed with the highest level of significance in the top and number of genes in (). Gene overlap exists between the annotated terms.

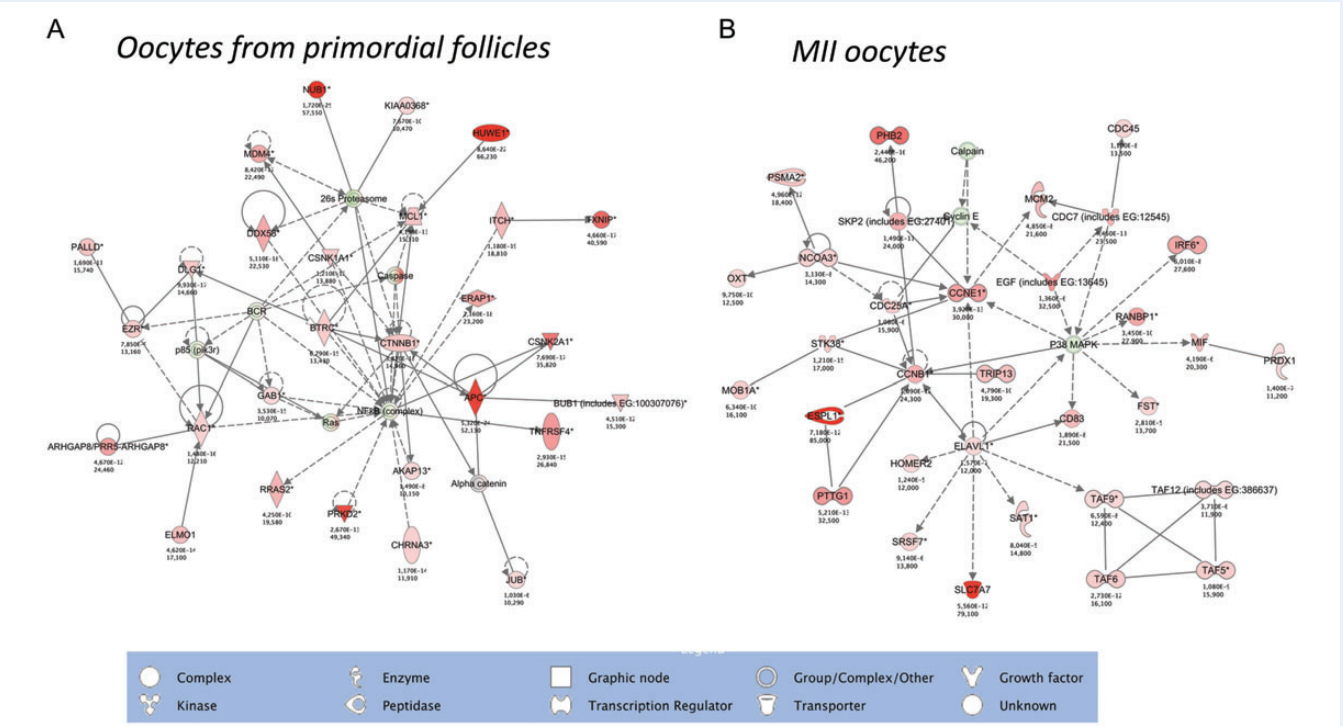

Figure 2 Enriched top cell cycle networks in the oocytes from primordial follicles and MII oocytes. (**A**) Top cell cycle network enriched in the oocytes from the primordial follicle is the network denoted 'Cell Death, Cell cycle, Cellular growth and proliferation' (enrichment score: 30) generated by Ingenuity Pathways Analysis. The network demonstrates high representation of tumor suppressors, i.e. Familial Adenomatous Polyposis (*APC*), budding uninhibited by benzimedazoles 1 (*BUB1*) and catenin beta 1 (*CTNNB1*). (**B**) Top cell cycle network enriched in the MII oocytes is the network denoted 'Cell cycle, Cell death, Cell growth and proliferation' (enrichment score: 30) generated by Ingenuity Pathways Analysis. The network contains genes with high representation of proliferative genes involved in cell cycle progression, i.e. cyclin B1 (*CCNB1*), cyclin E1 (*CCNE1*) and separase (*ESPL1*) and securing (*PTTG1*). Intensity of color represents fold change (red: higher expressed and green: lower expressed), and level of significance highlighted is meeting the criterion of being more than 10-fold differentially expressed. A key to identify node shapes is given in the figure. Lines without arrow indicate binding and full and dotted arrow lines represent direct and indirect interactions, respectively.

analysis. RNA was extracted from two independent pools of oocytes from primordial follicles and MII oocytes not used for the microarray analysis, respectively, and qPCR was performed on selected genes. Several standard housekeeping control genes were tested to find the most suitable control gene that differed the least between oocytes from primordial follicles and MII. The housekeeping control genes *RPLN13A* and *H2AFZ* showed more than 5- and 10-fold differences in Ct values between oocytes from primordial follicles and MII oocytes, respectively, and were thus excluded as good controls (data not shown). However, *GAPDH*, *PPIA* and *HPRT1* all showed smaller and comparable differences in Ct values between the two oocyte stages. Since *HPRT1* showed the least difference and the lowest Ct values, we used this gene as a housekeeping reference gene to normalize our qPCR data (Fig. 4). The normalization to *HPRT1* is comparable to the qPCR data normalized to both *GAPDH* and *PPIA*, respectively (Supplementary data, Fig. S1) and thus, combined, the qPCR data are strongly supported by three different housekeeping gene references (Ct values of control genes are described in material and methods). The selected qPCR control genes have distinct cellular functions, to avoid any co-regulations of the genes, which could bias the qPCR results by appearing falsely stable. The development-associated genes such as developmental pluripotency associated 3 (*DPPA3*), and *ZP3* were detected in oocytes from both primordial follicles and MII oocytes (Fig. 4). The detection of *MOS* and *BMP15* was restricted to MII oocytes, while *OOEP* were predominantly expressed in MII oocytes and lowly expressed in the oocytes of the primordial follicle. *FOLR1* were predominantly expressed in oocytes of the primordial follicle in contrast to a very low level in MII oocytes (Fig. 4). All findings were in accordance with the relative expression from the array data (Tables II and III).

Unique genetic requirements assigned to oocytes from primordial follicles, MII oocytes and granulosa cells

From the transcriptome lists numerous genes are restricted to the somatic cells alone, whereas several genes are restricted to the oocyte, which can be further divided to genes represented as being present in oocytes from the beginning or the end of folliculogenesis (Fig. 5). This reveals for the first time unique gene expressions associated with human oocytes from primordial follicles and MII oocytes and present candidates for downstream analysis to be performed from the listed genes (Tables II and III, respectively, and Fig. 5), which are likely to be of significance for essential biological questions related to female reproduction.

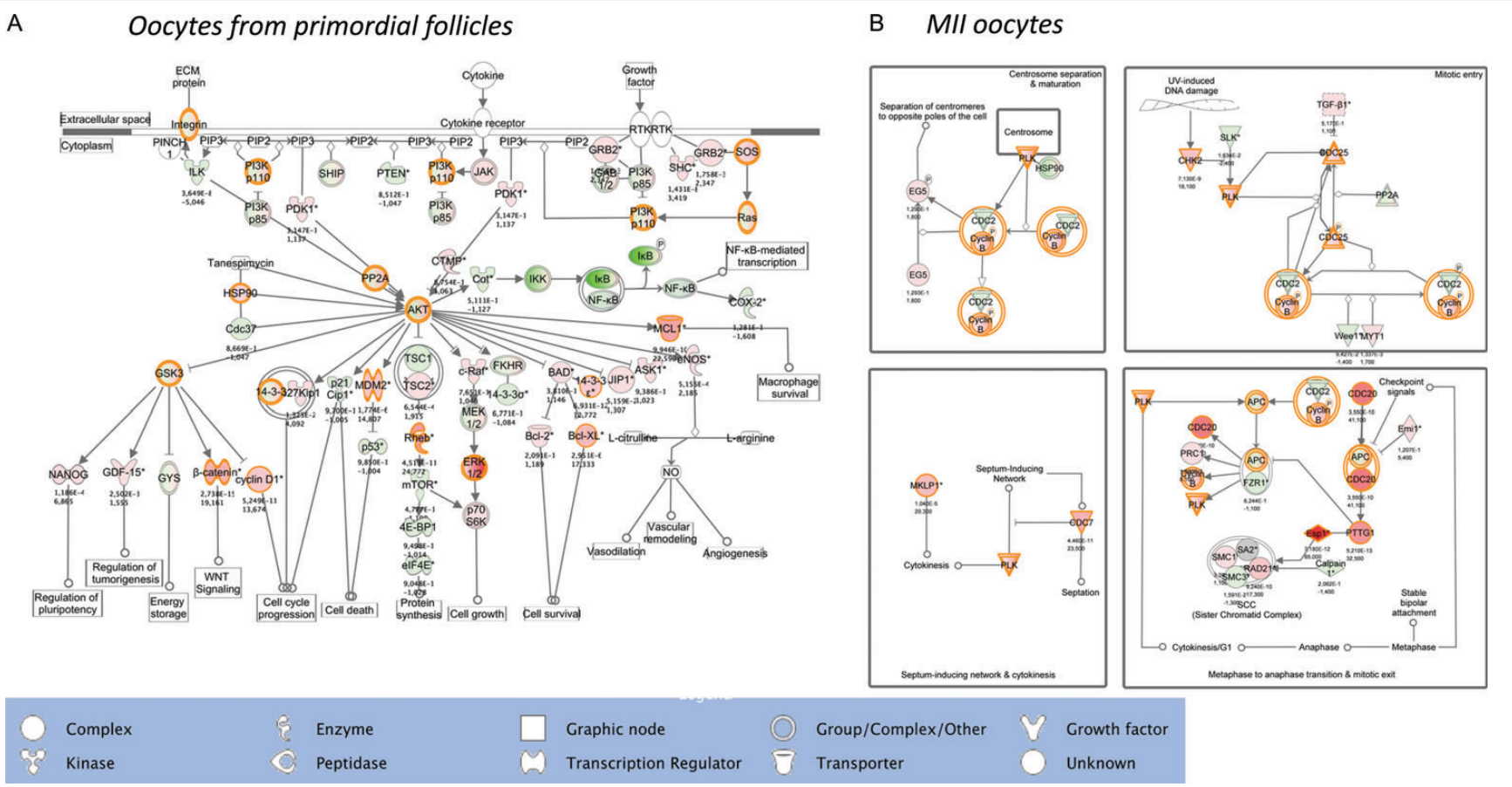

Figure 3 Top enriched signaling pathways in the oocytes from primordial follicles and MII oocytes. (**A**) Top canonical pathway enriched in the genes differentially expressed in the oocytes from the primordial follicle is the PI3K/AKT signaling pathway including *PTEN*, cyclin D (*CCND*), catenin beta 1 (*CTNNB1*) and heat shock protein 90 (*HSP90*). (**B**) Top canonical pathway enriched in the genes differentially expressed in the MII oocytes is the pathway denoted mitotic roles of polo-like kinases including anaphase promoting complex, several cell division cycle proteins (*CDC7*, *CDC20*, *CDC25*), checkpoint *CHK2* and the dominant cyclin B (*CCNB1*) as well as of *ESPL1* (separase) and *PTTG1* (securin). Intensity of color represents fold change (red: higher expressed and green: lower expressed), and level of significance highlighted is meeting the criterion of being more than 10-fold differentially expressed. A key to identify node shapes is given in the figure. Lines without arrow indicate binding and full and dotted arrow lines represent direct and indirect interactions, respectively.

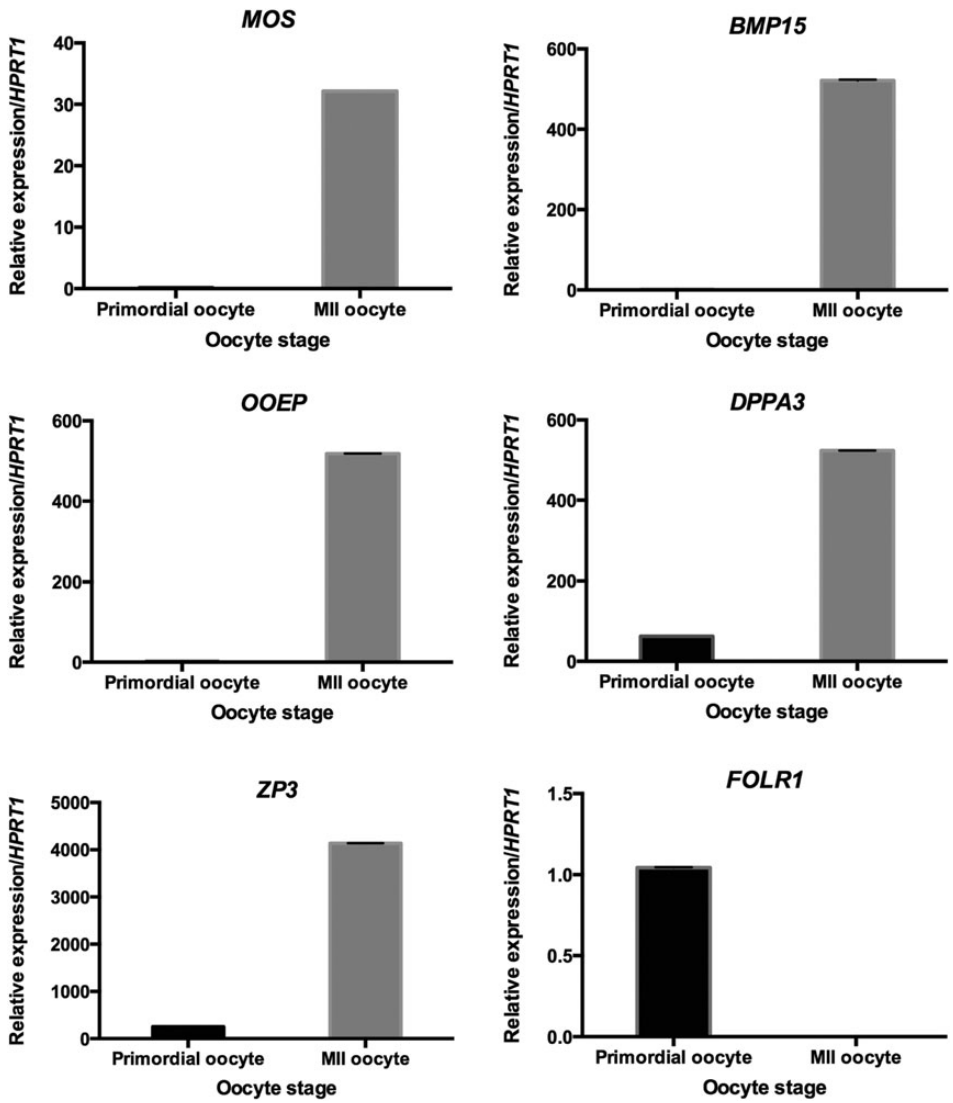

Figure 4 Relative qPCR of selected genes in oocytes from primordial follicles and MII oocytes. Quantification of relative abundance of *MOS*, *BMP15*, *FOLR1*, *DPPA3*, *ZP3* and *OOEP* transcripts in oocytes from primordial follicles and MII oocytes, as indicated (gray columns; oocytes from primordial follicles, blue columns; MII oocytes). All expression levels were normalized to *HPRT1* and the relative expression is displayed using Excel (Microsoft). Data are presented as the mean value of triplicate measurements including standard errors. An unpaired *t*-test with Welch's correction *P*-values; $P = 0.0003$ for *MOS*, $P = 0.0004$ for *BMP15*, $P = 0.0005$ for *OOEP*, $P = 0.009$ for *DPPA3*, $P = 0.0012$ for *ZP3* and $P = 0.0022$ for *FOLR1*.

Discussion

By comparing the transcriptome of oocytes from human primordial follicles with that of fully competent MII oocytes, the present study identified genes of specific importance at each of these unique developmental stages. These two types of oocytes represent the starting point and end of oocyte development during folliculogenesis and we assumed that genes present in both types of oocytes are of general importance, whereas genes specifically expressed in either one of the two developmental stages may be of special importance for oocytes at that particular stage. To the best of our knowledge this is the first such analysis being performed on human oocytes, which indeed are exceptional cells of the body and demonstrated a unique set of genes being active in the beginning and the end of folliculogenesis. The top functions of differentially expressed genes were similar in both types of oocytes and comprised 'cancer' and 'genetic disorders' involving, i.e. cell cycle checkpoint control and DNA damage response illustrating a broad spectrum of genes involved in processes ensuring the genetic stability of the oocyte in both developmental stages. These observations illustrate key biological events in the oocyte during folliculogenesis.

The *in silico* analysis may include potential batch effects since the cell populations were isolated differentially and RNA purified from paraffin-embedded (primordial) and media samples (MII and granulosa cells), respectively. The application of two different amplification protocols may contribute to bias in the data, despite linear amplification of small samples. Evaluation studies of the Ribo-SPIA protocol compared with the standard Affymetrix T7 linear amplification protocol has shown that hybridization of 2.5 μg of labeled

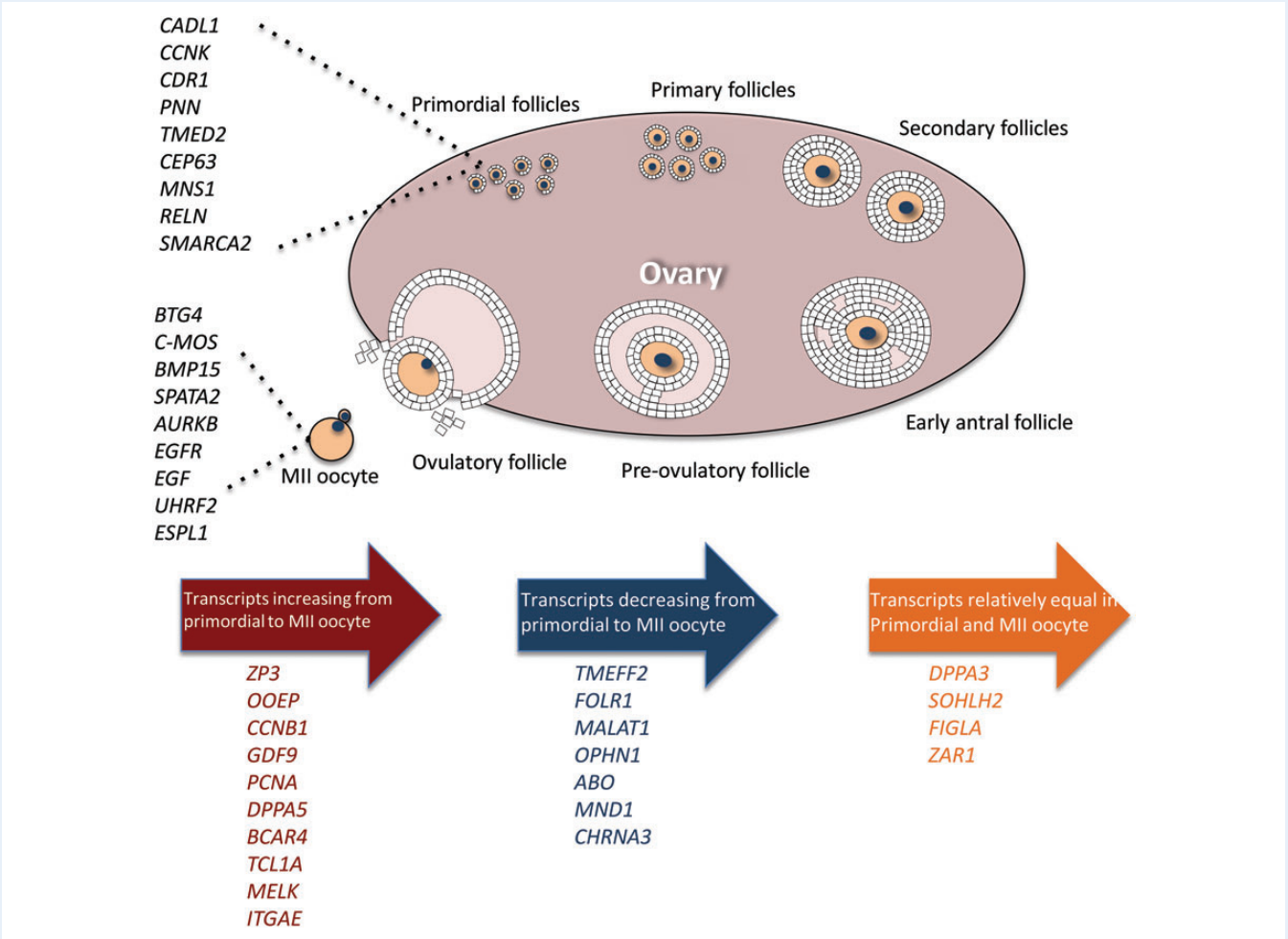

Figure 5 Expressed genes in human oocytes at the beginning and end of folliculogenesis. Expression profiling of human oocytes from primordial follicles and MII oocytes have identified several genes not previously associated with folliculogenesis, and thus, add to the current scenery of the genetic networks and pathways required during two hallmarks of oogenesis: the cell cycle dormant stage and the fully competent stage. Selected genes from the transcriptomes, both with and without previous reported functions in the oocyte, are placed according to their expression at the beginning or end of the folliculogenesis, as indicated with dotted lines, revealing genes specific to oocytes from primordial follicles (*CADL1*, *CCNK*, *CDR1*, *PNN*, *TMED2*, *CEP63*, *MNS1*, *RELN*, *SMARCA2*) and MII oocytes (*BTG4*, *C-MOS*, *BMP15*, *SPATA2*, *AURKB*, *EGFR*, *EGF*, *UHRF2*, *ESPL1*), respectively. Genes listed below red, blue and yellow arrows indicate transcripts increasing, decreasing or comparable in oocytes from primordial follicles and MII oocytes, respectively.

cDNA using Ribo-SPIA gives similar results to arrays that were hybridized with 10 μg cRNA, based on detection call and qRT–PCR analysis (Dafforn *et al.*, 2004; Singh *et al.*, 2005). Overall, the average pair-wise correlation of all signals between the two protocols was 0.73, compared with 0.99 within each protocol batch. Since it has been shown that the two protocols show considerable correlation, but also introduce some level of systemic bias, most pronounced for low expressed genes (Hu *et al.*, 2002), we have chosen to account for this by setting the threshold for differentially expressed genes to show a fold change ~10 and $P < 0.001$. We tested several different control genes to validate the gene expression based on reported oocyte control genes and their optimized used for both oligo-d(T)- and random hexamers-prepared cDNA (Mamo *et al.*, 2007; O'Connor *et al.*, 2012). In addition, the data were confirmed by both qRT–PCR and literature reporting both human and rodent studies, which collectively strongly support our observations.

The pool of oocytes from primordial follicles also contains oocytes from intermediate and primary follicles (Markholt *et al.*, 2012), although oocytes from intermediate and primary follicles are considered to be minor or negligible based on the absence of expression of BMP15 and the relative lower ZP1 expression when compared with MII, since mice studies have shown a dramatic rise in the oocyte BMP15 expression from primordial to primary follicle and a transient high expression of ZP1 in the primary follicle when compared with the MII oocyte (Pan *et al.*, 2005). Likewise, concerns regarding differences in female age, between patients donating oocytes from primordial follicles (11–21 years) and MII oocytes (28–39 years) seem to be negligible, since <1.6% of the transcripts highly enriched in MII were reported to be influenced in MII by increasing age of the woman (Grondahl *et al.*, 2010).

Cell cycle

The transcripts over-expressed in both types of oocytes revealed an enrichment of cell cycle networks, proliferation and related regulatory mechanisms. The PI3K/AKT signaling pathway being a top canonical pathway in the oocyte from the primordial follicle is in line with a suggestion that this pathway has a key role in initiation of follicle growth and hence maintenance of the oocyte pool (John *et al.*, 2008), as oocytes deficient in FOXO3 (substrate for AKT and inducing cell cycle arrest) and PTEN (inhibiting PI3K/AKT pathway) both result in global primordial follicle activation (John *et al.*, 2008). Thus, an enrichment of the PI3K/AKT signaling pathway and presence of both *PTEN* and *FOXO3* expressed at a low to moderate level in the oocytes from the primordial follicle may confirm a constant presence of positive and negative feedback loops (John *et al.*, 2008). Moreover, estradiol has recently been shown to increase PTEN expression in estrogen receptor (ER) positive cells (neuronal cell line; Yang *et al.*, 2011) and AR signaling suggested to inhibit PTEN transcription in prostate and breast cancers (Wang *et al.*, 2012). Both the ER signaling pathway and androgen signaling pathway were enriched in oocytes from primordial follicles and the estrogen receptors (*ERS1* and *ERS2*) as well as AR were present at a low level suggesting importance of these pathways in the oocytes from the primordial follicle potentially involved in the PTEN regulation and other pathways leading to the activation of growth in the primordial follicle. Testosterone has been reported to initiate follicle growth in the primate ovary (Vendola *et al.*, 1999) and the presence of AR expressed at a low level in the human oocyte in the primordial follicle support the suggestion that androgens act directly on the oocyte (Vendola *et al.*, 1999).

One of the genes with the highest relative expression in oocytes from primordial follicles, in contrast to its absence in MII oocytes, was a gene located on the X chromosome encoding the protein Cerebellar Degeneration-Related protein 1 (CDR1). The function of CDR1 is unknown; however, it was identified in a subset of patients with paraneoplastic cerebellar degeneration (PCD) and cell lines derived from cancers of neuroectodermal, kidney, and lung origin (Dropcho *et al.*, 1987) and further detected in tumor tissues from PCD patients (Furneaux *et al.*, 1989). It has been reported that *CDR1* expression in endothelial cell culture was significantly up-regulated by estradiol in a PI3K-dependent fashion (Pedram *et al.*, 2002) and, thus, it will be interesting to evaluate whether the high *CDR1* expression in the oocyte from the primordial follicle is linked to the enriched gene activity of *PI3K/AKT* and ER signaling.

Interestingly, the nicotine receptor cholinergic receptor, nicotinic, alpha 3 (*CHRNA3*) was represented in the top cell cycle/cell death network enriched in the oocytes from primordial follicles. This is the first report of a gene related to smoking being expressed in oocytes. Nicotine has been shown to dose-dependently impair the folliculogenesis in hamster ovaries by increasing the apoptotic cell death in granulosa cells (Bordel *et al.*, 2006). Whether the negative effect of smoking on female fecundity and fertility involves the oocyte nicotine receptor CHRNA3 needs further investigations.

The top bio-functions and pathways represented in the MII oocyte-specific transcriptome represent very diverse functions reflecting accumulation of transcripts during oocyte development and the many functions that the mature oocyte needs to accomplish to ensure reproductive success. However, the mature oocyte itself appears to undertake no or very low transcriptional activity, in line with the function 'transcription' being enriched in oocytes from the primordial follicle. Low transcriptional activities may partly be ensured by Suppression Of the Cytokine Signaling (SOCS) proteins, since several of the SOCS genes contributed to the observed enrichment of the JAK/STAT signaling in the MII oocyte. The enrichment of the ERK/MAPK pathway and the selectively high expression of MOS in MII oocytes enforce that the MOS–MAPK enzyme system is a critical regulator of the meiotic processes including the resumption of meiosis and cycle arrest upon fertilization (Dupre *et al.*, 2011). The enrichment of the 'mitotic roles of polo-like kinases' pathway involving the anaphase promoting complex, several cell division cycle proteins (*CDC7*, *CDC20*, *CDC25*), checkpoint *CHK2* and the dominant cyclin B (*CCNB1*) as well as the up-regulation of *ESPL1* (separase) and *PTTG1* (securin) reveal genes likely to be important in promotion of meiosis, mitosis and cytokinesis upon fertilization. In addition to genes (i.e. GDF9, BMP15 and ZAR1) previously reported as expressed in MII oocytes in other species (Vallee *et al.*, 2005) several genes not previously reported expressed in oocytes were highly expressed in the MII oocyte. One example is the selectively expressed *BOD1* (bi-orientation of chromosomes in cell division 1) that encodes a kinetochore protein (Compton, 2007), suggesting a role in the second meiosis and the subsequent mitosis.

Tumor suppressors and genome protection

Several of the genes highly expressed in the oocyte of the primordial follicle have been reported to be tumor suppressor genes representing both caretakers (repairing damaged genes and holding the cell cycle until repaired) and gatekeepers (inducing apoptosis or senescence).

Of the p53 family of tumor proteins, p63 has been suggested to control the quality and survival of the oocyte pool by involvement in the post-pachytene checkpoint and propensity of oocytes to undergo apoptosis (Levine *et al.*, 2011). In accordance, our data demonstrated that the p63 gene was substantially expressed in human oocytes from the primordial follicle while expression in MII oocytes and somatic cells were very low, confirming previous studies in mice (Suh *et al.*, 2006).

The transcript encoding the SKI-like oncogene (SkiL/SnoN) protein with vital roles in murine follicle development and inhibition of transforming growth factor beta (TGFβ) signaling (Xu *et al.*, 2009) was selectively expressed in oocytes from primordial follicles. In agreement with the TGFβ super family members being key regulators of the folliculogenesis and oogenesis (Trombly *et al.*, 2009), the transcripts of family members *BMP15* and *GDF9* were absent/very low expressed in oocytes from primordial follicles and both expressed at high levels in MII oocytes. This corresponds to recent findings in mice ovaries showing a gradual decline in *SkiL/SnoN* expression during folliculogenesis (Tang and Zhang, 2011), which might be associated with the activation of TGFβ leading to SkiL degradation after the primordial follicle stages and subsequently to promote expression of *GDF9* and *BMP15* mRNA in primary follicles and MII oocytes (McGrath *et al.*, 1995; Aaltonen *et al.*, 1999).

The reelin (*RELN*) gene encodes an extracellular glycoprotein involved in neuron migration in both the developing and adult nervous system (Barros *et al.*, 2011) and was moderately but selectively expressed in oocytes from the primordial follicle. Recently, *RELN* expression has been associated with cancer and suggested to be a possible tumor suppressor (Okamura *et al.*, 2011). Whether RELN is involved in retaining the follicle in the cell cycle dormant stage remains to be clarified, but a potential effect may act via the pregranulosa cells of the primordial follicle, since the *RELN* receptor gene (*LRP8*) has previously been localized

in bovine theca and granulosa cells during later stages of the folliculogenesis (Argov and Sklan, 2004) but no data have been reported from the early stages of folliculogenesis or in human.

Another highly up-regulated gene in the oocyte from the primordial follicle is *TMEFF2* that is also reported to be a tumor suppressor. The anti-proliferative effect of TMEFF2 has been reported to be regulated by androgens (Gery *et al.*, 2002) and Activin A (Tsai *et al.*, 2010), both suggested to be involved in the activation of the primordial follicle (McLaughlin and Telfer, 2010). Future functional studies will show whether TMEFF2 is of importance in keeping the oocyte at the special quiescent cell cycle stage.

To maintain DNA integrity, DNA damage responses coordinate diverse DNA repair and cell cycle checkpoint pathways resulting in cell cycle arrest, DNA repair or apoptosis (Yu and Cortez, 2011). With regard to the cell cycle checkpoint, the most abundant cyclin in the oocytes from the primordial follicle was cyclin K that was more than 100-fold higher expressed than in the mature oocyte and in the somatic cells, which indicates an important role. The cell cycle-dependent expression of cyclin K is new (Yu and Cortez, 2011) but it has been shown to be induced by DNA damage agents via a p53-dependent tumor suppressor pathway (Mori *et al.*, 2002). Experiments in cultured human cells depleted of cyclin K and cyclin-dependent kinase 9 (CDK9), respectively, suggest that CDK9-cyclin K complexes are required for genome maintenance (Yu and Cortez, 2011). Thus the role of the very high cyclin K expression may be to conserve genome integrity in oocytes from the primordial follicle.

One unique characteristic of DNA in oocytes is the high level of homologous recombination. Human *MND1* has been shown to be involved in inducing DNA strand exchange and ensuring the proper synapsis formation of homologous chromosomes in meiosis. An excess amount of the *MND1* protein is necessary to obtain stable homologous pairing in meiosis-specific homologous recombination (Pezza *et al.*, 2010). The observed high expression level of *MND1* in the oocytes from the primordial follicle may be involved in ensuring the stable recombination during the lifespan of the oocytes in the primordial follicle.

Maternal RNAs

Maternal supply of mRNAs to the early embryo is important, as the transition from oocyte to embryo occurs in the absence of transcription (Kronja and Orr-Weaver, 2011). Examples of highly enriched transcripts in the MII oocyte are maternal-effect genes such as the factor in the germline alpha (*FIGLA*), the Zygote Arrest 1 (*ZAR1*), the maternal embryonic leucine zipper kinase (*MELK*) and oocyte-expressed protein homolog (*OOEP*), previously detected in bovine, mouse, and *Xenopus laevis* MII oocytes (Vallee *et al.*, 2005; Raty *et al.*, 2011). Previous studies performed on mouse models reveal that deletion of many of these factors are associated with infertility, such as those encoded by FIGLA (Soyal *et al.*, 2000) and ZAR1 (Wu *et al.*, 2003). The main part of the maternal-effect genes showed a substantial increase in expression in MII oocytes when compared with the oocytes from the primordial follicle. Also the primate specific *NLRP11* (NACHT) was extensively expressed in MII oocytes and more than 12-fold higher than in the oocytes from the primordial follicle. Though, other of the NLRP (or NALP) maternal-effect genes as *NLRP5* (*MATER*) mRNA was highly expressed in both developmental oocyte stages as were *NLRP2* and *NLRP7*. The expression of *NLRP5* in the oocytes from primordial follicles confirms recent immunostaining data on human fetal ovary (Fowler *et al.*, 2009).

How oocytes store and subsequently activate mRNA for translation is not well understood. A recent study in mouse oocytes showed that the DCP1 decapping enzyme homolog A (DCP1A), known to be a part of the mRNA processing (P)-bodies in somatic cells (Sheth and Parker, 2003), re-localize to subcortical aggregates (a novel mRNA storage granules) as the oocyte meiotically matures and the products of the maternal mRNAs are needed (Flemr *et al.*, 2010). In accordance, the *DCP1A* transcript was found in the present data to be 35 times higher expressed in the MII oocytes when compared with the oocytes from primordial follicles. Moreover, we also found expression of transcripts encoding several other RNA-binding proteins, such as the DEAD (Asp-Glu-Ala-Asp) box polypeptide 6 (*DDX6*), the cytoplasmic polyadenylation element-binding protein 1 (*CPEB1*) and the Y box-binding protein 2 (*YBX2*) associated with subcortical accumulation as P-body compartments in maturing oocytes (Flemr *et al.*, 2010). Of these, CPEB1 that modulates poly(A) tail length was highly expressed in MII oocytes, while low expression was found in oocytes from primordial follicles in line with a report on involvement in the post-transcriptional and post-translational regulation during mouse oocyte meiotic maturation (Khan *et al.*, 2005).

Epigenetics and genetics

In the female germ line, initiation of imprinting occurs after birth during oocyte growth (Lucifero *et al.*, 2004; Hiura *et al.*, 2006; Kota and Feil, 2010). Many well-known genes associated with epigenetics were expressed in both oocytes from primordial follicle and in MII, such as the *DNMT*, *HDAC*, *HMT* and *MBD*. *DNMT1* that have been reported to be necessary to maintain DNA methylation imprints during maternal to zygotic development in mice (Hirasawa *et al.*, 2008) and the *DNMT1* transcript was highly expressed in the MII oocyte. The moderate but selective expression of *UHRF2* in MII oocytes may also be of importance for the methylation pattern because UHRF members represent putative regulators of inheritance of the epigenetic code (Pichler *et al.*, 2011). Another highly and selective MII-expressed transcript potentially related to imprinting is *TCL1A*, belonging to the proto-oncogene TCL1 family (Noguchi *et al.*, 2007). *TCL1A* has not previously been detected in the oocyte, but reported to be expressed in testis (Liu *et al.*, 2010), where *TCL1A* was found highly up-regulated in testicular germ cell tumor and categorized as an oncogene as well as a novel stem cell marker (Liu *et al.*, 2010). A recent study suggested *TCL1A* to act as an inhibition of *de novo* DNA methylation (Palamarchuk *et al.*, 2012). In the oocyte of the primordial follicle, another gene involved in chromatin modeling, the SWI/SNF-related, matrix-associated, actin-dependent regulator of chromatin 2 (*SMARCA2*) mRNA was high, and up to 38-fold higher expressed than observed in the MII oocyte, indicating a role in early oogenesis. The low expression level of *SMARCA2* transcripts in human MII oocytes confirms previous observations in murine MII oocytes (Oliveri *et al.*, 2007) and is in line with an increasing methylation of the *SMARCA2* gene during progression of oogenesis in the human ovary (Nagrani *et al.*, 2011).

Insufficient folate intake impairs fertility in animals (Mohanty and Das, 1982) and induces adverse pregnancy outcomes in human (early spontaneous abortions and birth defects) (George *et al.*, 2002), and a daily periconceptional supplementation is recommended by WHO. The high expression of the *FOLR1* in the oocyte from the primordial follicle,

contrasting the lack of expression in mature oocytes, suggests a function in early folliculogenesis. Folate deficiency has been shown to induce DNA breakage in various cell types *in vivo* and *in vitro* as well as cause genomic hypo-methylation in humans and in cells in culture (Crott *et al.*, 2008). Thus, the high expression of *FOLR1* may be involved in protection of the DNA as well as in sustaining appropriate levels of methylation.

Moreover, a recent paper associates *FOLR1* genotypes to oocyte fertilization rate, treatment outcome and risk of pregnancy loss in women undergoing IVF treatment connecting *FOLR1* to oocyte developmental competence (Sivakumaran *et al.*, 2010). Regulation of *FOLR1* expression in other cell types has recently been shown to be under exquisite control of steroid hormones (Sivakumaran *et al.*, 2010); thus the canonical steroid signaling pathways enriched in the oocytes from the primordial follicles may be involved in the regulation of the *FOLR1*.

A recent publication also links female fertility to genotype, suggesting that blood type O is associated with a reduced ovarian reserve, whereas type A was protective to the reserve independent of advancing age (Nejat *et al.*, 2011). Interestingly, we observed that *ABO* was moderately (specific probe set) to highly (less specific probe set) expressed in oocytes from primordial follicles, while low to absent in MII oocytes and granulosa cells, indicating that the *ABO* gene products, the glycosyltransferases may have a function in the primordial follicle.

Exploring epigenetic mechanisms in germ cell development appears to be important in relation to fertility and human health and the current study has highlighted genes that may be interesting to follow during various manipulations performed in connection with assisted reproduction.

Taken together, the present analysis identified new and known reproduction genes associated with specific stages of human oocyte development including genes centered on cell cycle regulation, DNA protection and epigenetics. The function enrichment analysis added novel genes and suggested molecular mechanisms associated with the unique functions of oocyte in its two extremes of the folliculogenesis. It is indeed intriguing that androgen and estrogen receptor signaling are enriched in the unique transcript profile in the oocyte from the primordial follicle and that several of the highly enriched genes in that oocyte stage such as *CDR1*, *FOLR1* and *TMEFF2* expression have been reported to be controlled by steroid hormones in other tissues.

In conclusion, the presented lists of genes being selectively or highly differentially expressed in either of the two developmental extremes of the human oocyte provide an important source for future downstream analysis to further identify genes of significance in human reproduction.

Supplementary data

Supplementary data are available at http://molehr.oxfordjournals.org/.

Acknowledgements

We thank Anders Heuck (Aarhus University) for his technical help on oocyte RNA isolation and qPCR.

Authors' roles

M.L.G. and K.L.-H. performed the study design, analysis and interpretation of data, and participated in writing and finalizing the manuscript. J.V. and R.B. performed the bioinformatic analysis. M.L.G. prepared Figs 1–3, Table I–IV as well as the Supplementary tables. K.L.-H. performed the qPCR, and prepared Table I and Figs 4 and 5 and Supplementary data, Fig. S1. C.Y.A. contributed to the study design, interpretation of data and manuscript preparation. E.E. was involved in patient recruitment.

Funding

This work was supported by an Aarhus University Research Grant (AUFF) to K.L.-H. and by an unrestricted grant from MSD Denmark to M.L.G.

Conflict of interest

None declared.

References

Aaltonen J, Laitinen MP, Vuojolainen K, Jaatinen R, Horelli-Kuitunen N, Seppa L, Louhio H, Tuuri T, Sjoberg J, Butzow R *et al.* Human growth differentiation factor 9 (GDF-9) and its novel homolog GDF-9B are expressed in oocytes during early folliculogenesis. *J Clin Endocrinol Metab* 1999;**84**:2744–2750.

Andersen CL, Jensen JL, Orntoft TF. Normalization of real-time quantitative reverse transcription-PCR data: a model-based variance estimation approach to identify genes suited for normalization, applied to bladder and colon cancer data sets. *Cancer Res* 2004;**64**:5245–5250.

Argov N, Sklan D. Expression of mRNA of lipoprotein receptor related protein 8, low density lipoprotein receptor, and very low density lipoprotein receptor in bovine ovarian cells during follicular development and corpus luteum formation and regression. *Mol Reprod Dev* 2004; **68**:169–175.

Barros CS, Franco SJ, Muller U. Extracellular matrix: functions in the nervous system. *Cold Spring Harb Perspect Biol* 2011;**3**:a005108.

Bolstad BM, Irizarry RA, Astrand M, Speed TP. A comparison of normalization methods for high density oligonucleotide array data based on variance and bias. *Bioinformatics* 2003;**19**:185–193.

Bordel R, Laschke MW, Menger MD, Vollmar B. Nicotine does not affect vascularization but inhibits growth of freely transplanted ovarian follicles by inducing granulosa cell apoptosis. *Hum Reprod* 2006;**21**:610–617.

Bracken CP, Wall SJ, Barre B, Panov KI, Ajuh PM, Perkins ND. Regulation of cyclin D1 RNA stability by SNIP1. *Cancer Res* 2008;**68**:7621–7628.

Brown N, Costanzo V. An ATM and ATR dependent pathway targeting centrosome dependent spindle assembly. *Cell Cycle* 2009;**8**:1997–2001.

Chuang CY, Lin KI, Hsiao M, Stone L, Chen HF, Huang YH, Lin SP, Ho HN, Kuo HC. Meiotic competent human germ cell-like cells derived from human embryonic stem cells induced by BMP4/WNT3A signaling and OCT4/EpCAM selection. *J Biol Chem* 2012;**287**:14389–14401.

Compton DA. Chromosome orientation. *J Cell Biol* 2007;**179**:179–181.

Crott JW, Liu Z, Keyes MK, Choi SW, Jang H, Moyer MP, Mason JB. Moderate folate depletion modulates the expression of selected genes involved in cell cycle, intracellular signaling and folate uptake in human colonic epithelial cell lines. *J Nutr Biochem* 2008;**19**:328–335.

Dafforn A, Chen P, Deng G, Herrler M, Iglehart D, Koritala S, Lato S, Pillarisetty S, Purohit R, Wang M *et al.* Linear mRNA amplification from as little as 5 ng total RNA for global gene expression analysis. *BioTechniques* 2004;**37**:854–857.

Dropcho EJ, Chen YT, Posner JB, Old LJ. Cloning of a brain protein identified by autoantibodies from a patient with paraneoplastic cerebellar degeneration. *Proc Natl Acad Sci USA* 1987;**84**:4552–4556.

Dupre A, Haccard O, Jessus C. Mos in the oocyte: how to use MAPK independently of growth factors and transcription to control meiotic divisions. *J Signal Transduct* 2011;**2011**:350412.

Edsgard D, Scheel M, Hansen NT, Ralfkiaer U, Jensen TS, Skakkebaek NE, Brunak S, Gupta R, Rajpert-De Meyts E, Ottesen AM. Heterozygous deletion at the RLN1 locus in a family with testicular germ cell cancer identified by integrating copy number variation data with phenome and interactome information. *Int J Androl* 2011;**34**:e122–e132.

Eppig JJ. Oocyte control of ovarian follicular development and function in mammals. *Reproduction* 2001;**122**:829–838.

Flemr M, Ma J, Schultz RM, Svoboda P. P-body loss is concomitant with formation of a messenger RNA storage domain in mouse oocytes. *Biol Reprod* 2010;**82**:1008–1017.

Fowler PA, Flannigan S, Mathers A, Gillanders K, Lea RG, Wood MJ, Maheshwari A, Bhattacharya S, Collie-Duguid ES, Baker PJ *et al*. Gene expression analysis of human fetal ovarian primordial follicle formation. *J Clin Endocrinol Metab* 2009;**94**:1427–1435.

Furneaux HM, Dropcho EJ, Barbut D, Chen YT, Rosenblum MK, Old LJ, Posner JB. Characterization of a cDNA encoding a 34-kDa Purkinje neuron protein recognized by sera from patients with paraneoplastic cerebellar degeneration. *Proc Natl Acad Sci USA* 1989;**86**:2873–2877.

George L, Mills JL, Johansson AL, Nordmark A, Olander B, Granath F, Cnattingius S. Plasma folate levels and risk of spontaneous abortion. *J Am Med Assoc* 2002;**288**:1867–1873.

Gery S, Sawyers CL, Agus DB, Said JW, Koeffler HP. TMEFF2 is an androgen-regulated gene exhibiting antiproliferative effects in prostate cancer cells. *Oncogene* 2002;**21**:4739–4746.

Gilchrist RB, Lane M, Thompson JG. Oocyte-secreted factors: regulators of cumulus cell function and oocyte quality. *Hum Reprod Update* 2008; **14**:159–177.

Godinho M, Meijer D, Setyono-Han B, Dorssers LC, van Agthoven T. Characterization of BCAR4, a novel oncogene causing endocrine resistance in human breast cancer cells. *J Cell Physiol* 2011;**226**:1741–1749.

Grondahl ML, Yding Andersen C, Bogstad J, Nielsen FC, Meinertz H, Borup R. Gene expression profiles of single human mature oocytes in relation to age. *Hum Reprod* 2010;**25**:957–968.

Grondahl ML, Andersen CY, Bogstad J, Borgbo T, Hartvig Boujida V, Borup R. Specific genes are selectively expressed between cumulus and granulosa cells from individual human pre-ovulatory follicles. *Mol Hum Reprod* 2012;**18**:572–584.

Gupta SK, Bansal P, Ganguly A, Bhandari B, Chakrabarti K. Human zona pellucida glycoproteins: functional relevance during fertilization. *J Reprod Immunol* 2009;**83**:50–55.

Hirasawa R, Chiba H, Kaneda M, Tajima S, Li E, Jaenisch R, Sasaki H. Maternal and zygotic Dnmt1 are necessary and sufficient for the maintenance of DNA methylation imprints during preimplantation development. *Genes Dev* 2008;**22**:1607–1616.

Hiura H, Obata Y, Komiyama J, Shirai M, Kono T. Oocyte growth-dependent progression of maternal imprinting in mice. *Genes Cells* 2006;**11**:353–61.

Holt LJ, Krutchinsky AN, Morgan DO. Positive feedback sharpens the anaphase switch. *Nature* 2008;**454**:353–357.

Hu L, Wang J, Baggerly K, Wang H, Fuller GN, Hamilton SR, Coombes KR, Zhang W. Obtaining reliable information from minute amounts of RNA using cDNA microarrays. *BMC Genomics* 2002;**3**:16.

Hsieh M, Zamah AM, Conti M. Epidermal growth factor-like growth factors in the follicular fluid: role in oocyte development and maturation. *Semin Reprod Med* 2009;**27**:52–61.

Jagarlamudi K, Rajkovic A. Oogenesis: transcriptional regulators and mouse models. *Mol Cell Endocrinol* 2012;**356**:31–39.

John GB, Gallardo TD, Shirley LJ, Castrillon DH. Foxo3 is a PI3K-dependent molecular switch controlling the initiation of oocyte growth. *Dev Biol* 2008; **321**:197–204.

Kevenaar ME, Themmen AP, van Kerkwijk AJ, Valkenburg O, Uitterlinden AG, de Jong FH, Laven JS, Visser JA. Variants in the ACVR1 gene are associated with AMH levels in women with polycystic ovary syndrome. *Hum Reprod* 2009;**24**:241–249.

Khan SA, Cook AC, Kappil M, Gunthert U, Chambers AF, Tuck AB, Denhardt DT. Enhanced cell surface CD44 variant (v6, v9) expression by osteopontin in breast cancer epithelial cells facilitates tumor cell migration: novel post-transcriptional, post-translational regulation. *Clin Exp Metas* 2005;**22**:663–673.

Kim SK, Suh MR, Yoon HS, Lee JB, Oh SK, Moon SY, Moon SH, Lee JY, Hwang JH, Cho WJ *et al*. Identification of developmental pluripotency associated 5 expression in human pluripotent stem cells. *Stem Cells* 2005;**23**:458–462.

Kim E, Yoon SJ, Kim EY, Kim Y, Lee HS, Kim KH, Lee KA. Function of COP9 signalosome in regulation of mouse oocytes meiosis by regulating MPF activity and securing degradation. *PLoS One* 2011;**6**:e25870.

Kirchmaier AL. Ub-family modifications at the replication fork: Regulating PCNA-interacting components. *FEBS Lett* 2011;**585**:2920–2928.

Ko M, Sohn DH, Chung H, Seong RH. Chromatin remodeling, development and disease. *Mutation Research* 2008;**647**:59–67.

Kremer BE, Adang LA, Macara IG. Septins regulate actin organization and cell-cycle arrest through nuclear accumulation of NCK mediated by SOCS7. *Cell* 2007;**130**:837–850.

Kota SK, Feil R. Epigenetic transitions in germ cell development and meiosis. *Dev Cell* 2010;**19**:675–686.

Kronja I, Orr-Weaver TL. Translational regulation of the cell cycle: when, where, how and why? *Philos Trans R Soc Lond B Biol Sci* 2011; **366**:3638–3652.

Lampson MA, Kapoor TM. The human mitotic checkpoint protein BubR1 regulates chromosome-spindle attachments. *Nat Cell Biol* 2005;**7**:93–98.

Leland S, Nagarajan P, Polyzos A, Thomas S, Samaan G, Donnell R, Marchetti F, Venkatachalam S. Heterozygosity for a Bub1 mutation causes female-specific germ cell aneuploidy in mice. *Proc Natl Acad Sci USA* 2009;**106**:12776–12781.

Le Masson F, Christians E. HSFs and regulation of Hsp70.1 (Hspa1b) in oocytes and preimplantation embryos: new insights brought by transgenic and knockout mouse models. *Cell stress & chaperones*. 2011; **16**:275–285.

Levine AJ, Tomasini R, McKeon FD, Mak TW, Melino G. The p53 family: guardians of maternal reproduction. *Nat Rev Mol Cell Biol* 2011; **12**:259–265.

Liu A, Cheng L, Du J, Peng Y, Allan RW, Wei L, Li J, Cao D. Diagnostic utility of novel stem cell markers SALL4, OCT4, NANOG, SOX2, UTF1, and TCL1 in primary mediastinal germ cell tumors. *Am J Surg Pathol* 2010;**34**:697–706.

Liu YJ, Nakamura T, Nakano T. Essential role of DPPA3 for chromatin condensation in mouse oocytogenesis. *Biol Reprod* 2012;**86**:40.

Lucifero D, Mann MR, Bartolomei MS, Trasler JM. Gene-specific timing and epigenetic memory in oocyte imprinting. *Hum Mol Genet* 2004; **13**:839–849.

Mamo S, Gal AB, Bodo S, Dinnyes A. Quantitative evaluation and selection of reference genes in mouse oocytes and embryos cultured in vivo and in vitro. *BMC Dev Biol* 2007;**7**:14.

Maran C, Tassone E, Masola V, Onisto M. The Story of SPATA2 (Spermatogenesis-Associated Protein 2): From Sertoli Cells to Pancreatic Beta-Cells. *Current Genomics* 2009;**10**:361–363.

Markholt S, Grondahl ML, Ernst EH, Andersen CY, Ernst E, Lykke-Hartmann K. Global gene analysis of oocytes from early stages in human folliculogenesis shows high expression of novel genes in reproduction. *Mol Hum Reprod* 2012;**18**:96–110.

Marshall OJ. PerlPrimer: cross-platform, graphical primer design for standard, bisulphite and real-time PCR. *Bioinformatics* 2004;**20**:2471–2472.

McGrath SA, Esquela AF, Lee SJ. Oocyte-specific expression of growth/differentiation factor-9. *Mol Endocrinol* 1995;**9**:131–136.

McLaughlin M, Telfer EE. Oocyte development in bovine primordial follicles is promoted by activin and FSH within a two-step serum-free culture system. *Reproduction* 2010;**139**:971–978.

McNatty KP, Smith DM, Makris A, Osathanondh R, Ryan KJ. The microenvironment of the human antral follicle: interrelationships among the steroid levels in antral fluid, the population of granulosa cells, and the status of the oocyte in vivo and in vitro. *J Clin Endocrinol Metab* 1979;**49**:851–860.

Mohanty D, Das KC. Effect of folate deficiency on the reproductive organs of female rhesus monkeys: a cytomorphological and cytokinetic study. *J Nutr* 1982;**112**:1565–1576.

Mori T, Anazawa Y, Matsui K, Fukuda S, Nakamura Y, Arakawa H. Cyclin K as a direct transcriptional target of the p53 tumor suppressor. *Neoplasia* 2002;**4**:268–274.

Nagrani SR, Levens ED, Baxendale V, Boucheron C, Chan WY, Rennert OM. Methylation patterns of Brahma during spermatogenesis and oogenesis: potential implications. *Fertil Steril* 2011;**95**:382–384.

Nejat EJ, Jindal S, Berger D, Buyuk E, Lalioti M, Pal L. Implications of blood type for ovarian reserve. *Hum Reprod* 2011;**26**:2513–2517.

Noguchi M, Ropars V, Roumestand C, Suizu F. Proto-oncogene TCL1: more than just a coactivator for Akt. *FASEB J* 2007;**21**:2273–2284.

O'Connor T, Wilmut I, Taylor J. Quantitative evaluation of reference genes for real-time PCR during in vitro maturation of ovine oocytes. *Reprod Domest Anim* 2012. doi:10.1111/rda.12112.

Okamura Y, Nomoto S, Kanda M, Hayashi M, Nishikawa Y, Fujii T, Sugimoto H, Takeda S, Nakao A. Reduced expression of reelin (RELN) gene is associated with high recurrence rate of hepatocellular carcinoma. *Ann Surg Oncol* 2011;**18**:572–579.

Oliveri RS, Kalisz M, Schjerling CK, Andersen CY, Borup R, Byskov AG. Evaluation in mammalian oocytes of gene transcripts linked to epigenetic reprogramming. *Reproduction* 2007;**134**:549–558.

Otsuka F, McTavish KJ, Shimasaki S. Integral role of GDF-9 and BMP-15 in ovarian function. *Mol Reprod Dev* 2011;**78**:9–21.

Palamarchuk A, Yan PS, Zanesi N, Wang L, Rodrigues B, Murphy M, Balatti V, Bottoni A, Nazaryan N, Alder H *et al.* Tcl1 protein functions as an inhibitor of de novo DNA methylation in B-cell chronic lymphocytic leukemia (CLL). *Proc Natl Acad Sci USA* 2012;**109**:2555–2560.

Pan H, O'Brien MJ, Wigglesworth K, Eppig JJ, Schultz RM. Transcript profiling during mouse oocyte development and the effect of gonadotropin priming and development in vitro. *Dev Biol* 2005;**286**:493–506.

Pedram A, Razandi M, Aitkenhead M, Hughes CC, Levin ER. Integration of the non-genomic and genomic actions of estrogen. Membrane-initiated signaling by steroid to transcription and cell biology. *J Biol Chem* 2002;**277**:50768–50775.

Pezza RJ, Camerini-Otero RD, Bianco PR. Hop2-Mnd1 condenses DNA to stimulate the synapsis phase of DNA strand exchange. *Biophys J* 2010;**99**:3763–3772.

Pichler G, Wolf P, Schmidt CS, Meilinger D, Schneider K, Frauer C, Fellinger K, Rottach A, Leonhardt H. Cooperative DNA and histone binding by Uhrf2 links the two major repressive epigenetic pathways. *J Cell Biochem* 2011;**112**:2585–2593.

Ramakers GJ. Rho proteins, mental retardation and the cellular basis of cognition. *Trends Neurosci* 2002;**25**:191–199.

Raty M, Ketoja E, Pitkanen T, Ahola V, Kananen K, Peippo J. In vitro maturation supplements affect developmental competence of bovine cumulus-oocyte complexes and embryo quality after vitrification. *Cryobiology* 2011;**63**:245–255.

Regassa A, Rings F, Hoelker M, Cinar U, Tholen E, Looft C, Schellander K, Tesfaye D. Transcriptome dynamics and molecular cross-talk between bovine oocyte and its companion cumulus cells. *BMC Genomics* 2011;**12**:57.

Saito K, Kondo E, Matsushita M. MicroRNA 130 family regulates the hypoxia response signal through the P-body protein DDX6. *Nucleic Acids Res* 2011;**39**:6086–6099.

Sheth U, Parker R. Decapping and decay of messenger RNA occur in cytoplasmic processing bodies. *Science* 2003;**300**:805–808.

Singh R, Maganti RJ, Jabba SV, Wang M, Deng G, Heath JD, Kurn N, Wangemann P. Microarray-based comparison of three amplification methods for nanogram amounts of total RNA. *Am J Physiol Cell Physiol* 2005;**288**:C1179–C1189.

Sivakumaran S, Zhang J, Kelley KM, Gonit M, Hao H, Ratnam M. Androgen activation of the folate receptor alpha gene through partial tethering of the androgen receptor by C/EBPalpha. *J Steroid Biochem Mol Biol* 2010;**122**:333–340.

Soyal SM, Amleh A, Dean J. FIGalpha, a germ cell-specific transcription factor required for ovarian follicle formation. *Development* 2000;**127**:4645–4654.

Suh EK, Yang A, Kettenbach A, Bamberger C, Michaelis AH, Zhu Z, Elvin JA, Bronson RT, Crum CP, McKeon F. p63 protects the female germ line during meiotic arrest. *Nature* 2006;**444**:624–628.

Tanaka M, Kihara M, Hennebold JD, Eppig JJ, Viveiros MM, Emery BR, Carrell DT, Kirkman NJ, Meczekalski B, Zhou J *et al.* H1FOO is coupled to the initiation of oocytic growth. *Biol Reprod* 2005;**72**:135–142.

Tang X, Zhang C. Relationship between Sloan-Kettering virus expression and mouse follicular development. *Endocrine* 2011;**40**:187–195.

Tashiro F, Kanai-Azuma M, Miyazaki S, Kato M, Tanaka T, Toyoda S, Yamato E, Kawakami H, Miyazaki T, Miyazaki J. Maternal-effect gene Ces5/Ooep/Moep19/Floped is essential for oocyte cytoplasmic lattice formation and embryonic development at the maternal-zygotic stage transition. *Genes Cells* 2010;**15**:813–828.

Tian X, Pascal G, Monget P. Evolution and functional divergence of NLRP genes in mammalian reproductive systems. *BMC Evol Biol* 2009;**9**:202.

Trombly DJ, Woodruff TK, Mayo KE. Roles for transforming growth factor beta superfamily proteins in early folliculogenesis. *Semin Reprod Med* 2009;**27**:14–23.

Tsai ZY, Singh S, Yu SL, Kao LP, Chen BZ, Ho BC, Yang PC, Li SS. Identification of microRNAs regulated by activin A in human embryonic stem cells. *J Cell Biochem* 2010;**109**:93–102.

Uzbekova S, Arlot-Bonnemains Y, Dupont J, Dalbies-Tran R, Papillier P, Pennetier S, Thelie A, Perreau C, Mermillod P, Prigent C *et al.* Spatio-temporal expression patterns of aurora kinases a, B, and C and cytoplasmic polyadenylation-element-binding protein in bovine oocytes during meiotic maturation. *Biol Reprod* 2008;**78**:218–233.

Vallee M, Gravel C, Palin MF, Reghenas H, Stothard P, Wishart DS Sirard MA. Identification of novel and known oocyte-specific genes using complementary DNA subtraction and microarray analysis in three different species. *Biol Reprod* 2005;**73**:63–71.

Vendola K, Zhou J, Wang J, Famuyiwa OA, Bievre M, Bondy CA. Androgens promote oocyte insulin-like growth factor I expression and initiation of follicle development in the primate ovary. *Biol Reprod* 1999;**61**:353–357.

Verdaasdonk JS, Bloom K. Centromeres: unique chromatin structures that drive chromosome segregation. Nat Rev *Mol Cell Biol* 2011;**12**:320–332.

Wang Y, He X, Ngeow J, Eng C. GATA2 negatively regulates PTEN by preventing nuclear translocation of androgen receptor and by androgen-independent suppression of PTEN transcription in breast cancer. *Hum Mol Genet* 2012;**21**:569–576.

Westergaard CG, Byskov AG, Andersen CY. Morphometric characteristics of the primordial to primary follicle transition in the human ovary in relation to age. *Hum Reprod* 2007;**22**:2225–2231.

Wu X, Viveiros MM, Eppig JJ, Bai Y, Fitzpatrick SL, Matzuk MM. Zygote arrest 1 (Zar1) is a novel maternal-effect gene critical for the oocyte-to-embryo transition. *Nat Genet* 2003;**33**:187–191.

Xu WW, Kong XB, An LG, Zhang C. Relationship between SnoN expression and mouse follicular development, atresia, and luteinization. *Zoolog Sci* 2009;**26**:66–73.

Yanagida M. Clearing the way for mitosis: is cohesin a target? *Nat Rev Mol Cell Biol* 2009;**10**:489–496.

Yang L, Wang Y, Chen P, Hu J, Xiong Y, Feng D, Liu H, Zhang H, Yang H, He J. Na(+)/H(+) exchanger regulatory factor 1 (NHERF1) is required for the estradiol-dependent increase of phosphatase and tensin homolog (PTEN) protein expression. *Endocrinology* 2011; **152**:4537–4549.

Yu DS, Cortez D. A role for CDK9-cyclin K in maintaining genome integrity. *Cell Cycle* 2011;**10**:28–32.

Zheng P, Dean J. Oocyte-specific genes affect folliculogenesis, fertilization, and early development. *Semin Reprod Med* 2007;**25**:243–251.

Zhou J, Yang F, Leu NA, Wang PJ. MNS1 is essential for spermiogenesis and motile ciliary functions in mice. *PLoS Genet* 2012;**8**:e1002516.

OPEN ACCESS Freely available online

PLoS one

Gene Bionetwork Analysis of Ovarian Primordial Follicle Development

Eric E. Nilsson[1], Marina I. Savenkova[1], Ryan Schindler[1], Bin Zhang[2], Eric E. Schadt[2], Michael K. Skinner[1]*

1 Center for Reproductive Biology, School of Molecular Biosciences, Washington State University, Pullman, Washington, United States of America, **2** Sage Bionetworks, Seattle, Washington, United States of America

Abstract

Ovarian primordial follicles are critical for female reproduction and comprise a finite pool of gametes arrested in development. A systems biology approach was used to identify regulatory gene networks essential for primordial follicle development. Transcriptional responses to eight different growth factors known to influence primordial follicles were used to construct a bionetwork of regulatory genes involved in rat primordial follicle development. Over 1,500 genes were found to be regulated by the various growth factors and a network analysis identified critical gene modules involved in a number of signaling pathways and cellular processes. A set of 55 genes was identified as potential critical regulators of these gene modules, and a sub-network associated with development was determined. Within the network two previously identified regulatory genes were confirmed (i.e., Pdgfa and Fgfr2) and a new factor was identified, connective tissue growth factor (CTGF). CTGF was tested in ovarian organ cultures and found to stimulate primordial follicle development. Therefore, the relevant gene network associated with primordial follicle development was validated and the critical genes and pathways involved in this process were identified. This is one of the first applications of network analysis to a normal developmental process. These observations provide insights into potential therapeutic targets for preventing ovarian disease and promoting female reproduction.

Citation: Nilsson EE, Savenkova MI, Schindler R, Zhang B, Schadt EE, et al. (2010) Gene Bionetwork Analysis of Ovarian Primordial Follicle Development. PLoS ONE 5(7): e11637. doi:10.1371/journal.pone.0011637

Editor: Hugh Clarke, McGill University, Canada

Received March 18, 2010; **Accepted** June 11, 2010; **Published** July 16, 2010

Funding: National Institutes of Health (NIH) R01 HD043093-01. The funders had no role in study design, data collection and analysis, decision to publish, or preparation of the manuscript.

Competing Interests: The authors have declared that no competing interests exist.

* E-mail: skinner@wsu.edu.edu

Introduction

An emerging concern in the field of biomedical research is that the common reductionist approach to studying biological processes may not be adequate to fully understand the complex interplay of cellular signaling, gene expression, and other complex molecular processes that occur within a tissue or organ. Examples of reductionist studies that have driven much of our understanding of biological processes associated with complex phenotypes like disease include the knockout mouse experiments and *in vitro* cytokine treatment to assess the effects of gene-specific perturbations on cell or tissue biology. Results from these types of studies provide information on candidate regulatory factors, but typically do not elucidate the network of factors or processes required for a normal developmental biology or pathobiology. A holistic, systems biology, approach to studying normal developmental processes can be a powerful tool that is complementary to the more reductionist experiments. In the spirit of a systems-based approach to development, the current study was designed to identify gene networks involved in ovarian primordial follicle development and to characterize critical regulatory factors involved in this development process.

In mammals, all the oocytes (eggs) that will be used over a female's lifetime are present in the ovary at birth in a finite pool. These oocytes are arrested in prophase of the first meiotic division and are each surrounded by flattened pre-granulosa cells to form a structure called a primordial follicle [1]. During the reproductive lifespan of a female, follicles gradually leave the arrested pool to undergo a primordial to primary follicle transition. A follicle undergoing follicle transition has an increase in oocyte diameter and the associated granulosa cells proliferate and change from a flattened to cuboidal in shape. Once primordial to primary follicle transition has occurred the follicle either continues to develop to the point of ovulation or undergoes atresia [1,2,3,4]. Previously cell-to-cell communication with extra-cellular growth factors has been shown to regulate the initiation of primordial follicle development. These studies have primarily used a reductionist approach to test candidate growth factors one at a time for their ability to affect follicle transition. A number of paracrine growth factors have been identified as having a role in early follicle development (reviews [4,5]).

To move beyond examining single gene effects on this development process, gene network analysis can be employed to identify groups (e.g. modules) of genes whose expression is regulated in a coordinated manner (gene network) [6,7,8]. In this type of analysis, a biological system is surveyed in the context of disease (or other interesting phenotypes) with microarrays multiple times with and without perturbations that cause the system to change. A novel bioinformatics analysis is used to identify modules of genes associated with biological systems (bionetwork). The great majority of network analyses have focused on disease states and been used to better understand the systems biology of disease processes and identify potential therapeutic targets [9,10,11, 12,13,14,15]. The current study was designed to determine if

network analysis can be applied to study a normal development process.

The current study used whole rat ovaries cultured *in vitro* in a manner that allowed primordial to primary follicle transition. The ovaries were treated with one of eight different growth factors previously shown to regulate primordial follicle transition in comparison to untreated control cultures. The mRNA was isolated from the ovaries and used for microarray transcriptome analysis to globally survey gene expression under these different treatment conditions. The effects of each growth factor on gene expression were analyzed to determine similarities and differences in gene expression between the different growth factor treatments. Those genes whose mRNA expression changed with any treatment were subjected to network analysis to identify pathways and genes with a high degree of connectivity between other genes and pathways. From the networks constructed from these data we identified a list of critical modules of regulated genes forming gene sub-networks that were used to identify regulatory genes involved in primordial follicle development. Not only were previously identified regulatory factors/genes associated with this process identified from this network analysis, but a number of putative regulators of follicle transition not previously associated with this process were also determined. One of the new candidate genes, connective tissue growth factor (Ctgf) [16], was tested experimentally and found to promote primordial to primary follicle transition. Observations demonstrate the utility of this network analysis to be used as a systems biology approach to study normal developmental processes in complex systems.

Number of Genes and Pathways Overlapped

	#PW	AMH	FGF2	BMP4	GDNF	FGF7	KITLG	LIF	PDGFab	CTGF
# genes		56	41	22	20	36	54	56	41	12
AMH	268		28	18	14	29	37	40	32	7
FGF2	248	10		13	11	19	27	29	17	7
BMP4	79	4	5		9	11	14	16	13	6
GDNF	148	14	7	3		9	9	11	11	3
FGF7	123	36	5	1	5		28	25	17	5
KITLG	271	8	5	3	1	2		39	24	8
LIF	349	7	18	13	4	3	18		30	9
PDGFab	275	18	22	3	14	5	7	10		6
CTGF	155	5	7	2	1	2	6	2	6	

Figure 1. Number of genes and pathways overlapped between signature (growth factor treatment group) lists. Total number of differentially expressed genes for each growth factor is shown in dark yellow column, number of genes overlapped between each pair of signature lists – in light yellow columns. Total number of KEGG pathways affected by each growth factor is shown in dark green row; number of KEGG pathways overlapped for each pair of growth factors is shown in light green row. CTGF analysis separate from the network analysis.
doi:10.1371/journal.pone.0011637.g001

Results

Primordial Follicle Transcriptome Analysis

A number of regulatory factors have been shown to affect primordial to primary follicle transition, including Amh [17,18], Fgf2 [19,20,21], Bmp4 [22,23], Gdnf [24], Fgf7/KGF [25], Kitlg [19,26,27], Lif [28] and Pdgfa [29]. In order to determine the underlying gene networks and processes involved in primordial follicle development, microarray analysis was performed on RNA from whole rat ovaries treated for two days in vitro with each of the above listed growth factors independently. There were three independent RNA samples of pooled ovaries for each growth factor treatment (except for GDNF, which had only two sample replicates), and corresponding control samples for a total of 38 RNA samples. These were evaluated using 38 Affymetrix Rat Gene 1.0 ST microarrays. The array data were analyzed together using normalization and pre-processing described in the Methods. Each growth factor treatment resulted in 79 to 349 genes with altered expression compared to controls (Figure 1). The lists of the genes affected by each treatment are presented in Table S1. There were relatively few genes with altered expression in common between the different treatments (Figure 1). Less than 10% of the genes changed by any one growth factor treatment were found to be changed in any other treatment. The exception was Fgf7/KGF, which had a more than 30% overlap of altered genes with Amh. There were no individual genes that changed expression levels in response to more than three of the eight original treatments (Table S1).

The complete list of genes whose expression levels changed with any of the treatments was compared to curated lists of genes from the KEGG database to identify processes that may be important for primordial follicle development. Automated unbiased matching of lists of affected genes to KEGG pathways was performed with Pathway Express (Intelligent Systems and Bioinformatics Laboratory; http://vortex.cs.wayne.edu/ontoexpress/). Pathways heavily impacted by genes whose expression altered in response to the growth factor treatments (Table 1) included pathways involved in cell surface and extracellular matrix regulation (cell adhesion molecules, adherens junction, focal adhesion, tight junction, gap junction, regulation of actin cytoskeleton), known signaling pathways (MAPK, notch, B-cell receptor, adipocytokine, toll-like receptor, ErbB, GnRH, Wnt, hedgehog, VEGF, Jak-STAT, TGF-beta, p53, insulin, PPAR), the complement cascade, axon guidance, glycan structure biosynthesis and pathways listing cell communication ligand-receptor interactions (cytokine-cytokine receptor, neuroactive ligand-receptor, ECM-receptor). There was a high degree of overlap of affected pathways between different growth factor treatments (Figure 1). For the list of pathways containing altered genes, from 70% to 82% of those pathways are shared with at least one other treatment. Application of the hypergeometrical Fisher Exact Test to assess whether the number of overlapped pathways was significantly greater than expected by chance, revealed that the majority were statistically significant. The pathways containing altered genes from several growth factor treatments are presented in Table 1. Although few altered genes were found to overlap between different treatments (Figure 1), each growth factor treatment influenced similar pathways, Table 1 and Table S1. Therefore, each growth factor affects similar pathways via different genes.

Bionetwork Analysis

The complete list of genes whose expression levels changed with any growth factor treatment was subjected to a network analysis as described in Methods. Potential batch effects for culture date, RNA processing data and microarray performance date were corrected during the analysis, with no major effect on the analysis. The data were fit using a robust linear regression model (rim function from R statistical package), and then the residuals with respect to the model fit were carried forward in all subsequent analysis. The network analysis scores each gene according to how

Table 1. Number of Regulated Genes in Pathways.

Pathway Name	Total List (1540)		Module Lists																Signature Lists								
	Total Overlap Number	Impact Factor	Short/Connected List	turquoise	blue	brown	yellow	green	red	black	pink	magenta	purple	green-yellow	tan	salmon	cyan	grey	AMH	bFGF	BMP4	GDNF	KGF	KL	LIF	PDGF	CTGF
Number of genes in the list			**55**	**194**	**182**	**158**	**150**	**139**	**112**	**99**	**85**	**68**	**45**	**32**	**29**	**28**	**22**	**157**	**268**	**248**	**79**	**148**	**123**	**271**	**349**	**275**	**155**
Neuroactive ligand-receptor interaction	**22**	**1.23**	1	2		5	2	1	3			1	1	2	1		1	3	4	5		1	4	5	4	6	3
Focal adhesion	**19**	**3.62**	3	7	1	7	1		1			1	1						3	3			4	8	3	1	
MAPK signaling pathway	**19**	**3.00**	6	7	1	3	4	1						1			1	1	6		4		5	4	6		
Cell adhesion molecules (CAMs)	**15**	**107**	1	1	3	2	1		1			3		1	1			2	6	2	3	2		3	2	2	1
Axon guidance	**15**	**6.34**	1	4	1	2	4	1						1	1				6		1	3	2	3	3	3	
Cytokine-cytokine receptor interaction	**15**	**2.24**	1	3	3	4	3			1								1	2	1	4		1	6	5		1
Calcium signaling pathway	**13**	**1.72**	1	3		5	1		2					1			1		3	2		1	2	3	4	1	
Regulation of actin cytoskeleton	**12**	**2.18**	2	5	1	4	2												4	2			5	4			
Cell Communication	**11**	**4.70**		2		4	3		1			1							3	1	2		1	4	1	1	
Jak-STAT signaling pathway	**11**	**1.88**		3	1	3	1			2				1					1	1			1	4	4		1
Adipocytokine signaling pathway	**10**	**2.94**		2			2	2			1		1	1		1			1	1	2				7	1	1
ECM-receptor interaction	**9**	**4.23**	2	2		4	2		1										1	2	1			5	2		
Complement and coagulation cascades	**9**	**3.63**		1	1	2	4							1						2	4			1	4		1
Apoptosis	**9**	**2.94**		1		2	2	1		2	1								2	1	2			2	5		
Toll-like receptor signaling pathway	**9**	**2.92**		3	1	1		1	1					1				1	2	1	1		1	2	1	1	
Leukocyte transendothelial migration	**9**	**2.74**		1	2	3	1					1						1	3	1				5	1		
Gap junction	**9**	**2.73**	1	2	1	2	2	1						1					2				1	3	1	3	
Insulin signaling pathway	**9**	**1.35**			1	1		1	2			1	2			1				2	1		1	4		2	1
Adherens junction	**8**	**33.1**		3		3						1						1	2					3	4	1	
Glycan structures - biosynthesis 2	**8**	**3.83**	1	2	2			1	1							1		1	1	3		1	3		1		
T cell receptor signaling pathway	**8**	**2.71**		2	1	1	1						1					2	3			1	2	2	1		
Tight junction	**7**	**3.28**		1		1	1	1	1			1						1		1				2	4		
GnRH signaling pathway	**6**	**2.84**	1	2		2											1	1	1				2	2	1		
TGF-beta signaling pathway	**6**	**1.40**		1	2						1	2							1		2	1	2		1	1	1

Table 1. Cont.

Pathway Name	Total List (1540)		Module Lists																Signature Lists								
	Total Overlap Number	Impact Factor	Short/Connected List	turquoise	blue	brown	yellow	green	red	black	pink	magenta	purple	green-yellow	tan	salmon	cyan	grey	AMH	bFGF	BMP4	GDNF	KGF	KL	LIF	PDGF	CTGF
Number of genes in the list			**55**	**194**	**182**	**158**	**150**	**139**	**112**	**99**	**85**	**68**	**45**	**32**	**29**	**28**	**22**	**157**	**268**	**248**	**79**	**148**	**123**	**271**	**349**	**275**	**155**
PPAR signaling pathway	**6**	**1.24**	1	1		1	1	1								1		1		1		1		1	2		
Antigen processing and presentation	**5**	**36.8**			1			1				2						1	1	1	1	1			1		
Melanogenesis	**5**	**3.34**	1	2		1	1				1								1	1				1	2	1	
B cell receptor signaling pathway	**5**	**2.95**		2	1	2													2	1		1		2			
Wnt signaling pathway	**5**	**2.84**		3			1								1				2	1				1	3		
Hematopoietic cell lineage	**5**	**1.28**		1	1		2											1	1	2	2		1		1		
ErbB signaling pathway	**4**	**2.89**				2	1											1	1				1	3			
Hedgehog signaling pathway	**4**	**2.38**		2		2													1	2					1	1	
VEGF signaling pathway	**4**	**2.17**		1		2							1						1					1	1	1	
p53 signaling pathway	**4**	**1.37**			1		1			1				1							1			1	2	1	
Glycan structures - biosynthesis 1	**4**	**0.85**		1	1				1										1	1	2	1	1				
Renin-angiotensin system	**3**	**3.21**															1	2		1				2			
Notch signaling pathway	**3**	**2.95**				1	1	1											1					1	1		1
mTOR signaling pathway	**3**	**2.82**				1						1	1							1				1	1	1	
Basal transcription factors	**3**	**2.03**							1		1					1				1		1	1				
Fc epsilon RI signaling pathway	**3**	**1.87**		1		1							1						1					2			
Nucleotide excision repair	**3**	**1.49**														1		2	2	1			1			1	
Cell cycle	**3**	**1.13**	1	1					1					1							1		1	1	1		
Ubiquitin mediated proteolysis	**3**	**0.98**	1	1		1					1									1			1	1			
Phosphatidylinositol signaling system	**2**	**28.0**						1										1							2		

Number of regulated genes in affected KEGG pathways for each of modules and signature (Growth Factor Treatment) lists.

Pathway enrichment analysis was performed using KEGG database, current for July 2009, for which gene symbols were used as input data. From 1,540 probe sets, 1,137 were identified as annotated genes using Affymetrix RaGene-1_0-st-v1 Transcript Cluster Annotations, release 28 (March, 2009). Top 44 pathways shown except for disease pathways (not shown). No KEGG pathways were affected by genes from light-cyan or midnight-blue modules.

doi:10.1371/journal.pone.0011637.t001

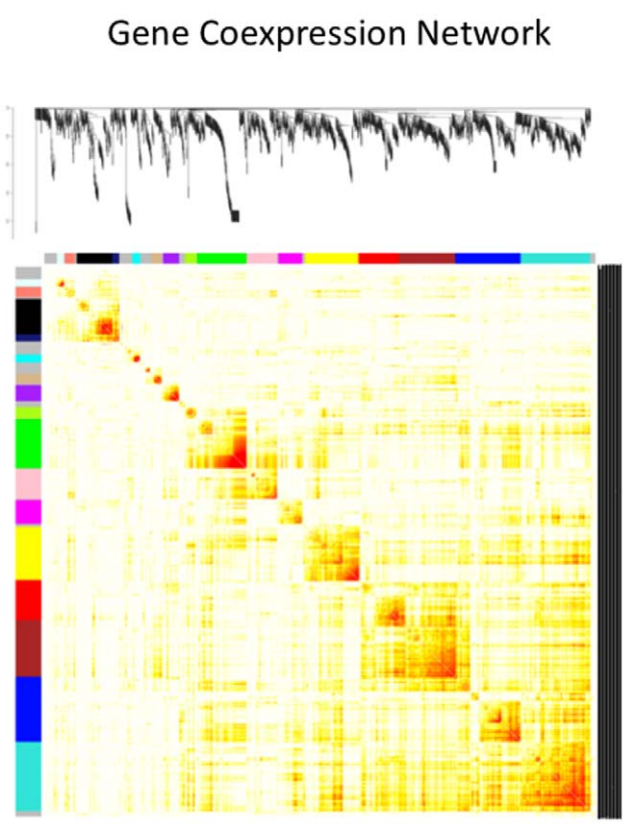

module	size
turquoise	194
blue	182
brown	158
yellow	150
green	139
red	112
black	99
pink	85
magenta	68
purple	45
greenyellow	32
tan	29
salmon	28
cyan	22
midnightblue	20
lightcyan	20

Figure 2. The ovary gene co-expression network and corresponding gene modules. A topological overlap matrix of the gene co-expression network consisting of the 1540 genes regulated by the various growth factors. Genes in the rows and columns are sorted by an agglomerative hierarchical clustering algorithm (see Methods). The different shades of color signify the strength of the connections between the nodes (from white signifying not significantly correlated to red signifying highly significantly correlated). The hierarchical clustering (top) and the topological overlap matrix strongly indicate highly interconnected subsets of genes (modules). Modules identified are colored along both column and row and are boxed. The number of genes in each module is listed as size of module.
doi:10.1371/journal.pone.0011637.g002

well, under different treatments, its changes in gene expression are correlated with the changes in expression of every other gene. This gives a connectivity score for each gene. High connectivity scores indicate that expression of this gene changes in concert with that of many other genes. In addition, the network analysis identifies gene modules in which the member genes have similar changes in expression in response to the various growth factor treatments. Gene modules are functional components of the network that are often associated with specific biological processes. To identify modules comprised of highly interconnected expression traits within the co-expression network, we examined the topological overlap matrix [30] associated with this network. The topological overlap between two genes not only reflects their more proximal interactions (e.g., two genes physically interacting or having correlated expression values), but also reflects the higher order interactions that these two genes may have with other genes in the network. Figure 2 depicts a hierarchically clustered topological overlap map in which the most highly interconnected modules in the network are readily identified. The specific details of the gene co-expression network analysis (Figure 2) are presented in the Methods section. To identify gene modules (sub-networks) formally from the topological overlap map, we employed a previously described dynamic cut-tree algorithm with near optimal performance on complicated dendrograms [31] (see Methods for details). Figure 2 shows the topological overlap map of the co-expression network with gene modules color-coded for the 16 modules identified. The membership of each module can be found in Table S1. The sixteen modules contained 1,383 genes with the remaining 157 genes (colored as gray) not failing into any module.

The pathways containing genes whose expression changed with growth factor treatment were compared to the genes from each module that were associated with specific pathways (Table 1 and Table S1 for full list). For most pathways genes from several network modules were present. However, several pathways were associated with selected modules. For example, out of 19 altered genes present in the focal adhesion pathway, seven were from the turquoise module and seven from the brown. Similarly, of the five altered genes in the Wnt signaling pathway three were from the turquoise module. For the fifteen changed genes in the cell adhesion molecule pathways three were from blue and three from magenta modules. Those genes whose expression changed with specific growth factor treatments were cross-matched with the genes assigned to each network module to determine if specific modules were heavily influenced by particular growth factors. Interestingly, each module was biased toward having many genes in common with selected growth factors (Table S1). In contrast, some growth factor treatments induced changes in genes that were distributed among several different modules.

In order to identify genes that could be key regulators of primordial follicle development, a shorter list of candidate genes was generated from the results of the network analysis. Six modules were chosen for having the highest numbers of known

regulatory genes and pathways (yellow, turquoise, blue, brown, red, purple). The top 10% of most connected transcripts in each of the six modules were identified as potential important regulators [13,15], except for the blue module for which the top 20% were chosen since so many of that module's most highly connected transcripts were not annotated as genes. The compiled list included 55 transcripts annotated as genes (Table 2), and these genes were subjected to more intensive investigation.

An automated unbiased analysis of published scientific literature was applied to the lists of differentially expressed genes described above using Genomatix/BiblioSphere software, as described in the Methods. Figure 3 shows a small integrated gene network among the short list of the 55 candidate regulators (Table 2). These relationships in literature raise the possibility that physiological interactions exist between these genes. The gene Ctgf (Connective tissue growth factor) was seen to relate to several other genes with high connectivity, Figure 3. Interestingly, two of the identified genes were previously shown to influence primordial follicle development, Pdgfa [29] and Fgfr2 [19,20,21].

The entire set of 1540 transcripts differentially expressed with growth factor treatment was also subjected to analysis using BiblioSphere. Only 632 were recognized by BiblioSphere and 613 were connected. A diagram of literature relationships between these genes is presented in Figure S1. Five major gene clusters were identified as associated with Nfkb1, Vegfa, Gadd45a, Esr1 and Egfr1. This analysis is useful to compare with the expression network analysis, but is biased toward the literature and finding relationships among more heavily studied factors.

Analysis of CTGF Actions

Critical regulatory candidates for primordial follicle development were selected due to their being differentially expressed in response to treatment with growth factors, having a high connectivity score, and being related in literature to other highly connected genes. For the purpose of the current study, candidate regulatory genes that were also extracellular growth factors were considered. Therefore, CTGF was selected based on all these criteria for further analysis. Experiments were performed to see if CTGF could regulate primordial to primary follicle transition. Ovaries from four-day old rats were treated with 50ng/ml CTGF protein for ten days in an organ culture system as described in the Methods (Figure 4A and 4B). Transforming growth factor beta 1 (TGFB1), which is known to interact with CTGF [32,33], was also tested. Untreated cultured ovaries were used as a negative control, and ovaries treated with 50ng/ml each of Kit ligand (KITL) and Fibroblast growth factor 2 (FGF2) were used as a positive control. CTGF treatment resulted in a significant ($p<0.05$) increase in developing follicles compared to untreated controls, as did treatment with the combination of KITL and FGF2 (Figure 4C). TGFB1 had no effect, either alone or in combination with CTGF.

RNA was collected from CTGF and control cultured ovaries as described in the Methods from three replicate experiments. The RNA was used for microarray analysis using the same criteria as for the other growth factors used in the network analysis. One hundred fifty-five transcripts were differentially expressed in CTGF-treated ovaries, Table S1. As was seen for the other growth factors used in the network analysis, there was little overlap of these changed genes with the genes showing changed expression in response to any other growth factor treatment, Figure 1. However, as seen among the other growth factors, there was a high degree of overlap between the pathways impacted by CTGF treatment and treatment with other growth factors (Figure 1). Therefore, a critical regulatory gene predicted from the network analysis was confirmed to regulate primordial follicle development.

Discussion

A systems biology approach was used to elucidate the changes in gene expression that are important for ovarian primordial to primary follicle transition. A gene network analysis was performed on the ovarian transcriptomes following treatment with 8 different growth factors. The rat ovary was used as a model system to test the utility of this approach in investigating a normal developmental process. This is one of the first applications of network analysis to a normal developmental process. The objective was to identify critical regulatory factors and pathways in primordial follicle development following a bionetwork analysis.

Microarray analysis determined the alterations in the ovarian transcriptome that occurred in response to treatment of ovaries with AMH, FGF2, BMP4, GDNF, FGF7, KITL, LIF, and PDGFB. All of these have previously been shown to effect follicle transition [17,18,19,20,21,22,23,24,25,26,27,28,29,34]. All these factors stimulate primordial follicle development except AMH that inhibits follicle development. The presence of both positive and negative factors provides a wider diversity of gene regulation to facilitate the network analysis. As expected the AMH regulated gene set is more distinct from the others. Surprisingly, there were few altered genes in common between all these growth factors and there were no genes that significantly changed in expression level in response to more than three of the eight growth factors. In contrast, the physiological processes impacted by these altered genes were found to have a higher level of overlap. Since a pathway includes groups of genes, it is expected that the overlap of pathways between growth factor treatments will be higher. The overlap of pathways was markedly high (70% to 82%) and statistically different, suggesting pathway associations provide a predicted capacity to identify regulatory factors. Certain pathways were significantly over-represented in the pool of genes with changed expression. This suggests that there are selected physiological pathways that are influenced by all the different growth factors (Figure 5), but that each growth factor affects different genes at different points in these pathways (Table 1). Multiple input points into these physiological pathways could allow for more precise regulation and more effective compensation between the growth factors. Since many growth factors are acting in parallel to regulate these pathways, any one pathway system is robust and maintains function if one growth factor becomes inoperative. Since primordial follicle development is essential for female reproduction, a complex network of regulatory factors influencing different aspects of critical signaling pathways has evolved.

For the eight growth factors evaluated the cellular processes affected in common (Figure 5) included changes in cell contact, morphogenesis, and cell proliferation and differentiation. These are processes that are necessary for the morphological changes that occur with primordial to primary follicle transition. During follicle transition granulosa cells change from squamous to cuboidal and the oocyte starts to grow in diameter (Figure 4B). Unexpectedly, what was also seen as an important affected cellular process was regulation of several key components of the complement and coagulation cascades (Figure S2). These genes are not known for having roles in ovary or follicle development, and merit further investigation.

Gene networks provide a convenient framework for exploring the context within which single genes operate. For gene networks associated with biological systems, the nodes in the network typically represent genes, and edges (links) between any two nodes indicate a relationship between the two corresponding genes. An important end product from the gene co-expression network analysis is a set of gene modules which member genes are more highly correlated with each other than with genes outside a module. It has been

Table 2. List of 55 Candidate Regulatory Genes.

Function	GeneSymbol	GeneBank	Probeset	k.in*	Module	Regulation by Growth Factor	GeneTitle
Apoptosis	Bcl2l10	NM_053733	10911690	10.0	red	KL-dwn	BCL2-like 10
Cell Cycle	Cdkn2c	NM_131902	10878705	7.6	red	KL-dwn	CDK4 inhibitor 2C
ECM	Cdh3	NC_005118	10807525	28.0	turq	AMH-dwn	cadherin 3, type 1, P-cadherin
	Col11a1	AJ005396	10818502	20.6	brown	KL-dwn	collagen, type XI, alpha 1
	Krt19	NM_199498	10747262	25.2	turq	AMH-dwn	keratin 19
	Lama5	NC_005102	10852270	30.9	turq	AMH-dwn	laminin, alpha 5
Development	Bnc2	NM_001106666	10877880	26.5	turq	AMH-dwn	basonuclin 2
	Emx2	NM_001109169	10716454	27.5	turq	KGF-dwn	empty spiracles homeobox 2
	Usmg5	NM_133544	10730633	13.5	blue	AMH, GDNF-dwn	muscle growth 5 homolog (mouse)
Epigenetics	Dnmt1	NM_053354	10915437	22.9	brown	KL-dwn	DNA (cytosine-5-)-methyltransferase 1
Golgi	B4galt6	NM_031740	10803394	11.7	blue	AMH-dwn, KGF-dwn	galactosyltransferase, polypeptide 6
Growth Factors	Ctgf	NM_022266	10717233	8.2	blue	KGF-up, LIF-dwn	connective tissue growth factor
	Il16	NM_001105749	10723351	31.9	turq	AMH-dwn, KGF-dwn	interleukin 16
	Pdgfa	NM_012801	10757129	27.0	turq	AMH-dwn, KGF-dwn	platelet-derived growth factor
Immune	LOC287167	NM_001013853	10741765	21.6	brown	KL-dwn	globin, alpha
Metabolism	Cacna2d3	NM_175595	10789819	19.9	brown	KL-dwn	calcium channel
	Hbq1	XM_001061675	10741761	24.0	brown	KL-dwn	hemoglobin, theta 1
	Hhatl	NM_001106868	10914424	15.7	yellow	PDGF-up	hedgehog acyltransferase-like
	Hmgcs2	NM_173094	10817759	19.5	brown	KL-dwn	Coenzyme A synthase 2
	Hsd11b1	NM_017080	10770795	17.0	yellow	BMP4-dwn	hydroxysteroid 11-beta dehydro
	Kirrel	NM_207606	10824123	14.1	yellow	AMH-dwn	kin of IRRE like (Drosophila)
	Plod2	NM_175869	10912255	18.3	brown	KL-dwn	procollagen lysine, 2-oxoglutarate
	Podxl	NM_138848	10861662	26.6	turq	AMH-dwn, KGF-dwn	podocalyxin-like
	Scn3a	NM_013119	10845809	17.4	brown	KL-dwn	sodium channel, type III, alpha
	Slc4a4	NM_053424	10775997	29.0	turq	AMH-dwn, KGF-dwn	solute carrier family 4
	Slc7a5	NM_017353	10811531	15.6	yellow	PDGF-up	solute carrier family 7
	Slc29a1	NM_031684	10921833	15.4	yellow	PDGF-up	solute carrier family 29
	Eno1	NM_012554	10874152	9.0	purple	PDGF-up	enolase 1, (alpha)
Receptors	Axl	NM_031794	10719900	15.4	yellow	BMP4-dwn	Axl receptor tyrosine kinase
	Ednrb	NM_017333	10785724	20.7	brown	KL-dwn	endothelin receptor type B
	Fgfr2	NM_012712	10726172	30.8	turq	AMH-dwn, KGF-dwn	fibroblueast growth factor receptor 2
	Itgb3bp	NM_001013213	10878272	11.0	blue	GDNF-dwn	integrin beta 3 binding protein
	Plxna4a	NM_001107852	10861678	30.9	turq	AMH-dwn, KGF-dwn	plexin A4, A
	Tmem151a	NM_001107570	10727725	26.2	turq	AMH-dwn, KGF-dwn	transmembrane protein 151A
Signaling	Nrgn	NM_024140	10916228	16.1	yellow	AMH, KGF-dwn, PDGF-up	neurogranin
	Dusp4	NM_022199	10792035	17.3	yellow	AMH-dwn	dual specificity phosphatase 4
	Dusp6	NM_053883	10895144	16.6	yellow	BMP4-dwn	dual specificity phosphatase 6
	Efna5	NM_053903	10930204	15.0	yellow	AMH, GDNF-dwn	ephrin A5
	Map3k1	NM_053887	10821276	26.8	turq	KGF-dwn	mitogen activated protein kinase
	Pde7b	NM_080894	10717069	17.8	brown	KL-dwn	phosphodiesterase 7B
	Rem1	NM_001025753	10840861	14.5	yellow	PDGF-up	RAS (RAD and GEM)-like
	Shc4	NC_005102	10849423	17.0	yellow	AMH-dwn	SHC family, member 4
	Ubash3b	AC_000076	10916476	16.9	yellow	PDGF-up	ubiquitin associated
Transcription	Btg4	NM_001013176	10909937	7.4	red	KL-dwn	B-cell translocation gene 4
	Etv5	NM_001107082	10752034	14.4	yellow	AMH-dwn	ets variant 5
	Fbxo15	NM_001108436	10803025	11.9	red	KL-dwn	F-box protein 15
Misc. & Unknown	Depdc2	NM_001107899	10875023	29.5	brown	KL-dwn	DEP domain containing 2
	Fam154a	AC_000073	10877890	11.4	red	KL-dwn	similarity 154, member A
	LOC686725	AC_000076	10915208	25.9	turq	AMH-dwn	hypothetical protein LOC686725

Table 2. Cont.

Function	GeneSymbol	GeneBank	Probeset	k.in*	Module	Regulation by Growth Factor	GeneTitle
	RGD1306186	BC090317	10881318	9.2	red	KL-dwn	similar to RIKEN cDNA 4930569K13
	RGD1306622	XM_001074493	10728647	32.6	turq	AMH-dwn, KGF-dwn	similar to KIAA0954 protein
	RGD1308023	XR_006437	10850490	17.6	brown	KL-dwn, LIF-dwn	similar to CG5521-PA
	RGD1566021	AC_000086	10800122	19.6	brown	KL-dwn	similar to KIAA1772

Short list of 55 genes that are the most connected genes with known functions in the modules of interest.
Selected from the top 10% most connected genes in each module (except blue module for which considered top 20% as many hubs are not annotated. Abbreviations used: dwn - down-regulated; up - up-regulated; (*)- k in. is connectivity coefficient obtained/calculated in network analysis.
doi:10.1371/journal.pone.0011637.t002

demonstrate that these types of modules are enriched for known biological pathways for genes that associate with disease traits and for genes that are linked to common genetic loci [6,35].

The current study employed a weighted gene co-expression network approach that has been extensively used for uncovering biologically meaningful gene modules [7,13,15] to explore novel pathways involved in primordial follicle development. An unsupervised and unbiased approach was used to nominate potential regulatory candidates for these modules based on gene network connectivity. The connectivity score shows how well under different treatments the changes in gene expression for a gene are correlated with the changes in expression for every other gene. In the current study, the gene co-expression network analysis helped select 55 highly connected genes for further functional analysis. An automated literature search of these 55 genes revealed a sub-network relationship among them as presented in Figure 3. This sub-network suggested regulatory roles for Pdgfa and Fgfr2 (the receptor) for Fgf2 and Fgf7 (KGF). PDGF, KGF/FGF7 and FGF2 proteins have previously been shown to regulate primordial to primary follicle transition [29,34]. Therefore, the bionetwork predicted to be involved in the regulation of primordial follicle development identified two previously known regulatory factors which validated the utility of the network analysis for identifying candidate regulatory genes, consistent with previous network studies [13,15]. This sub-network also identified connective tissue growth factor (Ctgf) [16,36] as a putative regulator of primordial follicle development. An ovarian organ culture experiment confirmed that CTGF promotes primordial to primary follicle transition. Therefore, a regulatory factor predicted to be important for primordial follicle development was confirmed to be involved which further validated the bionetwork approach. A microarray analysis of CTGF-treated ovaries showed an altered gene set similar to those of the other growth factors known to regulate follicle transition. These observations validate the network-based systems biology approach to elucidate the regulation of a complex developmental process.

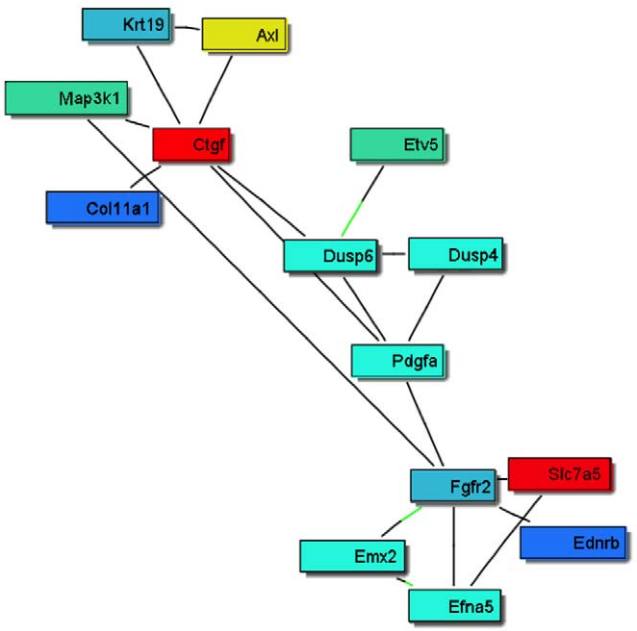

Figure 3. Sub-network connection scheme for the most highly connected 55 candidate genes obtained by global literature analysis. Only 15 connected genes from the list of 55 are shown, while the rest are not connected and not shown. Red and yellow colors represent up-regulated genes, blue and turquoise colors – down-regulated genes.
doi:10.1371/journal.pone.0011637.g003

Consideration of the 55 intra-module hub genes from critical regulatory modules revealed a number of signaling and cellular processes were influenced, Figure 5 and Figure S3. In the growth factor/chemokine family Pdgfa and Ctgf were confirmed to be involved. The IL16 identified is currently being investigated as a potential regulatory candidate. The specific genes identified in Table 2 and associated regulatory processes provide potential therapeutic targets to regulate primordial follicle development. The ability to inhibit or stimulate primordial follicle development with a therapeutic treatment has a number of clinical applications. A delay in primordial follicle development and maintenance of the primordial pool could delay the onset of menopause and extend the reproductive life span of a female. In addition, the ability to therapeutically inhibit primordial follicle development would provide a treatment for premature ovarian failure, a disease when the primordial pool is lost early in life causing female infertility. In contrast, the therapeutic stimulation of primordial follicle development could treat forms of female infertility [4]. The induction of primordial follicle development also could promote the loss of the primordial pool and induce female sterility. The bionetwork identified in the current study produced a number of potential therapeutic targets to manipulate primordial follicle development and female reproductive capacity.

The systems biology approach taken with this network analysis of primordial follicle development identified clusters and modules of genes involved in this critical development process. A number of the growth factors previously shown to be involved (e.g. PDGF and bFGF) were identified, but other factors known to be important for ovarian development were not identified. Often a reductionist approach such as a knockout mouse model can

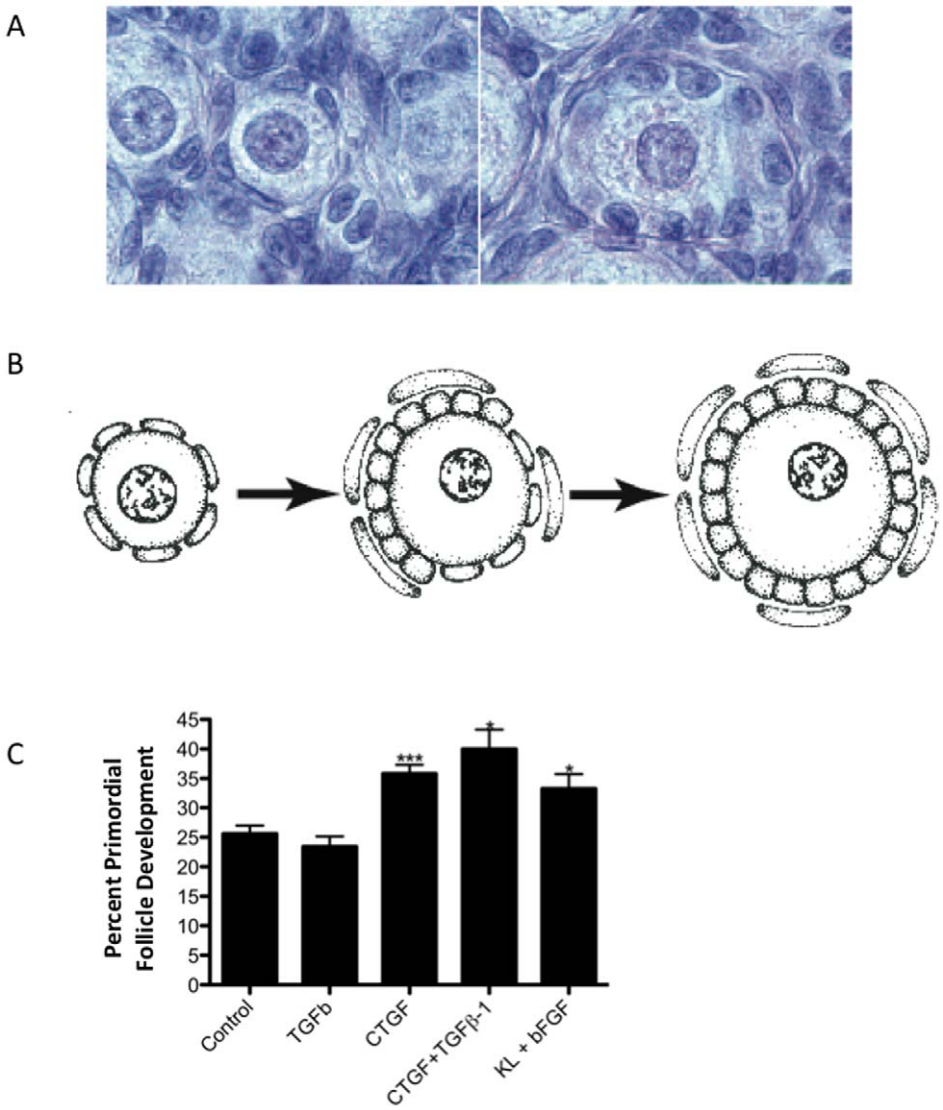

Figure 4. Analysis of the role of CTGF in primordial follicle transition. A) Hematoxylin-eosin stained ovary sections showing a representative arrested primordial follicle (left), and a developing primary follicle after having undergone primordial to primary follicle transition (right). **B**) Graphic representation of primordial and primary follicles. **C**) Effect of CTGF on cultured ovaries. Ovaries were cultured for 10 days with the treatments indicated. Ovarian histological analysis determined the percentage of primordial versus developing follicles for each ovary. Bars are the mean percent developing follicles ± SEM. N = 5–7 per treatment from four different replicate experiments. Asterisks indicate a significant (*$p<0.05$ or ***$p<0.01$) difference from control by Dunnet's post-hoc test after a significant result of ANOVA.
doi:10.1371/journal.pone.0011637.g004

identify a factor as being important for the maintenance of tissue development or function, but this does not mean the factor is regulated during the process. In addition, critical developmental processes such as primordial follicle development often have a set of compensatory factors that have evolved such that loss of any one will still allow the process to proceed. Therefore, knockout models often do not have phenotypes for these factors. This does not mean the factor is not important, but instead that the developmental process is essential and thus multiple factors compensate to assure the developmental process occurs. The current study takes a systems biology approach to identify networks of genes involved in the process without the bias of a reductionist model. Therefore, novel groups of factors and cellular processes were identified that now require further investigation.

The integrative analysis revealed a gene sub-network involved in primordial follicle development to elucidate the basic developmental biology of this process and provide potential therapeutic targets for ovarian disease and function. This sub-network was validated by the presence of two genes previously identified as being important. A new gene identified, Ctgf, was tested and found to regulate primordial follicle development. Therefore, the network based systems biology approach was partially validated for a normal developmental process. This type of approach will likely be invaluable to study development on a systems biology level in the future.

Materials and Methods

Ovarian organ culture

Four-day old female Sprague-Dawley rats (Harlan Laboratories, Inc., USA) were euthanized according to the laboratories Washington State University IACUC approved (#02568-014)

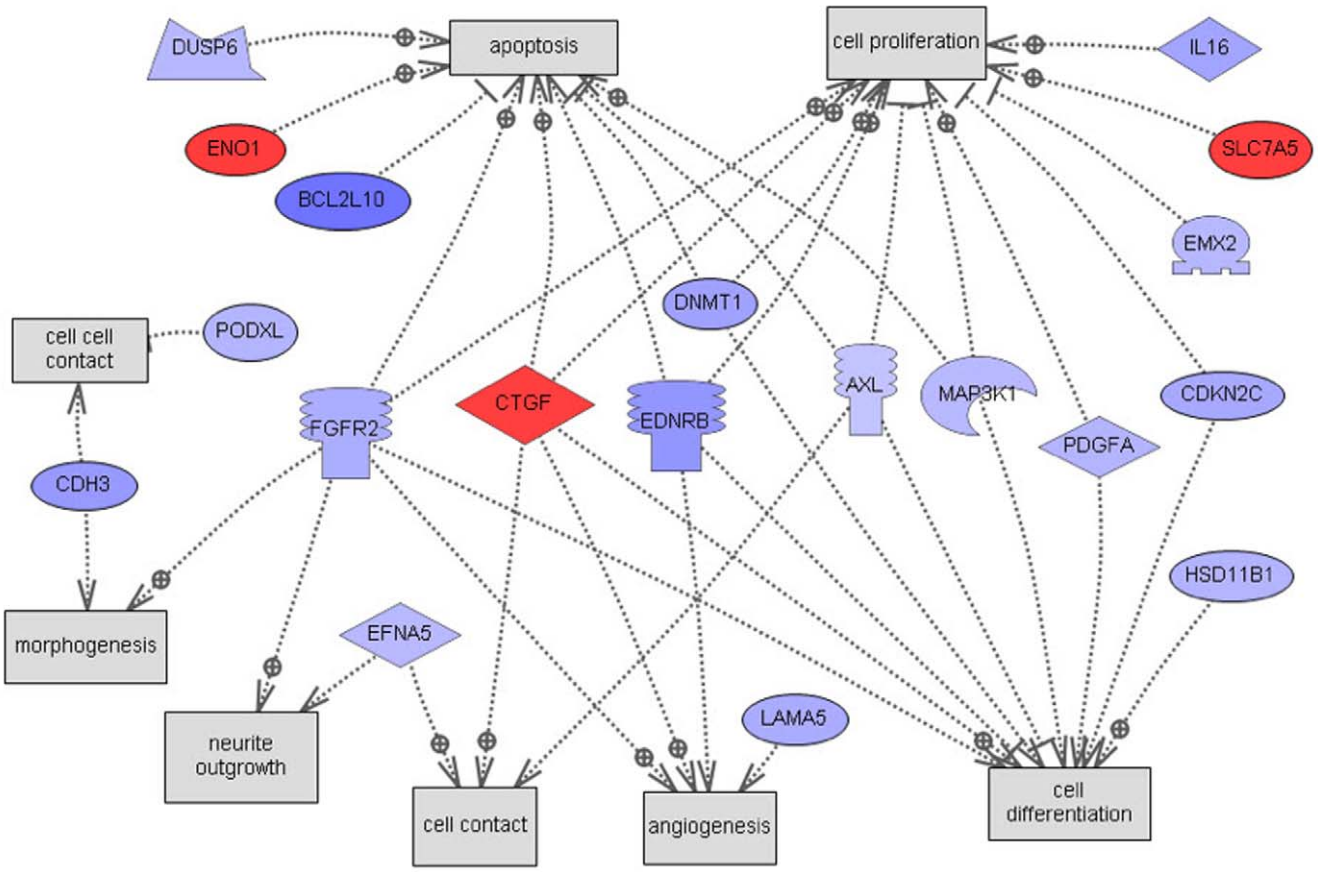

Figure 5. Scheme of direct connections to cellular processes for the 55 candidate regulatory genes obtained by global literature analysis. Only 19 connected genes from the list of 55 are shown, the rest are not connected and not shown. Node shapes code: oval and circle – protein; crescent – protein kinase and kinase; diamond – ligand; irregular polygon – phosphatase; circle/oval on tripod platform – transcription factor; ice cream cone – receptor. Red color represents up-regulated genes, blue color – down-regulated genes, grey rectangles represent cell processes; arrows with plus sign show positive regulation/activation, arrows with minus sign – negative regulation/inhibition.
doi:10.1371/journal.pone.0011637.g005

protocols and the ovaries removed and cultured whole as described previously [24]. Four-day old rat ovaries contain almost exclusively primordial follicles. For ovary culture experiments in which ovarian RNA was collected, 2–3 ovaries per well were cultured with media changes every 24 hours for two days in the absence (controls) or presence (treated) of either AMH (human Anti-Mülerian hormone)(50ng/mL, R&D Systems Inc., USA), FGF2 (rat Fibroblast growth factor 2)(50ng/mL, R&D Systems Inc., USA), BMP4 (human Bone morphogenetic protein 4)(50ng/mL, R&D Systems Inc., USA), GDNF (rat Glial derived neurotrophic factor)(50ng/mL, Calbiochem, USA), FGF7 (human fibroblast growth factor 7/keratinocyte growth factor)(50ng/mL, R&D Systems Inc., USA), KITLG (mouse Kit ligand)(50ng/mL, R&D Systems Inc., USA), LIF (rat leukemia inhibitory factor)(50ng/mL, Chemicon/Millipore, USA), PDGF-AB (rat platelet derived growth factor AB heterodimer)(50ng/mL, R&D Systems Inc., USA), TGFβ1 (human transforming growth factor beta 1)(50ng/mL, R&D Systems Inc., USA) or CTGF (human connective tissue growth factor)(50ng/mL, PeproTech Inc., NJ USA). After only two days of culture there are no morphological differences between control and growth factor-treated ovaries, so measurements of whole-ovary gene expression reflect differences in RNA transcription, rather than differing proportions of cell types due to differing cell proliferation between treatments.

In order to determine the effect of CTGF on primordial to primary follicle development, ovaries were cultured as above for ten days in the absence or presence of CTGF (50ng/mL), alone or in combination with TGF-beta1 (50ng/mL). After culture ovaries were fixed with Bouin's solution, paraffin embedded, sectioned onto microscope slides and stained with hematoxylin and eosin as described previously [24].

Morphometric Analysis

The number of follicles at each developmental stage was counted and averaged in two serial sections from the largest cross-section through the center of the ovary. Total follicle number has not been found to change between treatment groups. Rather, only the percentage of follicles at each developmental stage changes with treatment [28,34]. KL was used as a positive control for the organ culture experiments. Follicles in ovarian cross sections were classified as primordial (stage 0), or developing (stages 1–4: early primary, primary, transitional and preantral) as previously described [37]. Primordial follicles consist of an oocyte arrested in prophase I of meiosis that is partially or completely encapsulated by flattened squamous pregranulosa cells. Early transition primary follicles have initiated development (i.e., undergone primordial to primary follicle transition) and contain at least two cuboidal granulosa cells. Primary and preantral follicles exhibit one or more complete layers of cuboidal granulosa cells. Four-day old ovaries

contain predominately primordial follicles [26,38]. Hematoxylin/eosin stained ovarian sections were analyzed at 400× magnification using light microscopy. Follicles containing degenerating red eosin-stained oocytes were not counted.

RNA preparation

RNA was isolated from whole rat ovaries after homogenization in one ml Trizol™ reagent (Sigma-Aldritch, USA), according to manufacturer's instructions. Two or three ovaries from the same culture well (from different rat pups out of the same litter) and receiving the same treatment were pooled and homogenized together. On any given day a culture experiment was performed, the treatment groups included untreated control ovaries and one to three different growth factor treatments. Homogenized samples were stored at −70 C until the time of RNA isolation. After isolation from Trizol, RNA was further purified using RNeasy MinElute Cleanup Kits (Qiagen, USA) and stored in aqueous solution at −70 C.

Microarray Analysis

The microarray analysis was performed by the Genomics Core Laboratory, Center for Reproductive Biology, Washington State University, Pullman, WA using standard Affymetrix reagents and protocol. Briefly, mRNA was transcribed into cDNA with random primers, cRNA was transcribed, and single-stranded sense DNA was synthesized which was fragmented and labeled with biotin. Biotin-labeled ssDNA was then hybridized to the Rat Gene 1.0 ST microarrays containing 27,342 transcripts (Affymetrix, Santa Clara, CA, USA). Hybridized chips were scanned on Affymetrix Scanner 3000. CEL files containing raw data were then pre-processed and analyzed with Partek Genomic Suite 6.3 software (Partek Incorporated, St. Louis, MO) using an RMA GC-content adjusted algorithm. Raw data pre-processing was performed in 2 groups. The first group containing 38 samples CEL files were pre-processed in Partek all together as one experiment. Comparison of all array histogram graphs demonstrated the data for all 38 chips were similar and appropriate for further analysis. The second group of samples for microarray analysis consisting of 3 CTGF-treated and 3 corresponding control ovaries was run, pre-processed and analyzed *post factum*, separately from the rest of the samples as a result of a discovery from network analysis. Partek pre-processing algorithm for these 6 CEL files used the same criteria as used for the first group.

The microarray quantitative data involves over 10 different oligonucleotides arrayed for each gene and the hybridization must be consistent to allow a statistically significant quantitative measure of gene expression and regulation. In contrast, a quantitative PCR procedure only uses two oligonucleotides and primer bias is a major factor in this type of analysis. Therefore, we did not attempt to use PCR based approaches as we feel the microarray analysis is more accurate and reproducible without primer bias such as PCR based approaches.

All microarray CEL files (MIAME compliant raw data) from this study have been deposited with the NCBI gene expression and hybridization array data repository (GEO, http://www.ncbi.nlm.nih.gov/geo) (GEO Accession number: GSE20324), all arrays combined with one accession number, and can be also accessed through www.skinner.wsu.edu. For gene annotation, Affymetrix annotation file RaGene1_0stv1.na30.rn4.transcript.csv was used unless otherwise specified.

Network analysis

The network analysis was restricted to genes differentially expressed between the control and the treatment groups based on previously established criteria: (1) fold change of group means ≥ 1.2 or ≤ 0.83; (2) T test p-value ≤ 0.05; and (3) absolute difference of group means ≥ 10. The union of the differentially expressed genes from the different treatments resulted in 1,540 genes being identified and used for constructing a weighted gene co-expression network [7,8]. Unlike traditional un-weighted gene co-expression networks in which two genes (nodes) are either connected or disconnected, the weighted gene co-expression network analysis assigns a connection weight to each gene pair using soft-thresholding and thus is robust to parameter selection. The weighted network analysis begins with a matrix of the Pearson correlations between all gene pairs, then converts the correlation matrix into an adjacency matrix using a power function $f(x) = x^{\beta}$. The parameter β of the power function is determined in such a way that the resulting adjacency matrix (i.e., the weighted co-expression network), is approximately scale-free. To measure how well a network satisfies a scale-free topology, we use the fitting index proposed by Zhang & Horvath [7] (i.e., the model fitting index R^2 of the linear model that regresses $log(p(k))$ on $log(k)$ where k is connectivity and $p(k)$ is the frequency distribution of connectivity). The fitting index of a perfect scale-free network is 1. For this dataset, we select the smallest β $(=7)$ which leads to an approximately scale-free network with the truncated scale-free fitting index R^2 greater than 0.75. The distribution $p(k)$ of the resulting network approximates a power law: $p(k) \sim k^{-1.29}$.

To explore the modular structures of the co-expression network, the adjacency matrix is further transformed into a topological overlap matrix [30]. As the topological overlap between two genes reflects not only their direct interaction, but also their indirect interactions through all the other genes in the network. Previous studies [7,30] have shown that topological overlap leads to more cohesive and biologically meaningful modules. To identify modules of highly co-regulated genes, we used average linkage hierarchical clustering to group genes based on the topological overlap of their connectivity, followed by a dynamic cut-tree algorithm to dynamically cut clustering dendrogram branches into gene modules [39]. A total of sixteen modules were identified and the module size was observed to range from 20 to 194 genes.

To distinguish between modules, each module was assigned a unique color identifier, with the remaining, poorly connected genes colored grey. The hierarchical clustering over the topological overlap matrix (TOM) and the identified modules is shown. In this type of map, the rows and the columns represent genes in a symmetric fashion, and the color intensity represents the interaction strength between genes. This connectivity map highlights that genes in the ovary transcriptional network fall into distinct network modules, where genes within a given module are more interconnected with each other (blocks along the diagonal of the matrix) than with genes in other modules. There are a couple of network connectivity measures, but one particularly important one is the within module connectivity (k.in). The k.in of a gene was determined by taking the sum of its connection strengths (co-expression similarity) with all other genes in the module which the gene belonged.

Gene Co-expression Network Analysis Clarification

Gene networks provide a convenient framework for exploring the context within which single genes operate. Networks are simply graphical models comprised of nodes and edges. For gene co-expression networks, an edge between two genes may indicate that the corresponding expression traits are correlated in a given population of interest. Depending on whether the interaction strength of two genes is considered, there are two different approaches for analyzing gene co-expression networks: 1) an

unweighted network analysis that involves setting hard thresholds on the significance of the interactions, and 2) a weighted approach that avoids hard thresholds. Weighted gene co-expression networks preserve the continuous nature of gene-gene interactions at the transcriptional level and are robust to parameter selection. An important end product from the gene co-expression network analysis is a set of gene modules in which member genes are more highly correlated with each other than with genes outside a module. Most gene co-expression modules are enriched for GO functional annotations and are informative for identifying the functional components of the network that are associated with disease [6].

This gene co-expression network analysis (GCENA) has been increasingly used to identify gene sub-networks for prioritizing gene targets associated with a variety of common human diseases such as cancer and obesity [11,12,13,14,15]. One important end product of GCENA is the construction of gene modules comprised of highly interconnected genes. A number of studies have demonstrated that co-expression network modules are generally enriched for known biological pathways, for genes that are linked to common genetic loci and for genes associated with disease [6,7,11,13,14,15,40,41,42]. In this way, one can identify key groups of genes that are perturbed by genetic loci that lead to disease, and that define at the molecular level disease states. Furthermore, these studies have also shown the importance of the hub genes in the modules associated with various phenotypes. For example, GCENA identified ASPM, a hub gene in the cell cycle module, as a molecular target of glioblastoma [15] and MGC4504, a hub gene in the unfolded protein response module, as a target potentially involved in susceptibility to atherosclerosis [13].

Pathway Analysis

Resulting lists of differentially expressed genes for each growth factor treatment as well as for each module generated in the network analysis were analyzed for KEGG (Kyoto Encyclopedia for Genes and Genome, Kyoto University, Japan) pathway enrichment using Pathway-Express, a web-based tool freely available as part of the Onto-Tools (http://vortex.cs.wayne.edu) [43]. Global literature analysis of various gene lists was performed using BiblioSphere PathwayEdition (Genomatix Software GmbH, Munchen, Federal Republic of Germany) software which performs pathway and interaction analysis and labels genes which belong to certain known metabolic and signal transduction pathways. A program based on literature analysis Pathway Studio (Ariadne, Genomics Inc. Rockville MD) was used to evaluate cellular processes connected to differentially expressed genes.

Supporting Information

Figure S1 Network scheme for 1540 differentially expressed genes obtained by global literature analysis using BiblioSphere Pathway Edition Software (Genomatix Software GmbH, Munchen, Federal Republic of Germany). Different node colors represent different modules. A - the whole scheme clearly indicates 5 distinguished groups of genes (each group is shown separately on pp. 2–6) connected to 5 central genes: Nfkb1 (B, page 2), Vegfa (C, page 3), Egfr (D, page 4), and Gadd45a (F, page 6). Only connected genes are shown.
Found at: doi:10.1371/journal.pone.0011637.s001 (2.07 MB PDF)

Figure S2 KEGG Pathway "Complement and Coagulation Cascades" enriched by regulated genes from 1,540 gene list. Red nodes represent up-regulated genes, blue - down-regulated, green - not affected genes.
Found at: doi:10.1371/journal.pone.0011637.s002 (0.07 MB PDF)

Figure S3 Scheme of shortest connections to cellular processes for 55 candidate regulatory genes, as obtained by global literature analysis using Pathway Studio 7.0 (Ariadne Genomics, Inc., Rockville, MD; trial version). Only 22 connected genes from the list out of 55 are shown, the rest from the list are not connected and not shown. Node shapes code: oval and circle - protein; crescent - protein kinase and kinase; diamond - ligand; irregular polygon - phosphatase; circle/oval on tripod platform - transcription factor; ice cream cone - receptor. Red color represents up-regulated genes, blue color - down regulated genes, grey nodes represent genes closely connected (next neighbor) to the list genes; grey rectangles represent cell processes; arrows color: grey solid or dotted - regulation, blue - expression, green - promoter binding; arrows with plus sign show positive regulation/activation, arrows with minus sign - negative regulation/inhibition.
Found at: doi:10.1371/journal.pone.0011637.s003 (0.35 MB PDF)

Table S1 Rat Genes Expressed Differentially After Growth Factor Treatment of Ovary. Legends: * - absolute value of difference between means of Control and GF Treatment expression values ** - abbreviations used for modules' color: trq -turquoise; brw - brown; blu- blue; ylw- yellow; prp - purple; gr - grey; grn - green; grlw - green-yellow; blc- black; mbl - midnight-blue; slm - salmon; lcn - light cyan; ***- k in. is connectivity coefficient determined in network analysis.
Found at: doi:10.1371/journal.pone.0011637.s004 (1.37 MB PDF)

Author Contributions

Conceived and designed the experiments: EES MKS. Performed the experiments: EEN MIS RS BZ. Analyzed the data: EEN MIS RS BZ EES MKS. Wrote the paper: EEN MIS RS BZ EES MKS.

References

1. Hirshfield AN (1991) Development of follicles in the mammalian ovary. Int Rev Cytol 124: 43–101.
2. Rajah R, Glaser EM, Hirshfield AN (1992) The changing architecture of the neonatal rat ovary during histogenesis. Dev Dyn 194: 177–192.
3. Peters H, Byskov AG, Himelstein-Braw R, Faber M (1975) Follicular growth: the basic event in the mouse and human ovary. J Reprod Fertil 45: 559–566.
4. Skinner MK (2005) Regulation of primordial follicle assembly and development. Hum Reprod Update 11: 461–471.
5. Pangas SA (2007) Growth factors in ovarian development. Semin Reprod Med 25: 225–234.
6. Lum PY, Chen Y, Zhu J, Lamb J, Melmed S, et al. (2006) Elucidating the murine brain transcriptional network in a segregating mouse population to identify core functional modules for obesity and diabetes. J Neurochem 97 Suppl 1: 50–62.
7. Zhang B, Horvath S (2005) A general framework for weighted gene co-expression network analysis. Stat Appl Genet Mol Biol 4: Article17.
8. Zhu J, Wiener MC, Zhang C, Fridman A, Minch E, et al. (2007) Increasing the power to detect causal associations by combining genotypic and expression data in segregating populations. PLoS Comput Biol 3: e69.
9. Schadt EE, Lamb J, Yang X, Zhu J, Edwards S, et al. (2005) An integrative genomics approach to infer causal associations between gene expression and disease. Nat Genet 37: 710–717.
10. Winrow CJ, Williams DL, Kasarskis A, Millstein J, Laposky AD, et al. (2009) Uncovering the genetic landscape for multiple sleep-wake traits. PLoS ONE 4: e5161.

11. Chen Y, Zhu J, Lum PY, Yang X, Pinto S, et al. (2008) Variations in DNA elucidate molecular networks that cause disease. Nature 452: 429–435.
12. Emilsson V, Thorleifsson G, Zhang B, Leonardson AS, Zink F, et al. (2008) Genetics of gene expression and its effect on disease. Nature 452: 423–428.
13. Gargalovic PS, Imura M, Zhang B, Gharavi NM, Clark MJ, et al. (2006) Identification of inflammatory gene modules based on variations of human endothelial cell responses to oxidized lipids. Proc Natl Acad Sci U S A 103: 12741–12746.
14. Ghazalpour A, Doss S, Zhang B, Wang S, Plaisier C, et al. (2006) Integrating genetic and network analysis to characterize genes related to mouse weight. PLoS Genet 2: e130.
15. Horvath S, Zhang B, Carlson M, Lu KV, Zhu S, et al. (2006) Analysis of oncogenic signaling networks in glioblastoma identifies ASPM as a molecular target. Proc Natl Acad Sci U S A 103: 17402–17407.
16. Leask A, Abraham DJ (2003) The role of connective tissue growth factor, a multifunctional matricellular protein, in fibroblast biology. Biochem Cell Biol 81: 355–363.
17. Durlinger AL, Kramer P, Karels B, de Jong FH, Uilenbroek JT, et al. (1999) Control of primordial follicle recruitment by anti-Mullerian hormone in the mouse ovary. Endocrinology 140: 5789–5796.
18. Nilsson E, Rogers N, Skinner MK (2007) Actions of anti-Mullerian hormone on the ovarian transcriptome to inhibit primordial to primary follicle transition. Reproduction 134: 209–221.
19. Nilsson EE, Skinner MK (2004) Kit ligand and basic fibroblast growth factor interactions in the induction of ovarian primordial to primary follicle transition. Mol Cell Endocrinol 214: 19–25.
20. Garor R, Abir R, Erman A, Felz C, Nitke S, et al. (2009) Effects of basic fibroblast growth factor on in vitro development of human ovarian primordial follicles. Fertil Steril 91: 1967–1975.
21. Matos MH, Lima-Verde IB, Bruno JB, Lopes CA, Martins FS, et al. (2007) Follicle stimulating hormone and fibroblast growth factor-2 interact and promote goat primordial follicle development in vitro. Reprod Fertil Dev 19: 677–684.
22. Nilsson EE, Skinner MK (2003) Bone morphogenetic protein-4 acts as an ovarian follicle survival factor and promotes primordial follicle development. Biol Reprod 69: 1265–1272.
23. Tanwar PS, O'Shea T, McFarlane JR (2008) In vivo evidence of role of bone morphogenetic protein-4 in the mouse ovary. Anim Reprod Sci 106: 232–240.
24. Dole G, Nilsson EE, Skinner MK (2008) Glial-derived neurotrophic factor promotes ovarian primordial follicle development and cell-cell interactions during folliculogenesis. Reproduction 135: 671–682.
25. Kezele P, Nilsson EE, Skinner MK (2005) Keratinocyte growth factor acts as a mesenchymal factor that promotes ovarian primordial to primary follicle transition. Biol Reprod 73: 967–973.
26. Parrott JA, Skinner MK (1999) Kit-ligand/stem cell factor induces primordial follicle development and initiates folliculogenesis. Endocrinology 140: 4262–4271.
27. Hutt KJ, McLaughlin EA, Holland MK (2006) KIT/KIT ligand in mammalian oogenesis and folliculogenesis: roles in rabbit and murine ovarian follicle activation and oocyte growth. Biol Reprod 75: 421–433.
28. Nilsson EE, Kezele P, Skinner MK (2002) Leukemia inhibitory factor (LIF) promotes the primordial to primary follicle transition in rat ovaries. Mol Cell Endocrinol 188: 65–73.
29. Nilsson EE, Detzel C, Skinner MK (2006) Platelet-derived growth factor modulates the primordial to primary follicle transition. Reproduction 131: 1007–1015.
30. Ravasz E, Somera AL, Mongru DA, Oltvai ZN, Barabasi AL (2002) Hierarchical organization of modularity in metabolic networks. Science 297: 1551–1555.
31. Langfelder P, Zhang B, Horvath S (2008) Defining clusters from a hierarchical cluster tree: the Dynamic Tree Cut package for R. Bioinformatics 24: 719–720.
32. Cicha I, Goppelt-Struebe M (2009) Connective tissue growth factor: context-dependent functions and mechanisms of regulation. Biofactors 35: 200–208.
33. Gressner OA, Gressner AM (2008) Connective tissue growth factor: a fibrogenic master switch in fibrotic liver diseases. Liver Int 28: 1065–1079.
34. Nilsson E, Parrott JA, Skinner MK (2001) Basic fibroblast growth factor induces primordial follicle development and initiates folliculogenesis. Mol Cell Endocrinol 175: 123–130.
35. Ghazalpour A, Doss S, Sheth SS, Ingram-Drake LA, Schadt EE, et al. (2005) Genomic analysis of metabolic pathway gene expression in mice. Genome Biol 6: R59.
36. Harlow CR, Hillier SG (2002) Connective tissue growth factor in the ovarian paracrine system. Mol Cell Endocrinol 187: 23–27.
37. Oktay K, Schenken RS, Nelson JF (1995) Proliferating cell nuclear antigen marks the initiation of follicular growth in the rat. Biol Reprod 53: 295–301.
38. Kezele PR, Ague JM, Nilsson E, Skinner MK (2005) Alterations in the ovarian transcriptome during primordial follicle assembly and development. Biol Reprod 72: 241–255.
39. Langfelder P, Horvath S (2007) Eigengene networks for studying the relationships between co-expression modules. BMC Syst Biol 1: 54.
40. Schadt EE, Molony C, Chudin E, Hao K, Yang X, et al. (2008) Mapping the genetic architecture of gene expression in human liver. PLoS Biol 6: e107.
41. Zhu J, Zhang B, Schadt EE (2008) A systems biology approach to drug discovery. Adv Genet 60: 603–635.
42. Zhu J, Zhang B, Smith EN, Drees B, Brem RB, et al. (2008) Integrating large-scale functional genomic data to dissect the complexity of yeast regulatory networks. Nat Genet 40: 854–861.
43. Draghici S, Khatri P, Tarca AL, Amin K, Done A, et al. (2007) A systems biology approach for pathway level analysis. Genome Res 17: 1537–1545.